NASA Contractor Report 190147

STS-48 CASE STUDY
17-18 SEPTEMBER 1991

Michael K. Atchison
Mark M. Wheeler
Gregory E. Taylor
John D. Warburton
Applied Meteorology Unit

Prepared For:
Kennedy Space Center
under Contract No. C-NAS10-11844

NASA
National Aeronautics and
Space Administration

Office of Management

Scientific and Technical
Information Program

1992

TABLE OF CONTENTS

LIST OF ILLUSTRATIONS

LIST OF ILLUSTRATIONS

LIST OF ILLUSTRATIONS

LIST OF ILLUSTRATIONS

1.0 INTRODUCTION

The purpose of this report is to document weather conditions prior to and during the STS-48 attempted landing at the Shuttle Landing Facility (SLF) at the Kennedy Space Center (KSC) on 18 September 1991. Major emphasis will be placed on trends in meteorological data during 17 and 18 September and their relationship to the overall weather pattern seen over the KSC region. Major landing rules of concern for the landing support forecaster during STS-48 were the formation of showers within 10 nautical miles of the SLF and any ceiling less than 10,000 feet. The following sections will describe each of the meteorological data sets available for analysis during the attempted KSC landing of STS-48. Section 2 of this report will describe the surface weather patterns affecting the KSC region on 17 and 18 September. Section 3 will present an analysis of upper-air conditions over Florida and the southeastern United States plus a detailed look at soundings taken from the Cape Canaveral Air Force Station (CCAFS). Section 4 will present an analysis of radar and satellite imagery from the KSC vicinity. Section 5 contains a brief summary of this analysis while Section 6 will discuss any recommendations suggested by the AMU. Section 7 contains the acknowledgments and Section 8 a list of references.

2.0 SURFACE ANALYSIS

As shown by the Meteorological Interactive Data Display System (MIDDS), the surface pressure pattern at 1200 UTC on 17 September 1991 (Figure 1) featured a weak high pressure ridge over Tennessee through the Carolinas and out into the Atlantic for several hundred miles. During the daylight hours on 17 September and the early morning hours on 18 September this ridge gradually weakened and moved slowly off to the northeast. This weakening and movement of the ridge can be seen by a series of surface analysis charts (Figures 2-4) over the southeast U.S. Note specifically the break down of the ridge over the Tennessee, northern Alabama and Mississippi regions with time.

As the intensity and position of the ridge changed throughout 17 and 18 September the surface flow over the KSC region became more southeasterly. This can be seen in time series plots of wind data from Towers 513 and 003 (see Figures 5 and 6). Tower 513 is located along the SLF while Tower 003 is located near the tip of the Cape (see Figure 7). Winds from Tower 513 early in the morning (0400-1200 UTC) on 17 September showed the presence of a weak land breeze over the Merritt Island area (see Figure 6). By late morning and early afternoon on 17 September the winds turned more to the northeast and by sundown (2300 UTC) they had shifted to the east. During the early morning hours on 18 September the winds gradually shifted more to the southeast (110-120 degrees). The same type of wind shift can also be seen at Tower 003. However, no land breeze was noted at this coastal location.

Also noted in the time series in Figures 5 and 6 was a sharp shift in wind speed and direction from 1800 to 2100 UTC on 17 September. This was caused by showers that were moving through the area especially along coastal sections. In addition, one other significant feature of the low-level winds over the KSC area can be seen in the wind speed time series at Tower 003 (see Figure 5). During the daylight hours on 17 September the wind speed was averaging close to 10 knots. After the showers passed (1900-2000 UTC), the wind speeds decreased to 2-3 knots and then increased to 10 knots early on 18 September and stayed at those speeds until attempted landing time (0609 UTC 18 September). However, winds at Tower 513 were much lighter during the early morning hours as shown in Figure 6. With wind speeds still 10 knots along the coast but much lighter inland there would be some speed convergence occurring near the coast. This combined with several other mechanisms such as weak convergence lines east of the

Cape and a increase in low-level moisture probably contributed to the development of clouds and showers near the coast.

The pressure field over Florida indicates the persistent southeasterly winds along the east coast were being enhanced by a slightly stronger pressure gradient along the east coast of the state. This can be seen by examining the surface maps (Figures 1-4). In Figure 2 the pressure difference between Orlando and West Palm Beach was approximately 0.7 mb but by 0000 UTC on 18 September it had increased to 1.0 mb and remained at this strength until at least 0600 UTC.

2.1 SURFACE SUMMARY

- Weakening high pressure ridge north of Florida moves off to the northeast
- Winds shift NE-E-SE with time as ridge weakens
- Slightly stronger pressure gradient early on 18 September
- Weak convergence along coastal sections during early morning hours of 18 September

3.0 UPPER-AIR ANALYSIS

During 17 September, MIDDS analyses of 850, 700 and 500 mb upper-air data showed a ridge extending across the southeastern portions of the country from Louisiana to Georgia then off the North Carolina coast out into the Atlantic Ocean (see Figures 8-10). As a result of this ridge position, easterly flow was present at all levels up to at least 200 mb. This easterly flow can be seen by the CCAFS rawinsonde at 1000 UTC on 17 September as shown in Figure 11. At this time winds from the surface to 800 mb were averaging 5-10 knots with winds at 700 to 500 mb in the 10-20 knot range.

Between 1200 UTC on 17 September and 1200 UTC on 18 September, the ridge weakened slightly and changed orientation over the southeast U.S. (compare the upper-air charts in Figures 8-10, especially at 850 and 700 mb). This weakening resulted in a reduction in winds as observed by the CCAFS rawinsondes (compare the 1000 and 2336 UTC CCAFS soundings in Figure 12). As shown in Figure 12, the most noticeable change occurred around 700 mb where winds were 10-15 knots at 1000 UTC but by 2336 UTC they had decreased to near 5 knots. At 700 mb throughout the early morning hours of 18 September (see CCAFS soundings in Figures 13-16) the winds at this level remained weak and even shifted to the southwest by 1000 UTC on 18 September (see Figure 16). This mid-level weakening in winds was also seen at Tampa as shown in Figures 17-19.

This change in winds around 700 mb can also be seen by looking at the KSC Doppler radar wind profiler data at the 3061 m (10040 ft.) level (see Figures 20 and 21). Between 1800 UTC 17 September and 0200 UTC 18 September winds at this level were from a northeast direction at speeds of 6-9 knots. At around 0200 UTC winds started to become very light with speeds of only 2-4 knots. By 0400 UTC winds had become very light with speeds of less than 2 knots and even started to shift more to the southwest as shown in Figure 20. By 0600 UTC winds had taken a definite shift to the southwest and had increased in speed up to 4-6 knots. This type of trend in the wind speed and direction, as shown by both the KSC wind profiler and CCAFS rawinsondes, appears to be related to a very weak mid-level disturbance moving east to west in the general easterly synoptic flow pattern. This weak disturbance could not be seen at levels above 500 mb. As shown in Figures 22 and 23 at 6061m (near 500 mb), no significant changes could be seen in either wind speed or direction during the early morning hours of 18 September.

Other minor changes in the CCAFS soundings were also noted between the surface and 6000 feet. At 1000 UTC on 17 September (see Figure 12), winds 0-6000 feet were easterly at 5-8 knots but by 2336 UTC the winds had become more southeasterly and increased to 15 knots. Between 0000-0600 UTC on 18 September winds at these levels remained southeasterly at 10-15 knots. In addition, between 2336 UTC on 17 September and 0336 UTC on 18 September, both temperature and moisture increased slightly in these lower levels making the atmosphere more unstable (see Figure 24). This trend in relative humidity from 2336 UTC on 17 September to 0506 UTC on 18 September is shown in Figure 25. At the 914 m level the relative humidity at 2336 UTC was 62% but had increased to 93% by 0506 UTC. In addition, the lifted index decreased from -1 at 2336 UTC to -4 at 0336 UTC and the precipitable water increased from 38 to 42 mm. All of these indicators show that the lower atmosphere was becoming more unstable during the early morning hours prior to the attempted landing time of 0609 UTC supporting an increasing possibility of cloud and shower development.

3.1 SUMMARY OF UPPER-AIR CONDITIONS

- Upper-air ridge to the north provides easterly flow at most levels
- Ridge weakens with winds diminishing around 700 mb throughout 17-18 September
- Weak mid-level disturbance indicated by wind profiler and rawinsondes
- Shift in winds from east to southeast in the low-levels
- Increase in temperature and moisture below 700 mb early on 18 September

4.0 RADAR AND SATELLITE ANALYSIS

This section will discuss GOES IR satellite and McGill radar data collected during 17 and 18 September 1991. The McGill system, which is located at the Range Operations Control Center (ROCC), processes WSR-74C radar data at Patrick AFB (PAFB) in volumetric mode and is updated at 5 minute intervals. Figures 26-34 show radar images from early afternoon on 17 September (1900 UTC) to attempted landing time of near 0600 UTC on 18 September. Figures 35-41 show IR satellite images and their corresponding enhancements from 0000-0731 UTC on 18 September. No satellite data was available from 0500 to 0731 UTC due to a satellite in eclipse.

During the afternoon (1600-1800 UTC) on 17 September, radar loops indicated showers were forming in a band of cloudiness approximately 25-30 nm east of the Cape. The precipitation echoes were moving westward at 10 nm/hr. These showers and clouds affected the coastal regions of the Cape between 1900 and 2200 UTC. Figure 26 shows a radar image at 1859 UTC showing showers near the tip of the Cape extending down the coast to offshore of Melbourne. Radar loops showed the showers quickly dissipated once they moved inland. By 2358 UTC on 17 September (Figure 27), almost all showers were gone with very few discernible echoes within 30 nm of the Cape. In fact, at this time as shown by satellite data (Figure 35), there were very few clouds over the KSC region. During this time the SLF reported only high thin scattered clouds with less than 2/10 cloud cover below 8000 feet (see complete surface weather observations in Table 1).

Between 0100 and 0230 UTC patches of clouds and few showers started to form in a couple of bands over the area. At 0058 UTC (Figure 28) the McGill radar showed a few showers west of (PAFB) and to the south and southeast of Melbourne. These showers can be seen in the enhanced IR satellite image (Figure 36a) at 0101 UTC. There were also a few showers approximately 40 nm to the northeast of the Cape. Showers during this time were all moving in a northwest direction in response to the shift in the low-level winds (surface to 10,000 feet) as observed by the CCAFS rawinsondes. This was a significant change from the afternoon on 17 September when cell movement had been primarily westward. Around 0228 UTC a few showers passed over the northern portions of the Indian River approximately 12-15 nm northwest of the SLF (Figure 30). The enhanced IR image at 0201 UTC (Figure 37a) just began to indicate a slight enhancement of clouds over the northern portions of the Cape at this time.

During the period 0300-0400 UTC there was very little shower activity detected by the PAFB radar within 30 nm of the CAPE (Figure 31 and 32). The only significant precipitation echoes were east of Daytona Beach moving toward the northwest away from the Cape. In addition, IR imagery also showed very little in the way of organized cloudiness. However, post-analyses using different IR enhancements to bring out the lower level cloudiness showed a band of clouds approximately 15 nm south of the tip of the Cape extending out into the ocean for greater than 50 nm (see GOES IR image at 0401 and 0501 UTC - Figures 39 and 40). At shuttle landing decision time (0455 UTC) a few showers were just beginning to develop within this band of cloudiness (see PAFB radar at 0458 UTC in Figure 33). At this time a heavy rain shower formed near Cocoa with a few more cells forming about 20 nm southeast of the Cape. All the shower cells were moving northwest at 15 nm/hr.

Between 0500-0600 UTC, the showers near Cocoa moved northwest to just west of the Titusville-Cocoa airport (TIX). In addition, a small rain shower formed in the Indian River between the SLF and TIX (Figure 34) and more showers were beginning to develop in the band of clouds approximately 15 nm southeast of the Cape. As shown in Table 1, near the first landing opportunity time of 0609 UTC the surface weather conditions at the SLF were 3/10 cloud cover below 10000 feet with 2/10 at 2700 feet and 1/10 at 7500 feet. Surface winds were reported as calm.

The IR satellite loops through the evening hours revealed another interesting feature. First a warm area (dark pixels) can be seen east of the Cape region on all of the images (see Figures 35-41). It appears this region was experiencing some subsidence. This seems possible since it has already been noted that there was a lull in shower activity over this area at this time. As the evening progressed this area enlarged and spread toward the coast. After 0500 UTC the area shrank in size as the cloud band to the south expanded and high level clouds from an upper-air low north of the Bahamas (about 100 nm to the east) moved toward the Cape. The cirrus shield from thunderstorms near this upper-air low can be seen moving toward the Cape but did not affect the Cape's weather until after 0731 UTC.

Table 1.
Shuttle Landing Facility Weather Observations (X68) 17 and 18 September 1991

Day	Time (UTC)	Vis (nm)	Press. (mb)	Temp. (F)	Dew Pt. (F)	Wind Dir.	Wind Speed (Knots)	Clouds < 10K (Feet)
17 Sep	1155	5	1018.3	73	71	340	4	2/10
17 Sep	1255	6	1018.6	79	75	340	4	2/10
17 Sep	1355	7	1019.0	84	71	050	5	2/10
17 Sep	1455	7	1019.0	86	70	040	3	2/10
17 Sep	1555	7	1018.6	86	70	030	7	2/10
17 Sep	1655	7	1018.0	86	71	060	9	2/10
17 Sep	1755	7	1017.3	86	71	060	8	4/10
17 Sep	1855	7	1016.6	85	71	060	5	4/10
17 Sep	1955	7	1016.3	85	72	070	6	4/10
17 Sep	2055	7	1016.3	84	73	130	6	5/10
17 Sep	2155	7	1015.6	83	72	120	4	4/10
17 Sep	2255	7	1015.6	81	73	120	2	2/10
17 Sep	2355	8	1015.6	79	72	110	1	0
18 Sep	0055	8	1016.6	78	72	000	0	0
18 Sep	0155	8	1017.3	77	73	140	4	2/10
18 Sep	0255	8	1017.3	76	72	120	4	2/10
18 Sep	0325	8	1017.3	76	73	140	3	1/10
18 Sep	0355	8	1016.9	76	72	090	2	2/10
18 Sep	0425	8	1017.3	75	72	000	0	3/10
18 Sep	0455	8	1016.9	73	71	140	2	2/10
18 Sep	0525	8	1016.9	74	71	080	2	3/10
18 Sep	0555	8	1016.9	74	71	110	2	3/10
18 Sep	0606	8	1016.6	73	71	000	0	3/10
18 Sep	0655	8	1016.6	73	70	140	2	3/10

5.0 SUMMARY

The key to the weather on 17 and 18 September over the KSC area was a high pressure ridge that was gradually weakening and moving off slowly to the northeast. As this occurred the low-level flow over the KSC area was switching from a easterly to a southeasterly direction. This change in low-level wind direction was evident by shower cell movement on the McGill radar. On the afternoon of 17 September, cells were moving basically westward, while by early on 18 September, they were moving northwest. Analysis of CCAFS rawinsondes during this time indicates that the boundary layer became slightly more unstable which may have aided in the formation of clouds and isolated small showers. In addition, analyses of data from the KSC wind profiler and CCAFS rawinsondes indicated a possible mid-level disturbance in the easterly flow pattern near the 700 mb level. This weak upper-air low may have made the atmosphere a little more unstable during the early morning hours of 18 September. Also, stronger winds along the coast and weaker winds inland may have also been responsible for speed convergence over the area which would have aided cloud and shower development along the coast. Finally, embedded within this southeasterly flow were several bands of low clouds. These clouds were rather difficult to see in the IR satellite imagery available to forecasters in real time. However, post analyses using several different enhancement curves, adapted from NESDIS (Clark, 1983), clearly reveals the presence of these clouds.

6.0 RECOMMENDATIONS

By analyzing the meteorological data surrounding the STS-48 attempted landing at KSC on 18 September 1991, the AMU has identified two meteorological aspects that need further attention. First, forecasters need to become more aware of selecting the optimum satellite enhancements curves to visualize low clouds in IR imagery during the nighttime hours. By using NESDIS products as a guideline both the Space Flight Meteorology Group (SMG) and the AMU have developed enhancements that more easily detect lower level cloudiness. Using these types of enhancements is especially important during easterly flow cases and even low stratus and fog situations over the St. John's River valley. Second, since the development of showers and the presence of cloud ceilings less than 10,000 feet are of prime concern for Shuttle landings, identifying the stability in the low levels of the atmosphere is very important, especially in easterly flow situations. A low-level stability index should be developed and evaluated for use in easterly flow situations. Currently, MIDDS provides the forecasters with estimates of the K-Index (George, 1960), the Lifted Index (Galway, 1956), the Total Totals Index (Miller, 1972), and the Severe Weather Threat Index (SWEAT Index) (Miller, 1975). Although valuable for evaluating the potential for thunderstorm and severe thunderstorm development, these tools are not optimal for evaluating the potential for low-level shower development along the east coast of Florida in easterly flow situations.

The Lifted Index, the Total Totals Index, and the SWEAT Index estimate the potential for the development of deep penetrative convection using low-level (e.g., 850 mb or below) temperature and moisture and upper-level (e.g., 500 mb) temperature data. These indices do not incorporate any information regarding the moisture content or temperature of the atmosphere between these two levels. Thus, they will not, in all cases, accurately reflect the static stability of the lower atmosphere (e.g., surface to 700 mb) nor will they reflect the stabilizing effect of entraining dry environmental air into a shower updraft. Since the tops of low-level east coast Florida showers may not extend far above the 700 mb level and since entrainment of dry air will tend to inhibit low-level shower development, these indices may not provide an accurate assessment of the potential for low-level shower development.

The K-Index does incorporate a measure of mid-level moisture, the 700 mb dew point depression, in addition to low-level (e.g., 850 mb) and upper level (e.g., 500 mb) data. Consequently, it does reflect the potential for air mass thunderstorm development which

is inhibited by entrainment of dry environmental air in mid-levels. However, it is still a measure of the stability of the atmosphere from the 850 mb level to the 500 mb. Thus, it also may not properly reflect the static stability of the atmosphere from the surface to 700 mb, the region of low-level shower development.

Since these four stability indices all have one or more deficiencies regarding their capability of estimating the potential for low-level shower development, it is recommended that a low-level stability index should be developed and evaluated for use in easterly flow situations. The index should focus on the stability of the lower atmosphere from the surface to 700 mb and should take into account the stabilizing effect of entrainment of environmental air into the shower updraft.

In addition to a low-level stability index, a quick-look trend analysis (comparison of successive rawinsonde data) would also be very helpful to the landing support forecaster in identifying subtle but critical changes in atmospheric conditions over short periods of times.

7.0 ACKNOWLEDGMENTS

The AMU would like to thank personnel from both the CCFF and SMG for their careful and constructive review of this report. In addition, we would also like to thank Computer Sciences Raytheon (CSR) Meteorology Section for providing much of the data that was used in this report.

8.0 REFERENCES

Clark, J.D., 1983: *The GOES User's Guide*, U.S. Department of Commerce, National Oceanic and Atmospheric Administration, 156 pp.

Galway, J.G., 1956: The Lifted Index as a predictor of latent instability, *Bulletin of the American Meteorological Society, 37*, 528-529.

George, J.J., *et al.*, 1960: *Weather Forecasting for Aeronautics*, Academic Press, New York, 673 pp.

Miller, R.C., 1972: Notes on Analysis and Severe Storm Forecasting Procedures of the Air Force Global Weather Central, *Air Weather Service Technical Report 200* (Revised), 102 pp.

Miller, R.C. and R.A. Maddox, 1975: Use of the SWEAT and SPOT Indices in Operational Severe Storm Forecasting, *Preprints, Ninth Conference on Severe Local Storms*, Norman, OK, American Meteorological Society, Boston, 1-6.

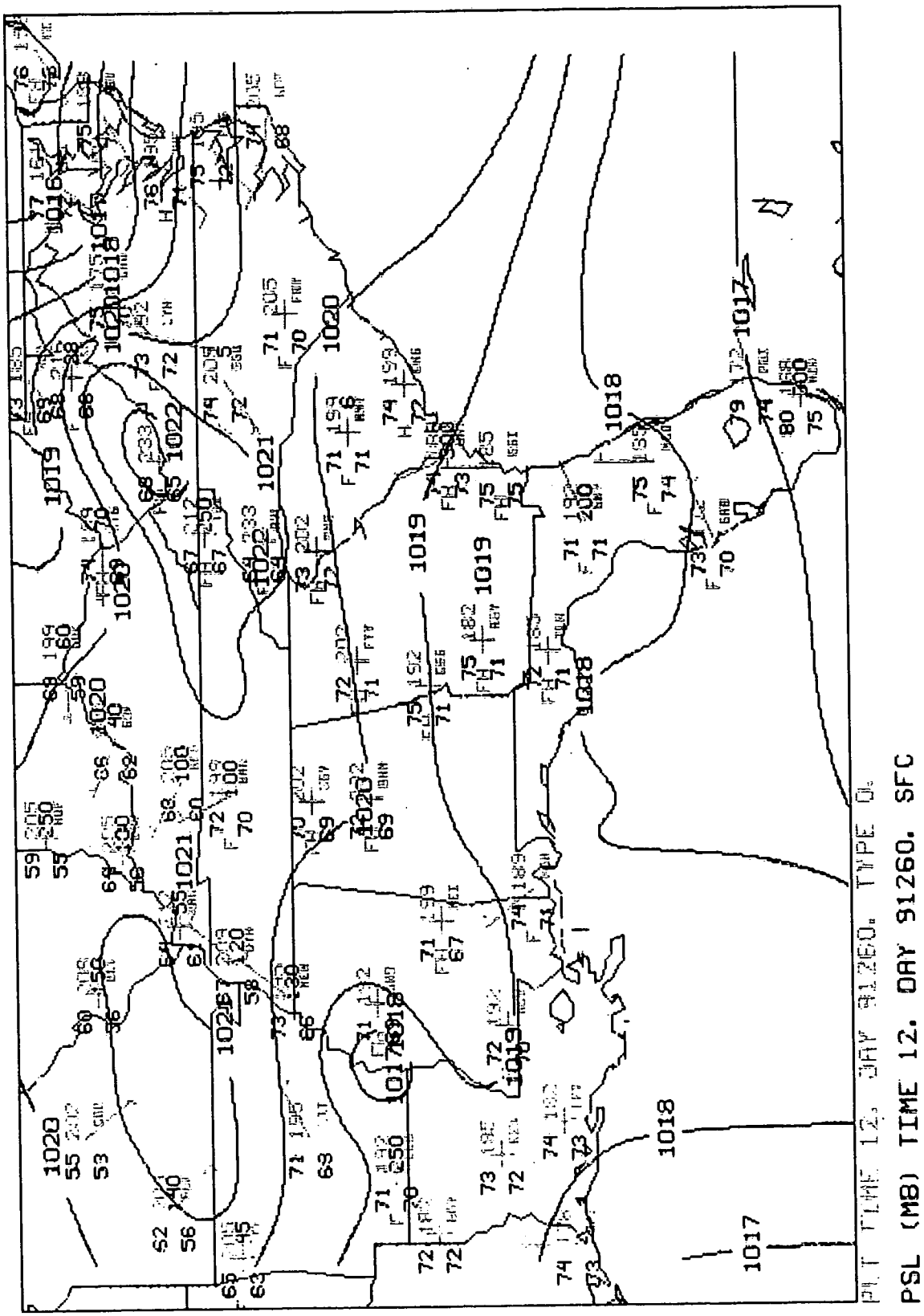

Figure 1 Surface Analysis at 1200 UTC on 17 September 1991.

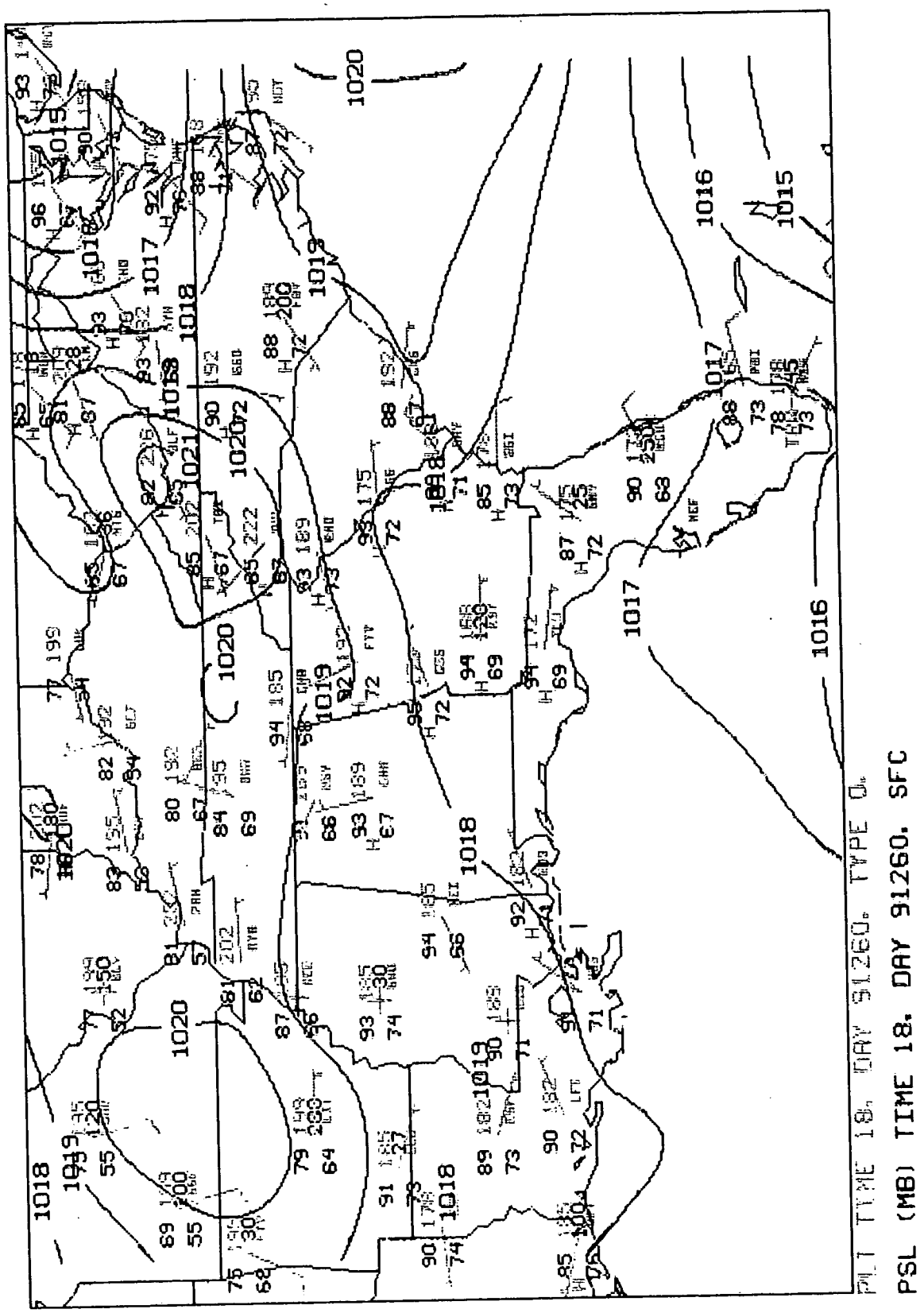

Figure 2 Surface Analysis at 1800 UTC on 17 September 1991.

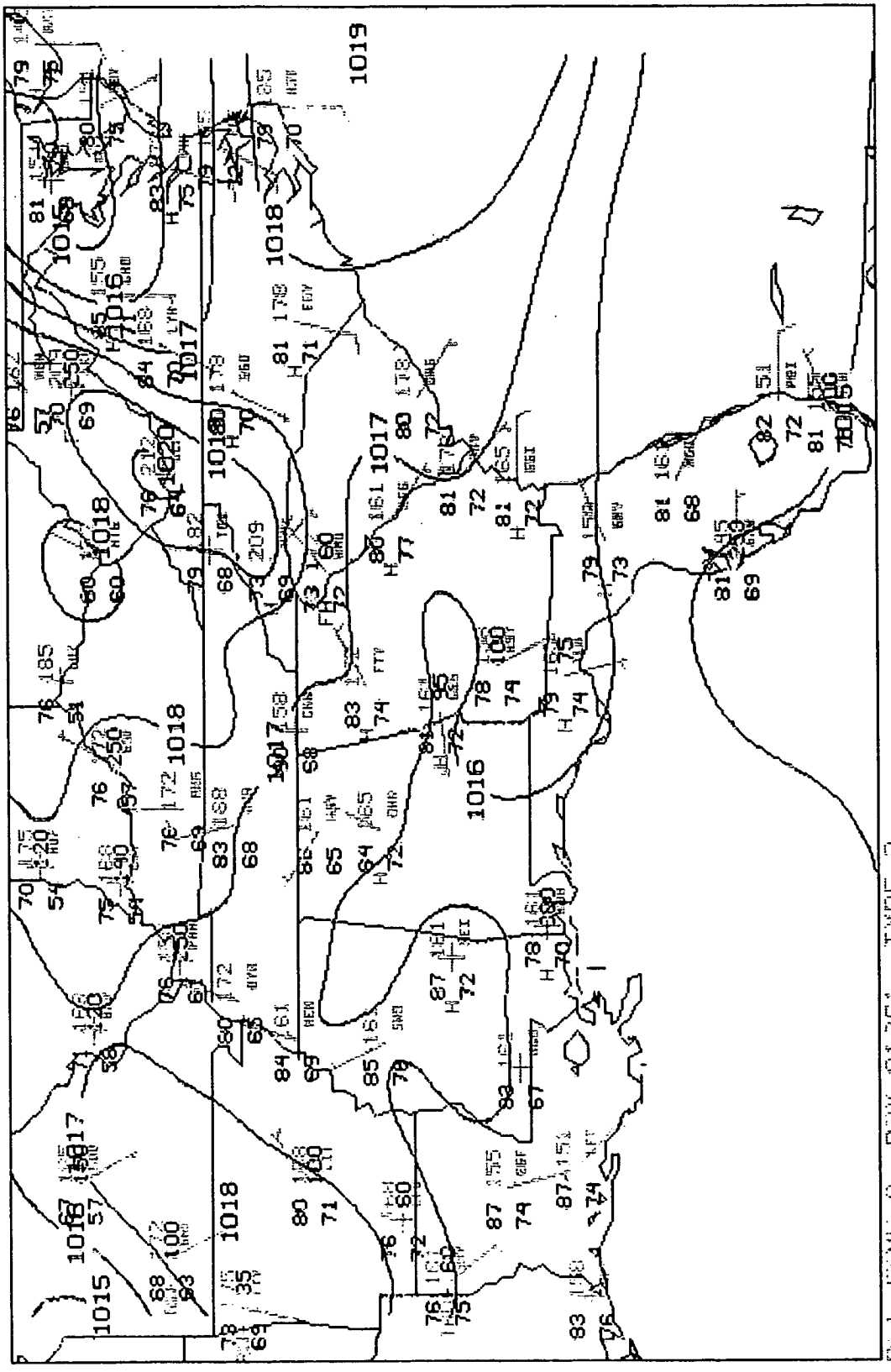

Figure 3 Surface Analysis at 0000 UTC on 18 September 1991.

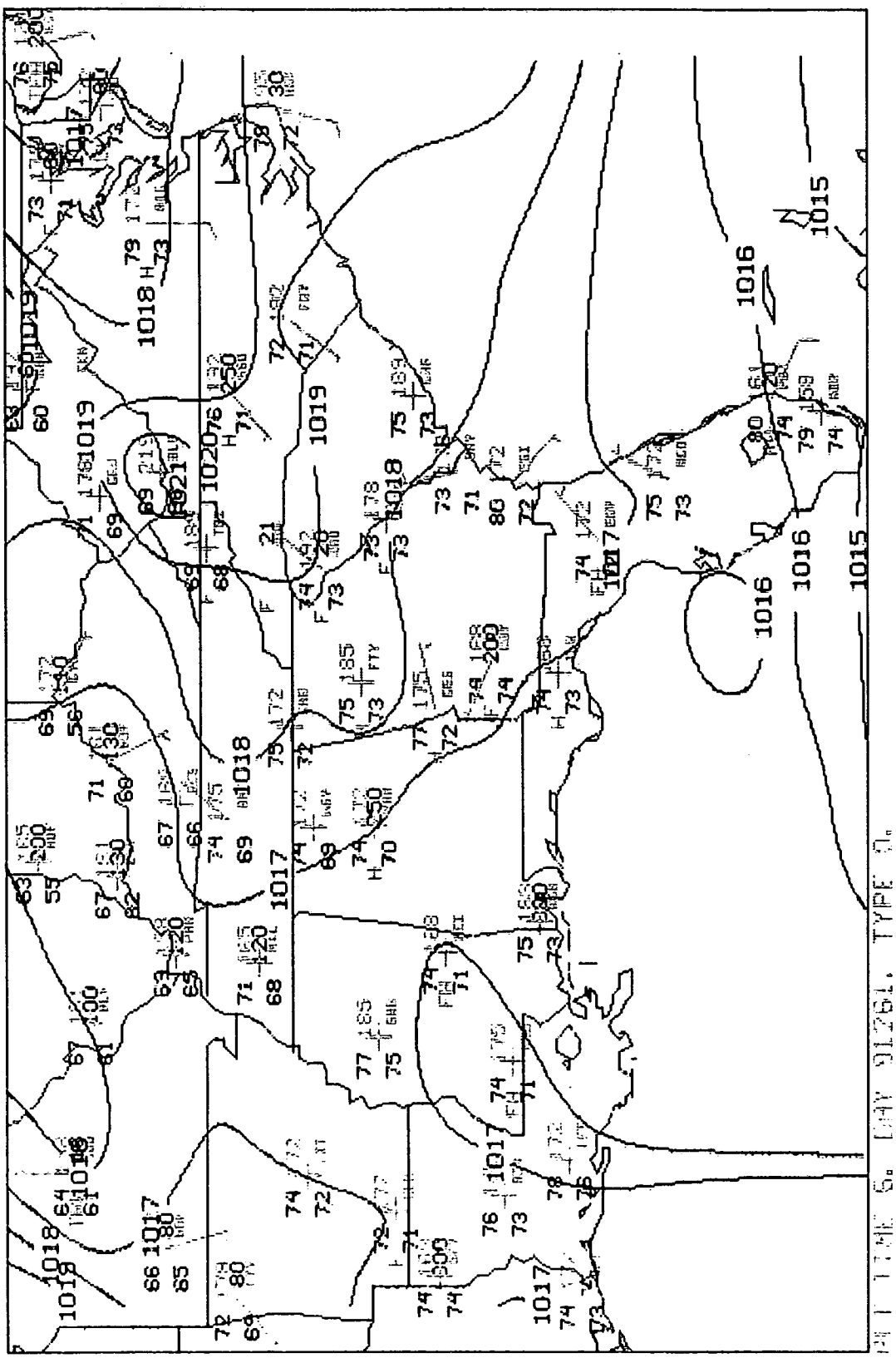

Figure 4 Surface Analysis at 0600 UTC on 18 September 1991.

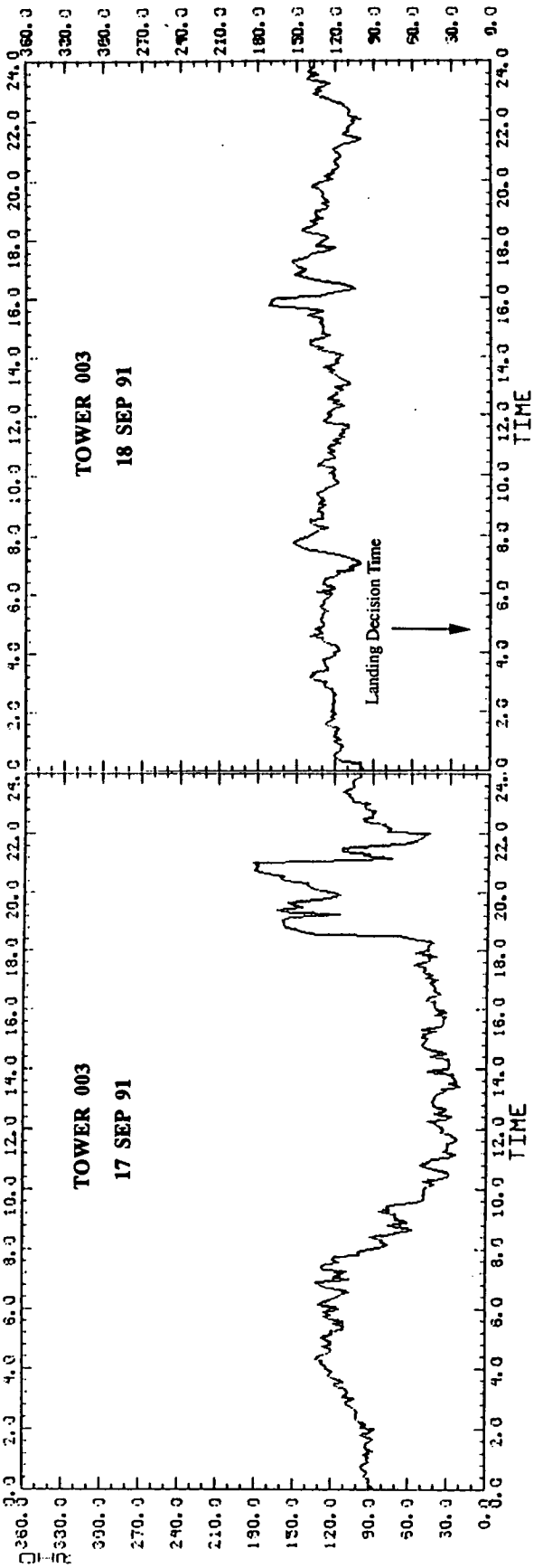

Figure 5a Time series of Wind Direction at the 16.5m (54 ft.) level at Tower 0003 on 17 and 18 September 1991.

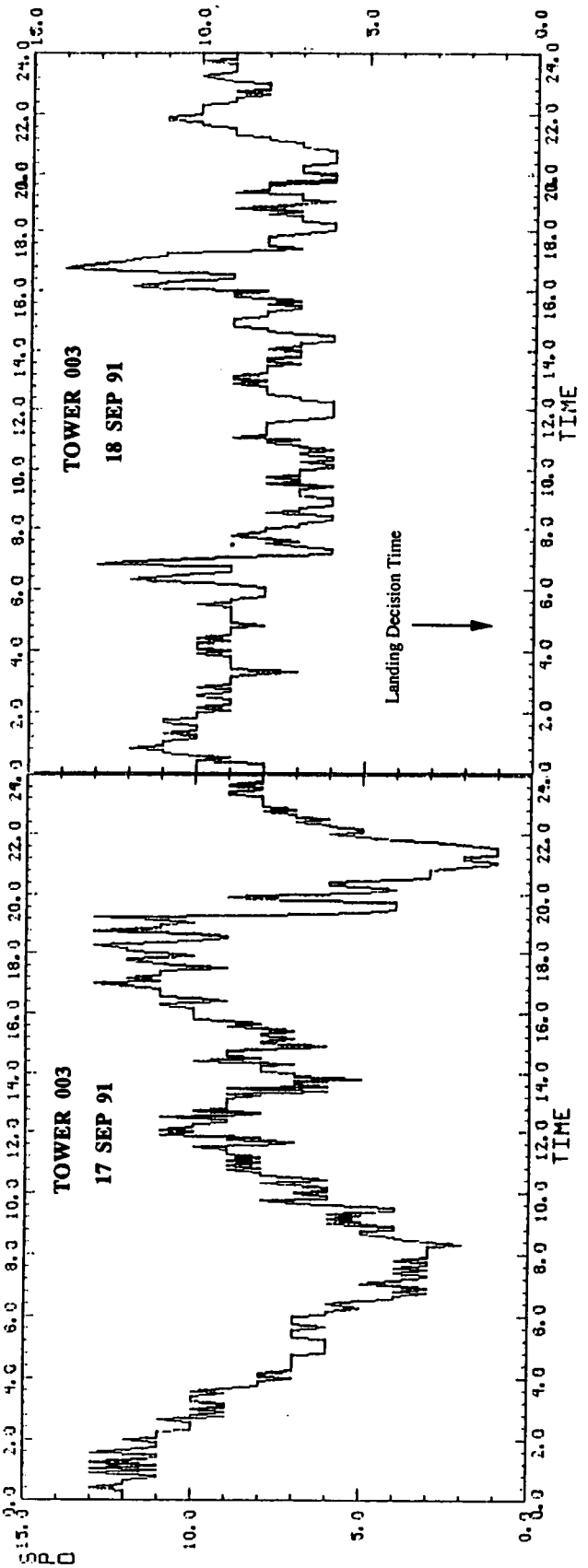

Figure 5b Time series of Wind Speed at the 16.5m (54 ft.) level at Tower 0003 on 17 and 18 September.

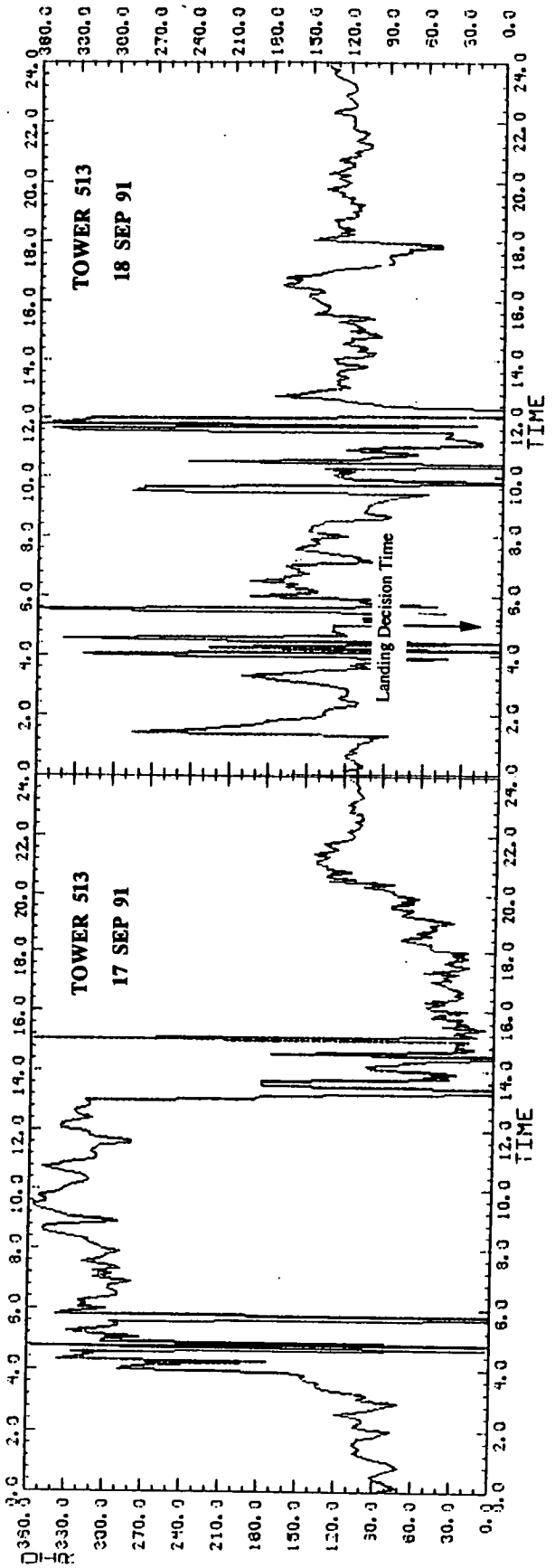

Figure 6a Time series of Wind Direction at the 9.1m (30 ft.) level at Tower 0513 on 17 and 18 September 1991.

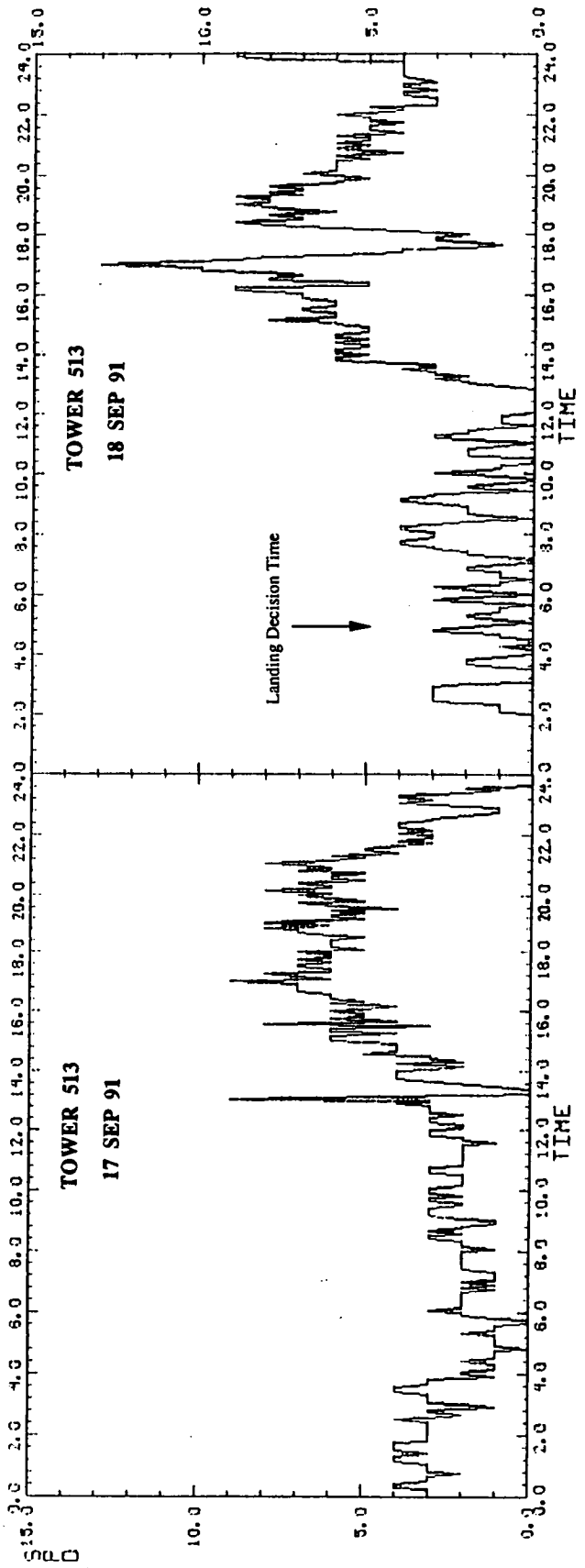

Figure 6b Time series of Wind Speed at the 9.1m (30 ft.) level at Tower 0513 on 17 and 18 September.

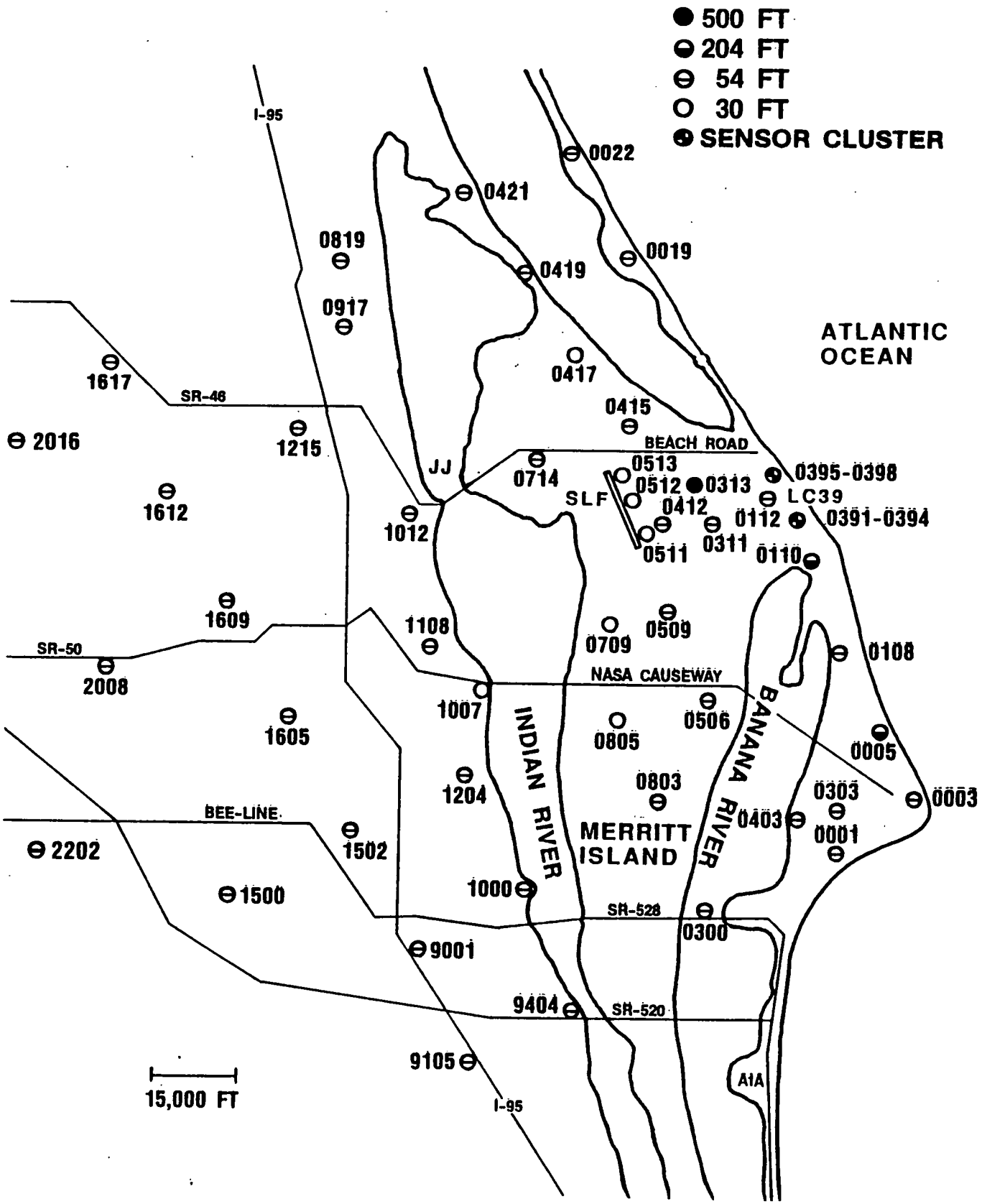

Figure 7 WINDS Towers locations.

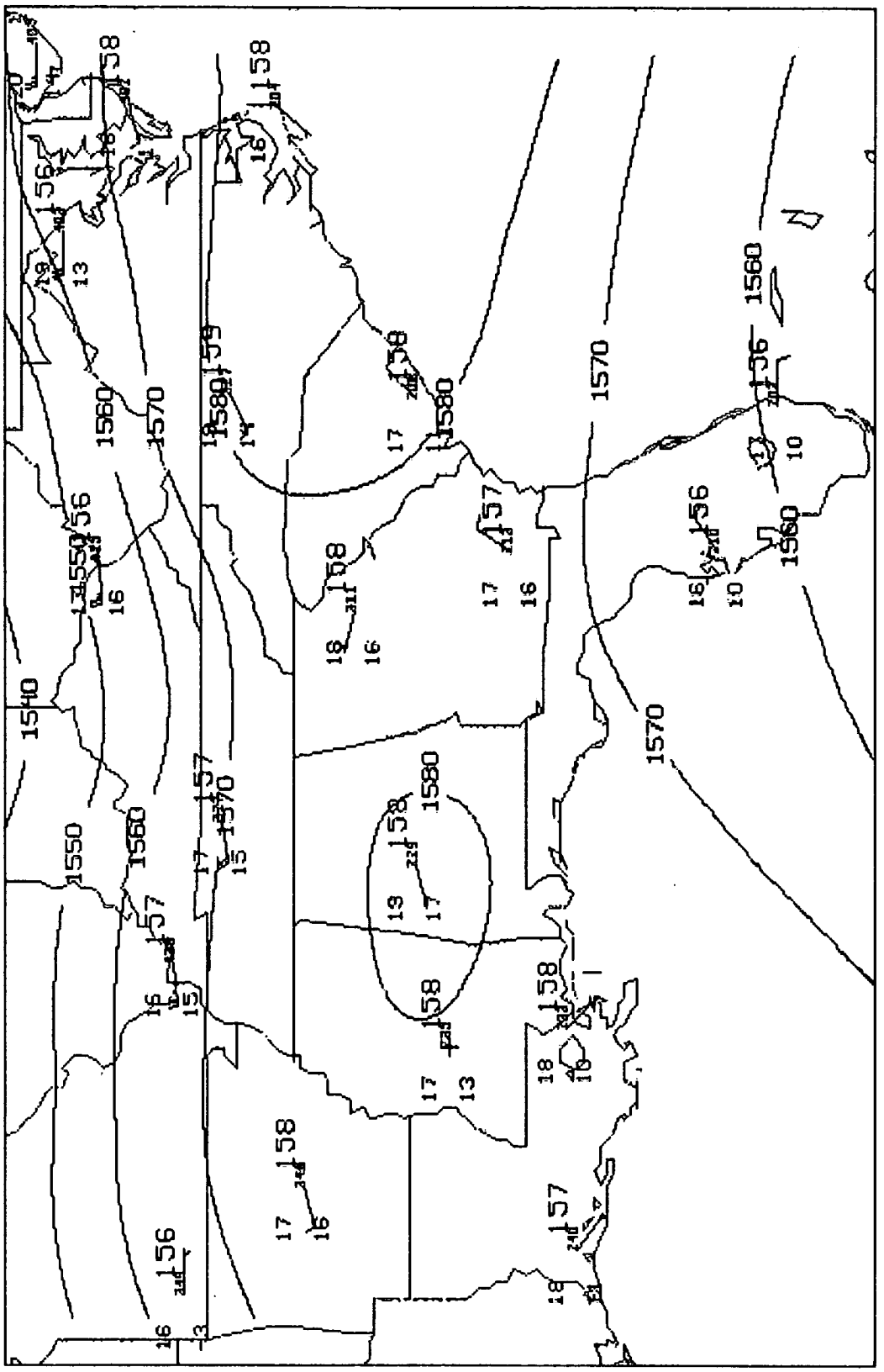

Figure 8a 850 mb Analysis at 1200 UTC on 17 September 1991.

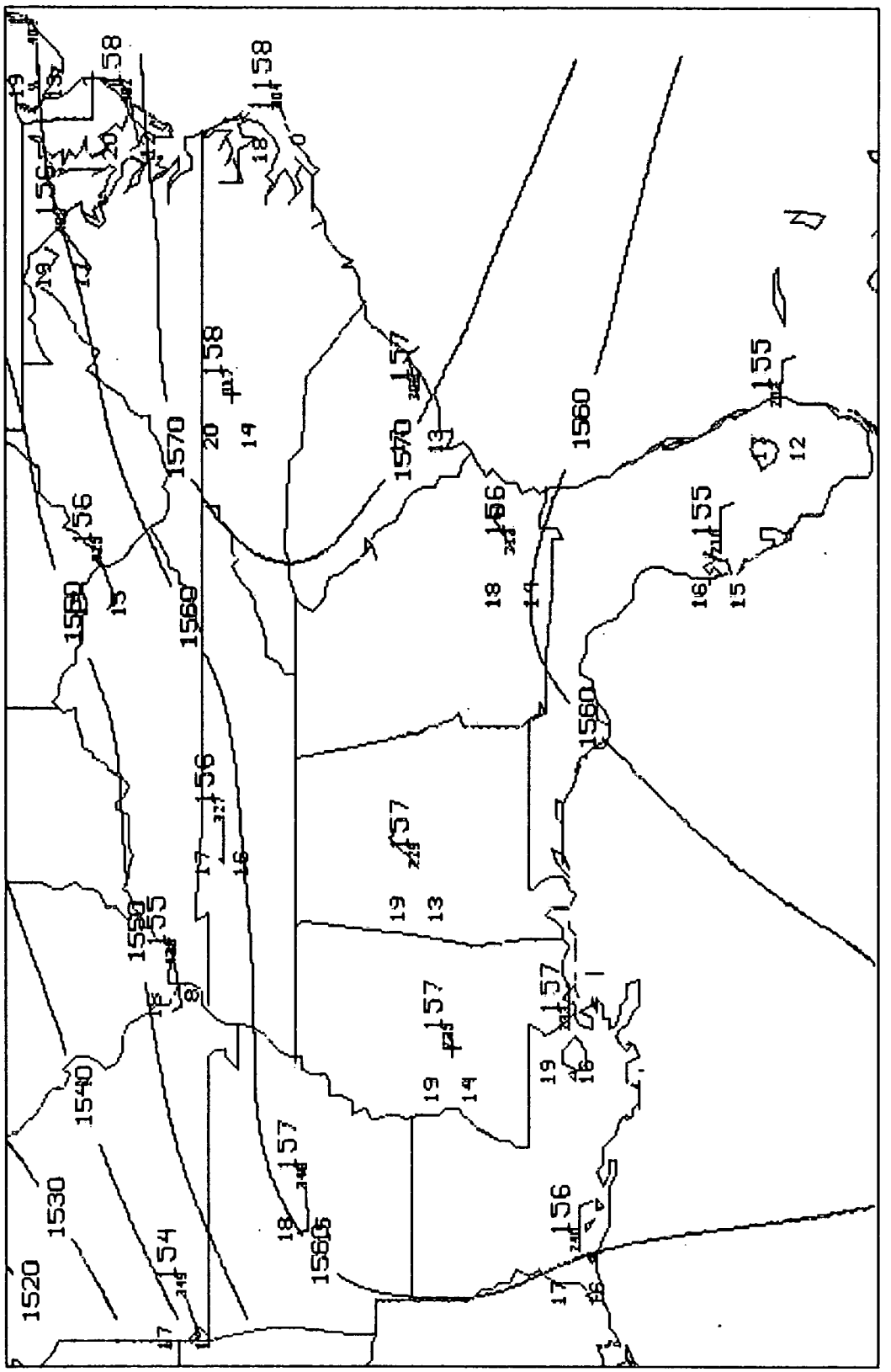

Figure 8b 850 mb Analysis at 0000 UTC on 18 September 1991.

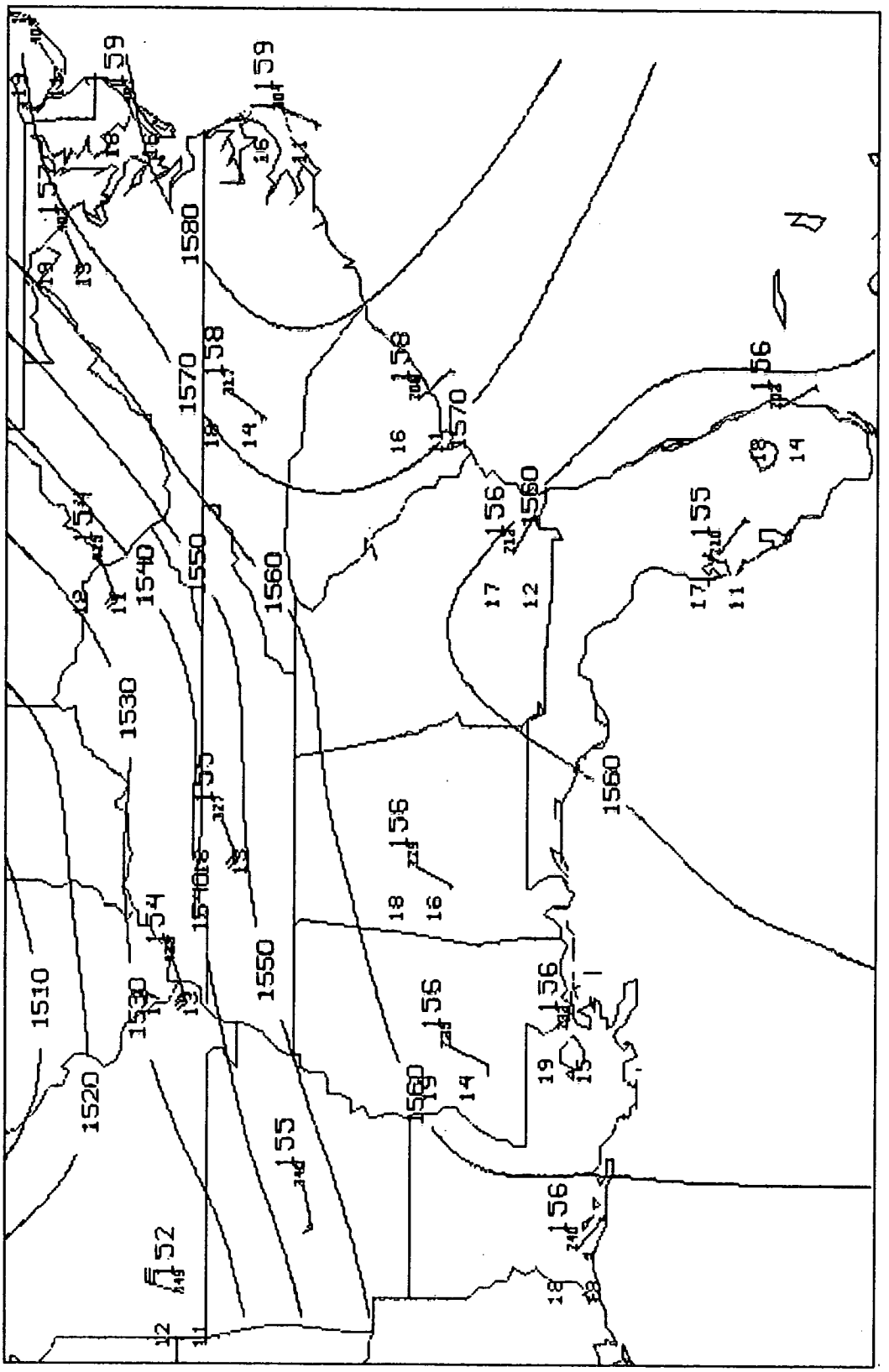

Figure 8c 850 mb Analysis at 1200 UTC on 18 September 1991.

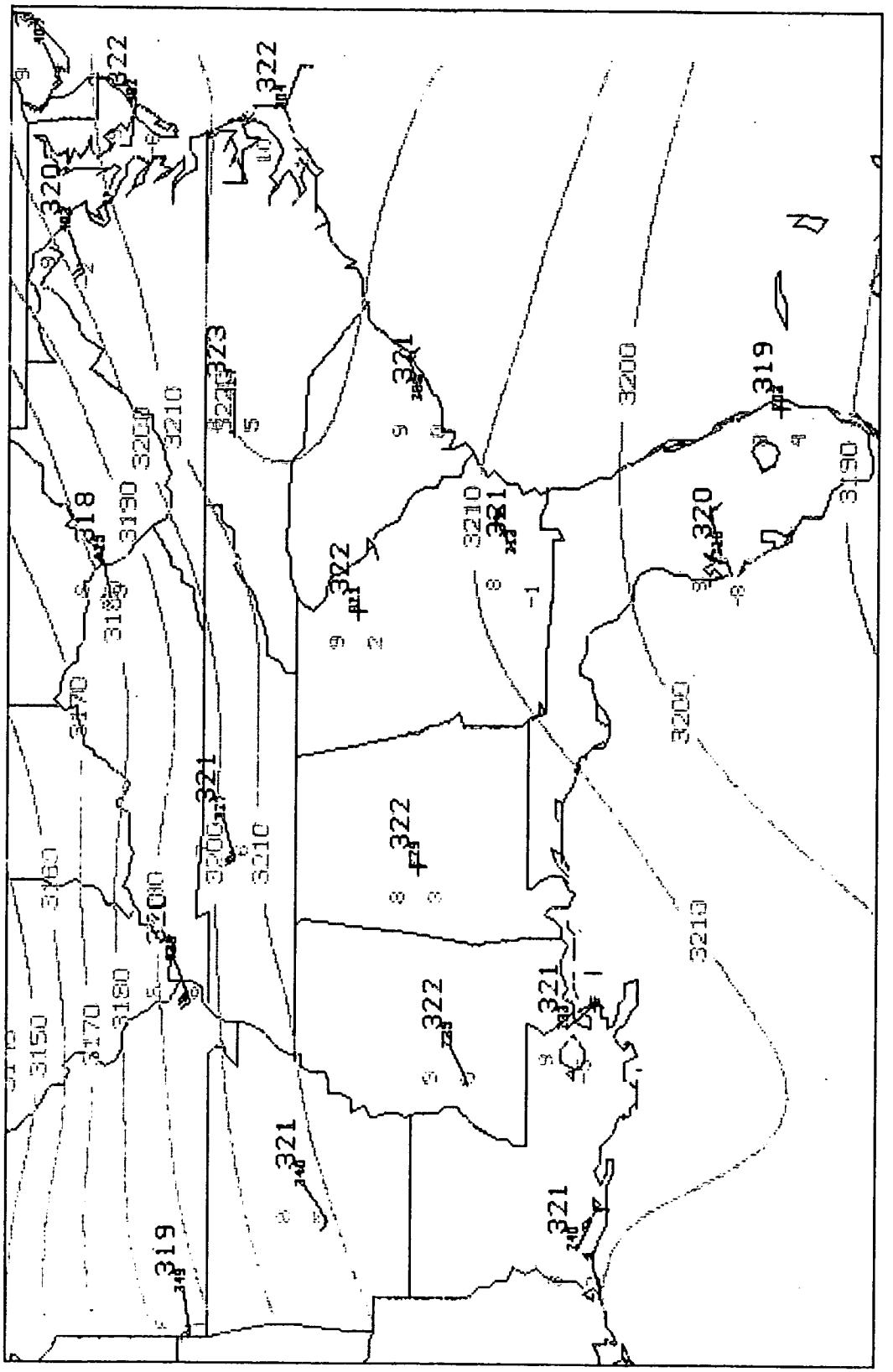

Figure 9a 700 mb Analysis at 1200 UTC on 17 September 1991.

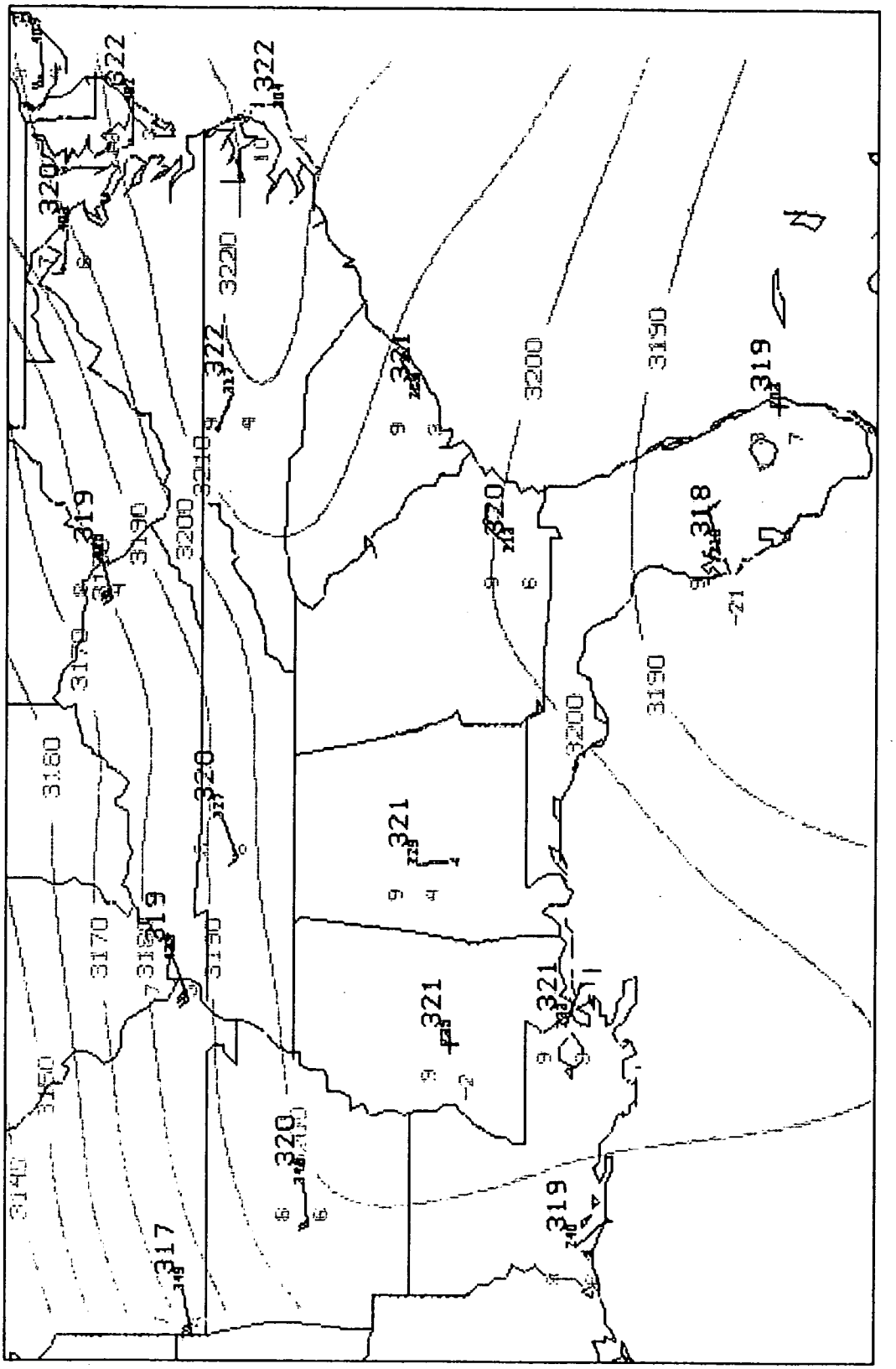

Figure 9b 700 mb Analysis at 0000 UTC on 18 September 1991.

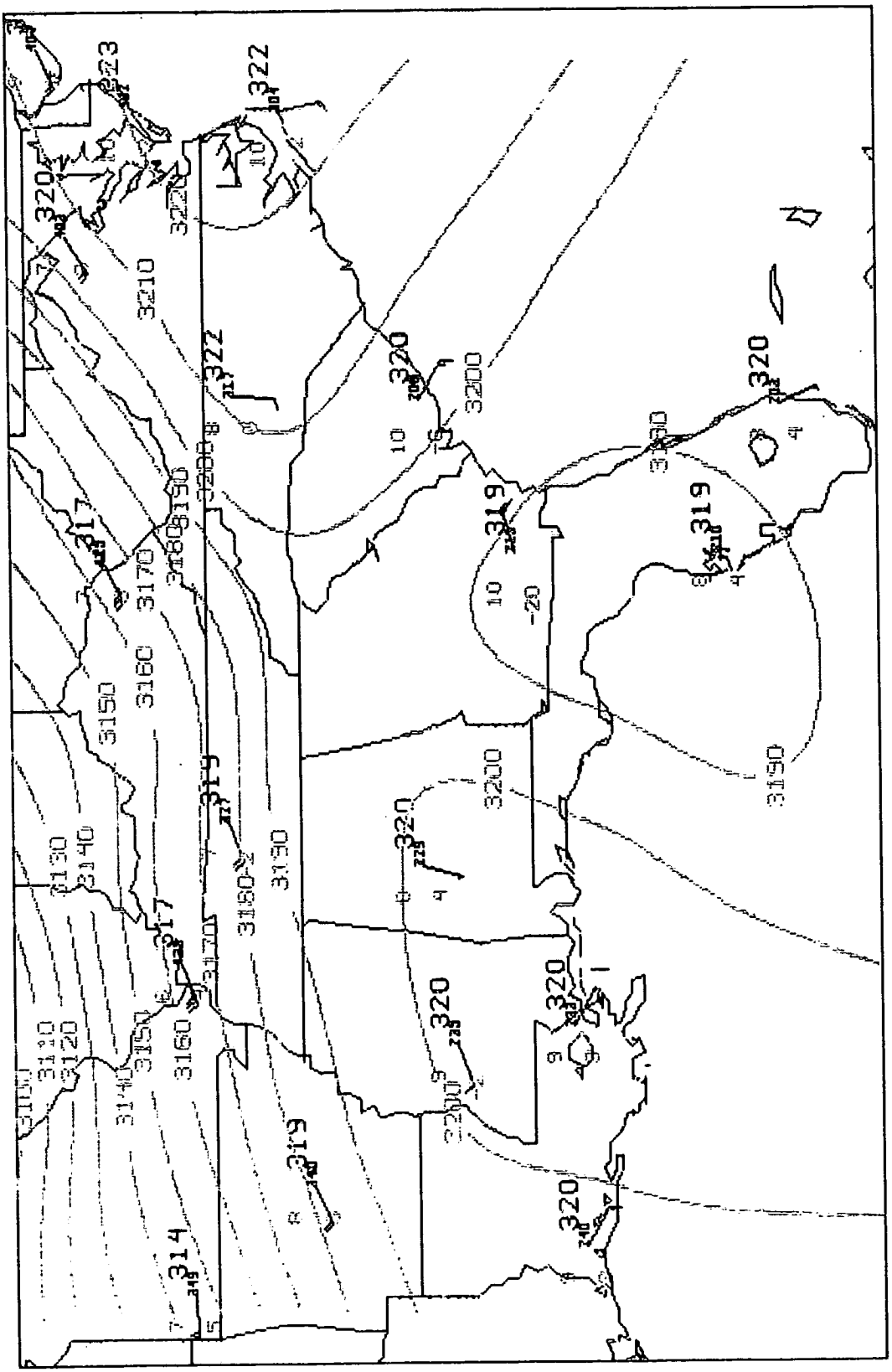

Figure 9c 700 mb Analysis at 1200 UTC on 18 September 1991.

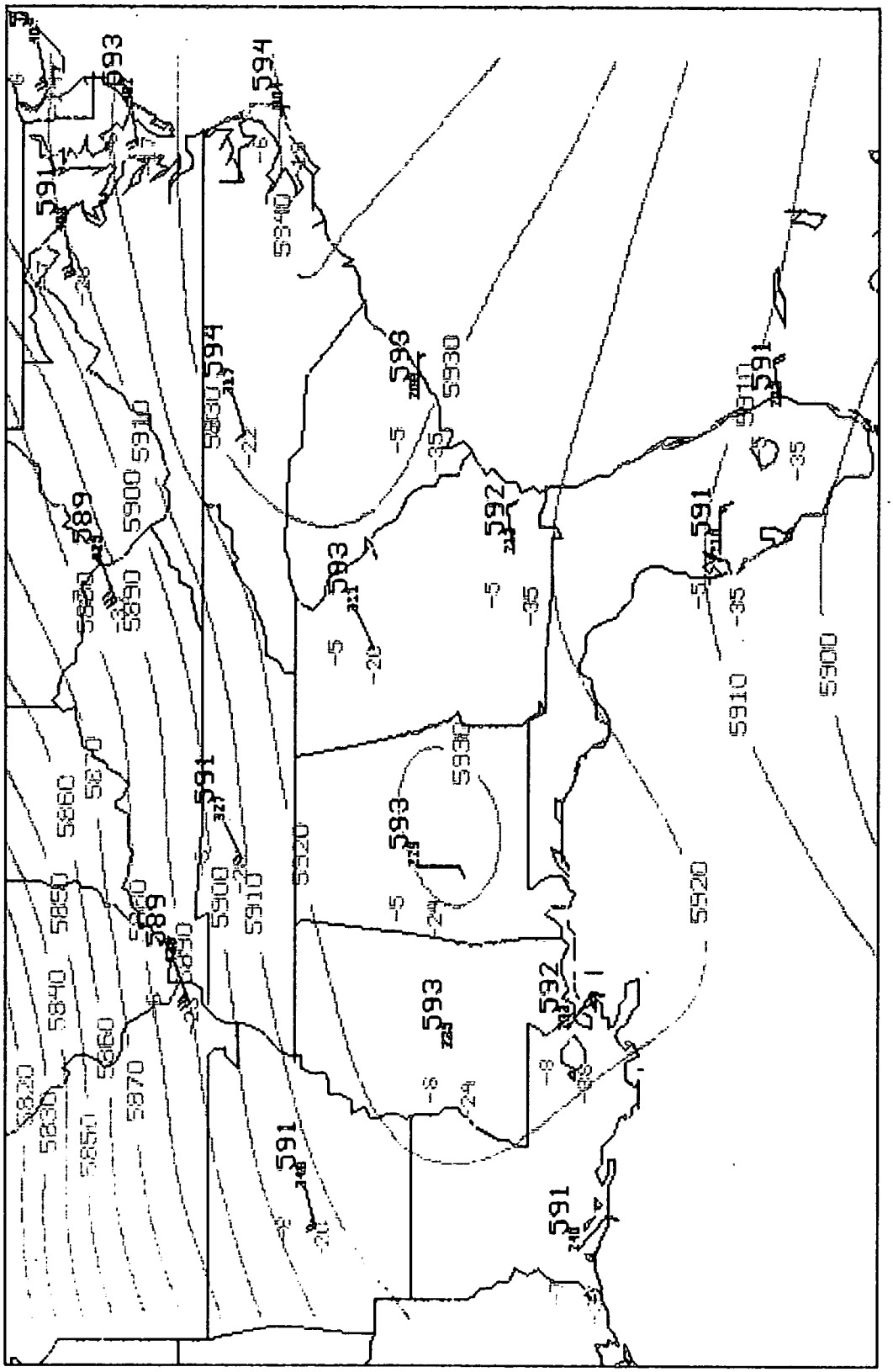

Figure 10a 500 mb Analysis at 1200 UTC on 17 September 1991.

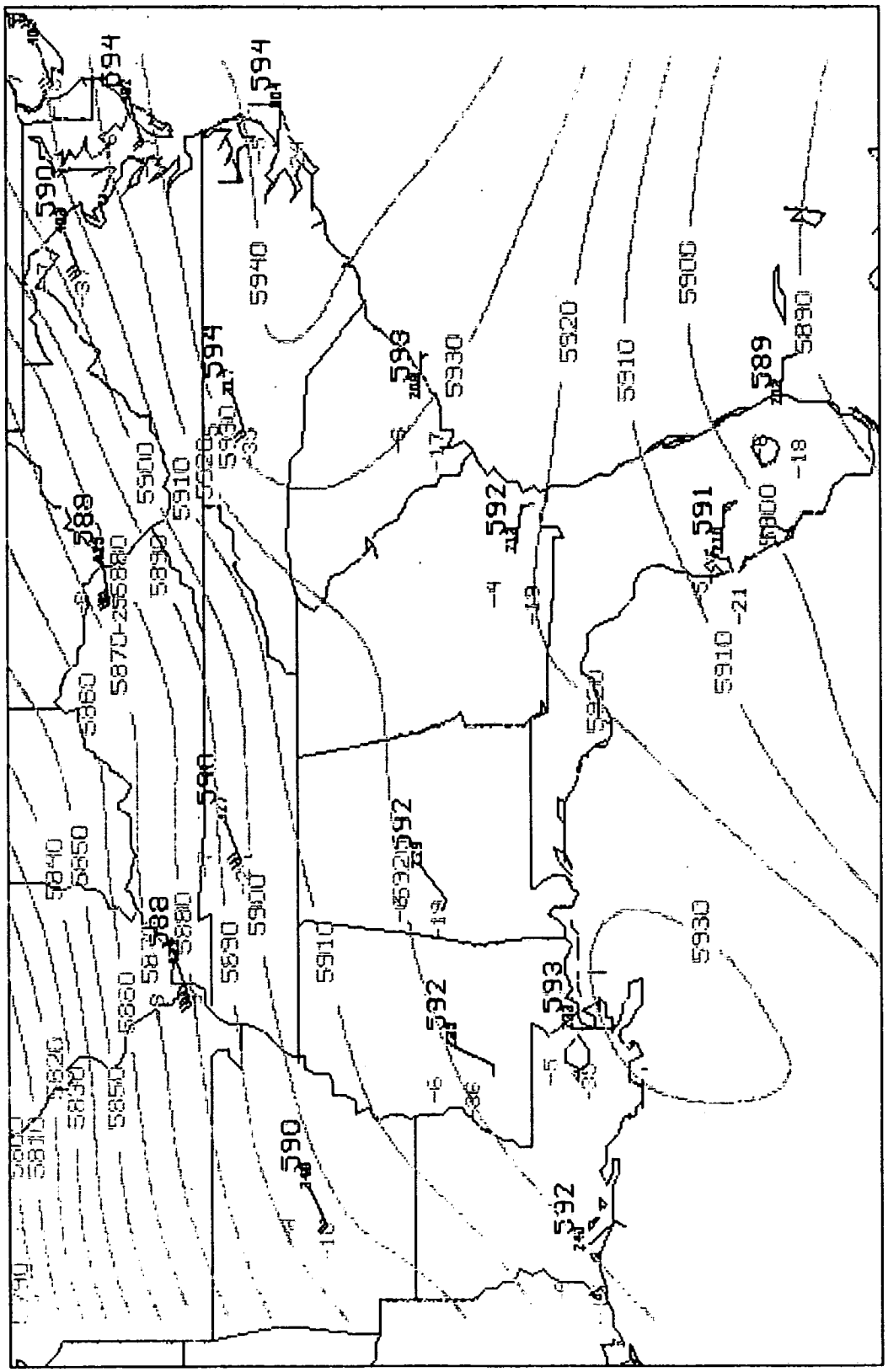

Figure 10b 500 mb Analysis at 0000 UTC on 18 September 1991.

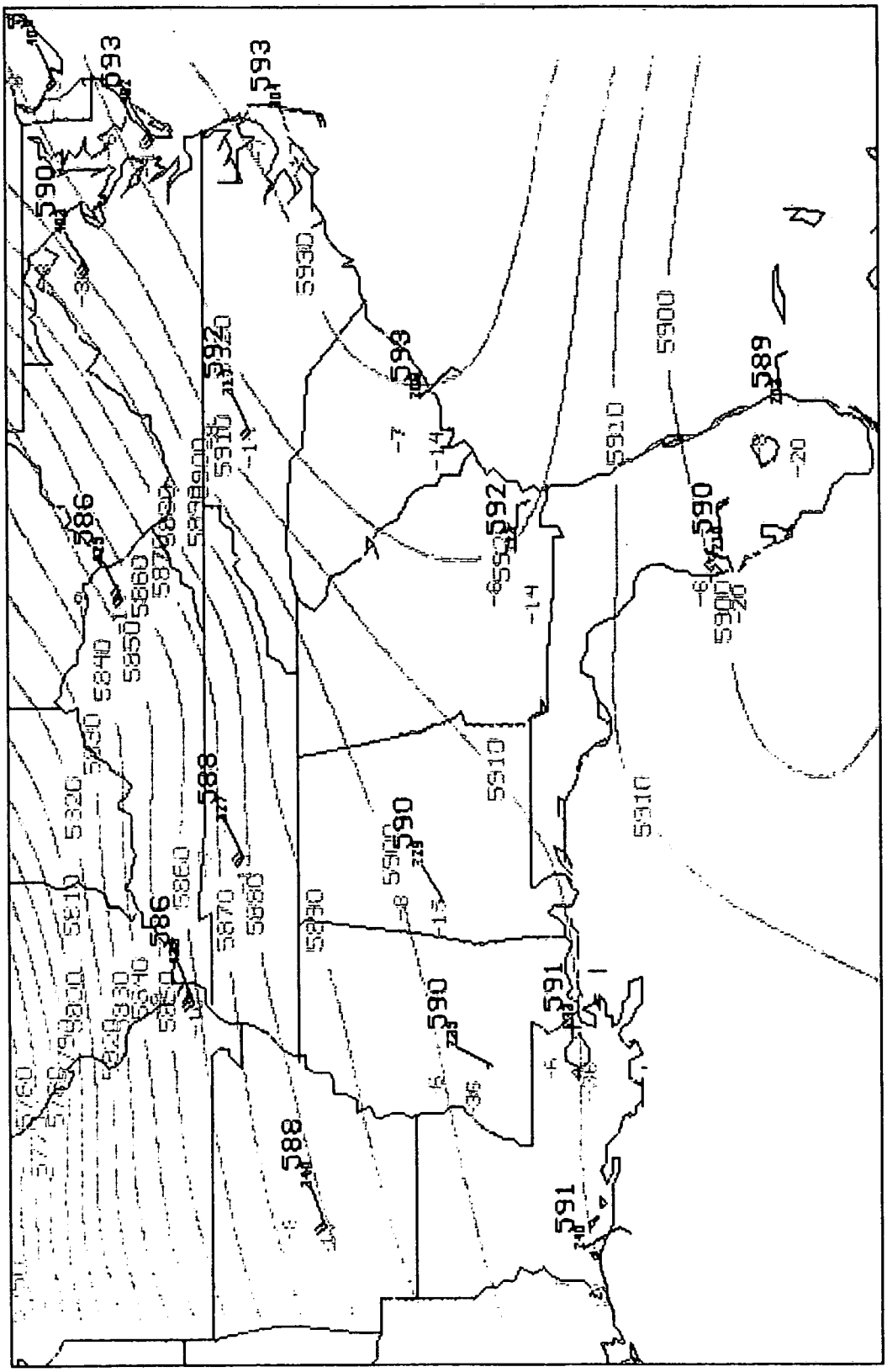

Figure 10c 500 mb Analysis at 1200 UTC on 18 September 1991.

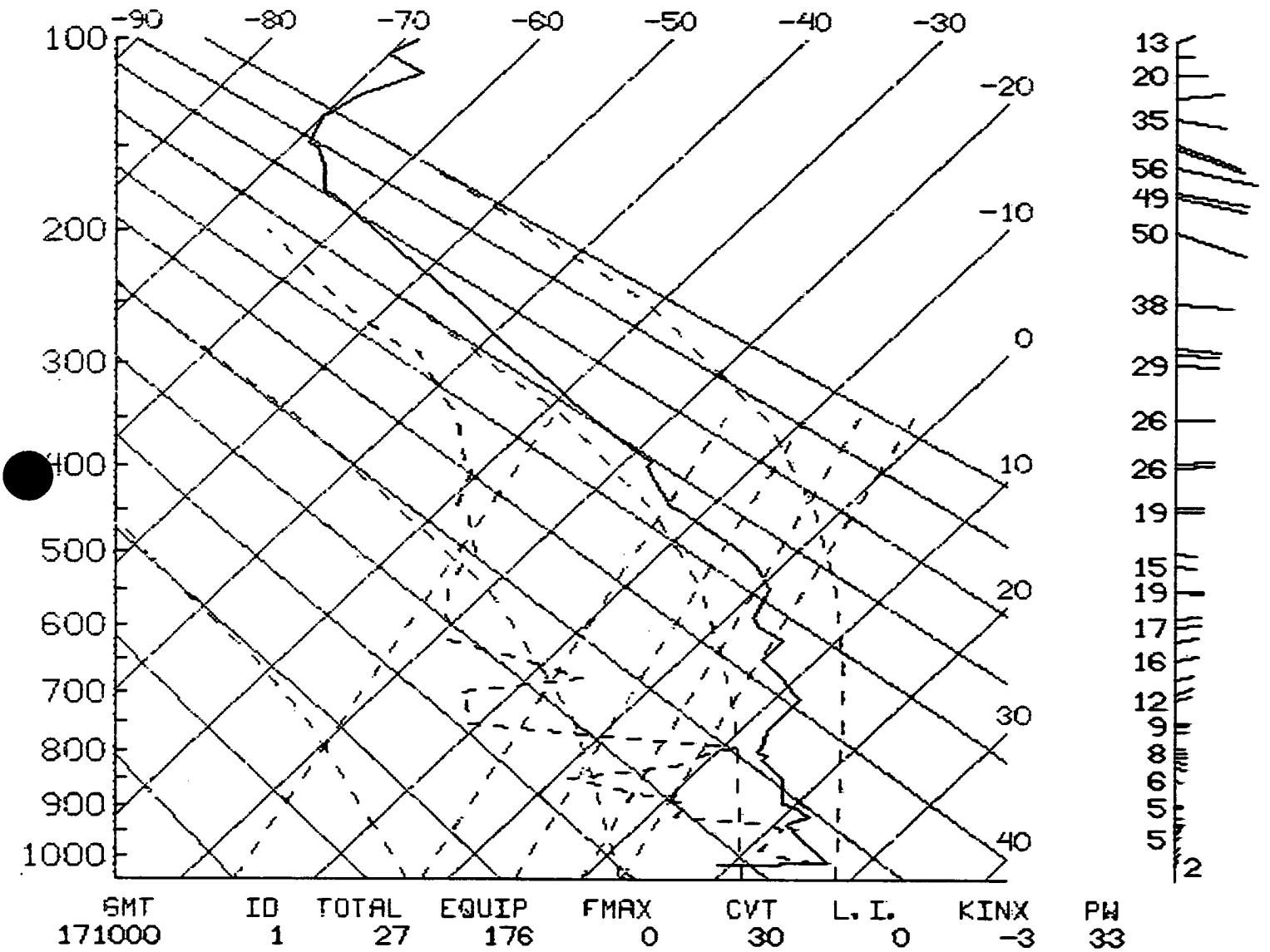

Figure 11 CCAFS Rawinsonde at 1000 UTC 17 September 1991.

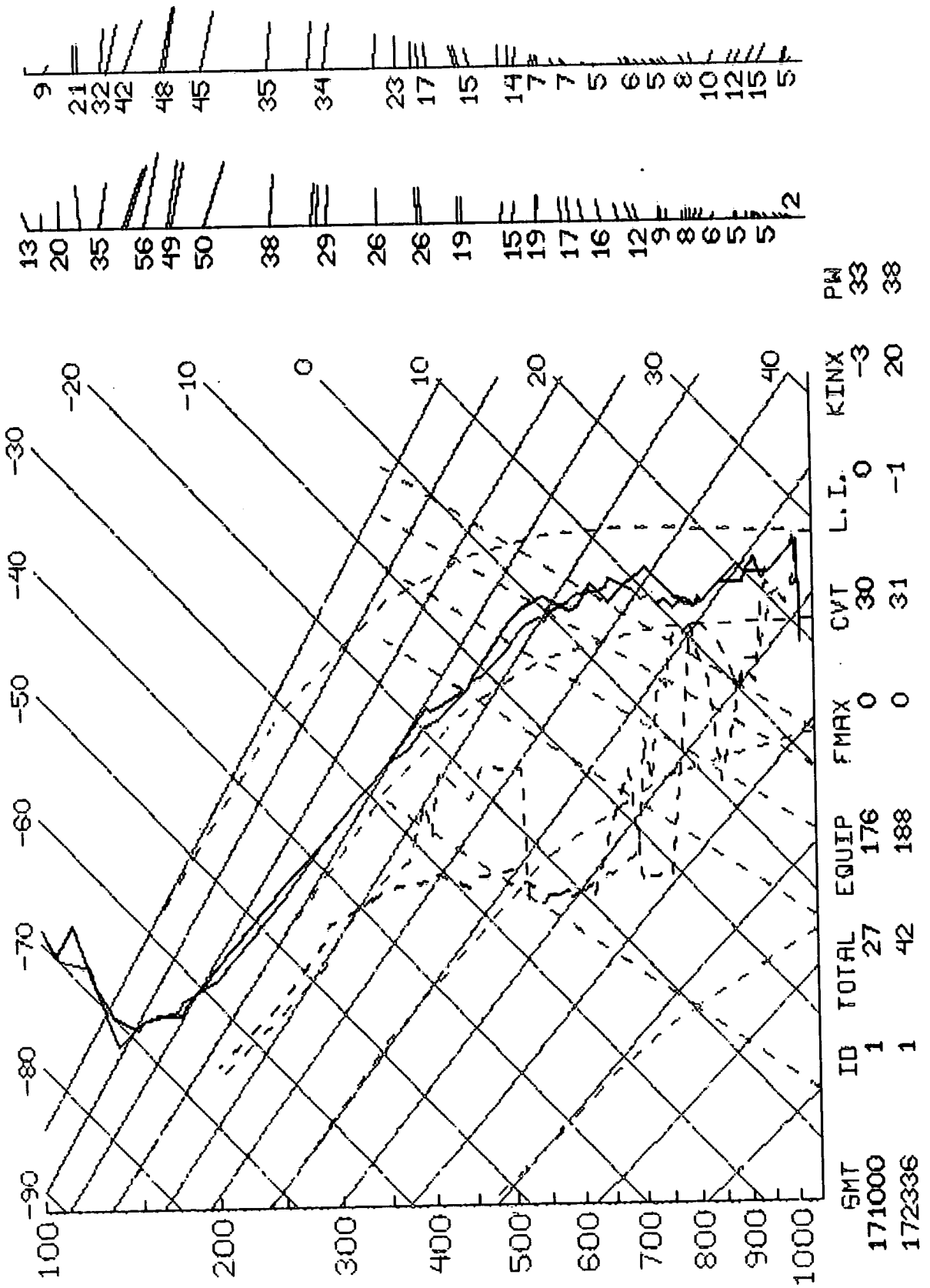

Figure 12 CCAFS Rawinsonde at 1000 UTC and 2336 UTC on 17 September 1991.

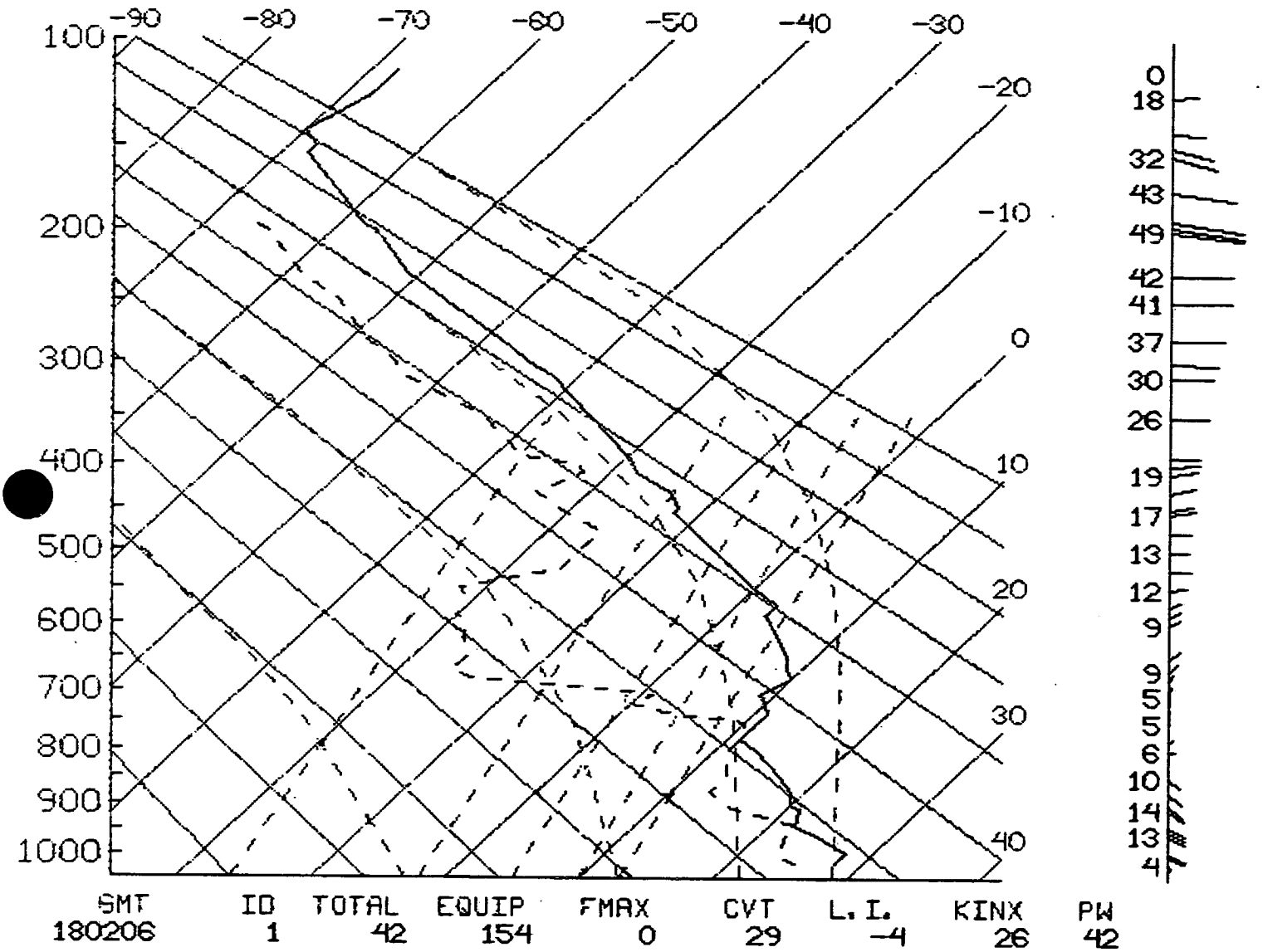

Figure 13 CCAFS Rawinsonde at 0206 UTC on 18 September 1991.

ORIGINAL PAGE
COLOR PHOTOGRAPH

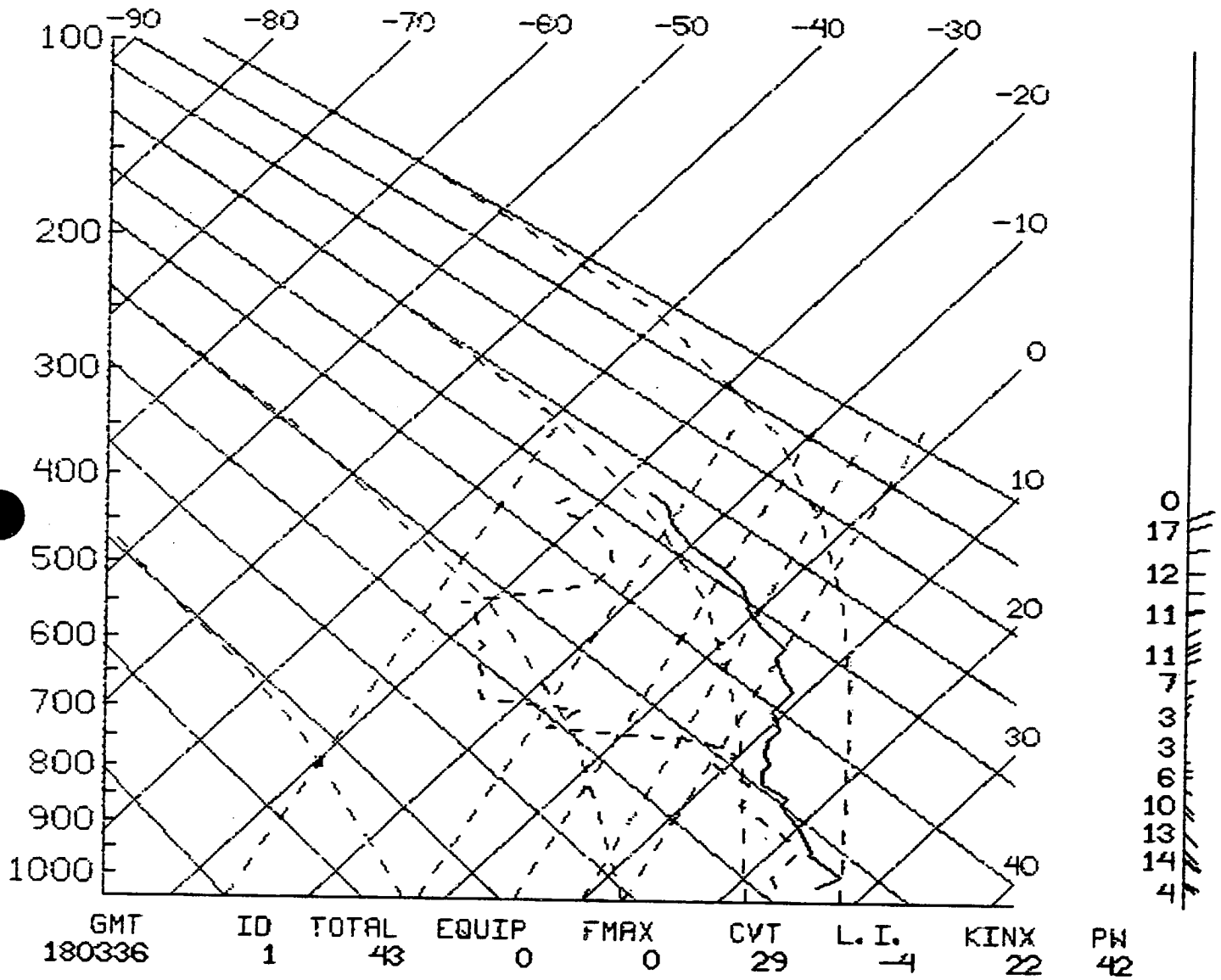

Figure 14 CCAFS Rawinsonde at 0336 UTC on 18 September 1991.

ORIGINAL PAGE
COLOR PHOTOGRAPH

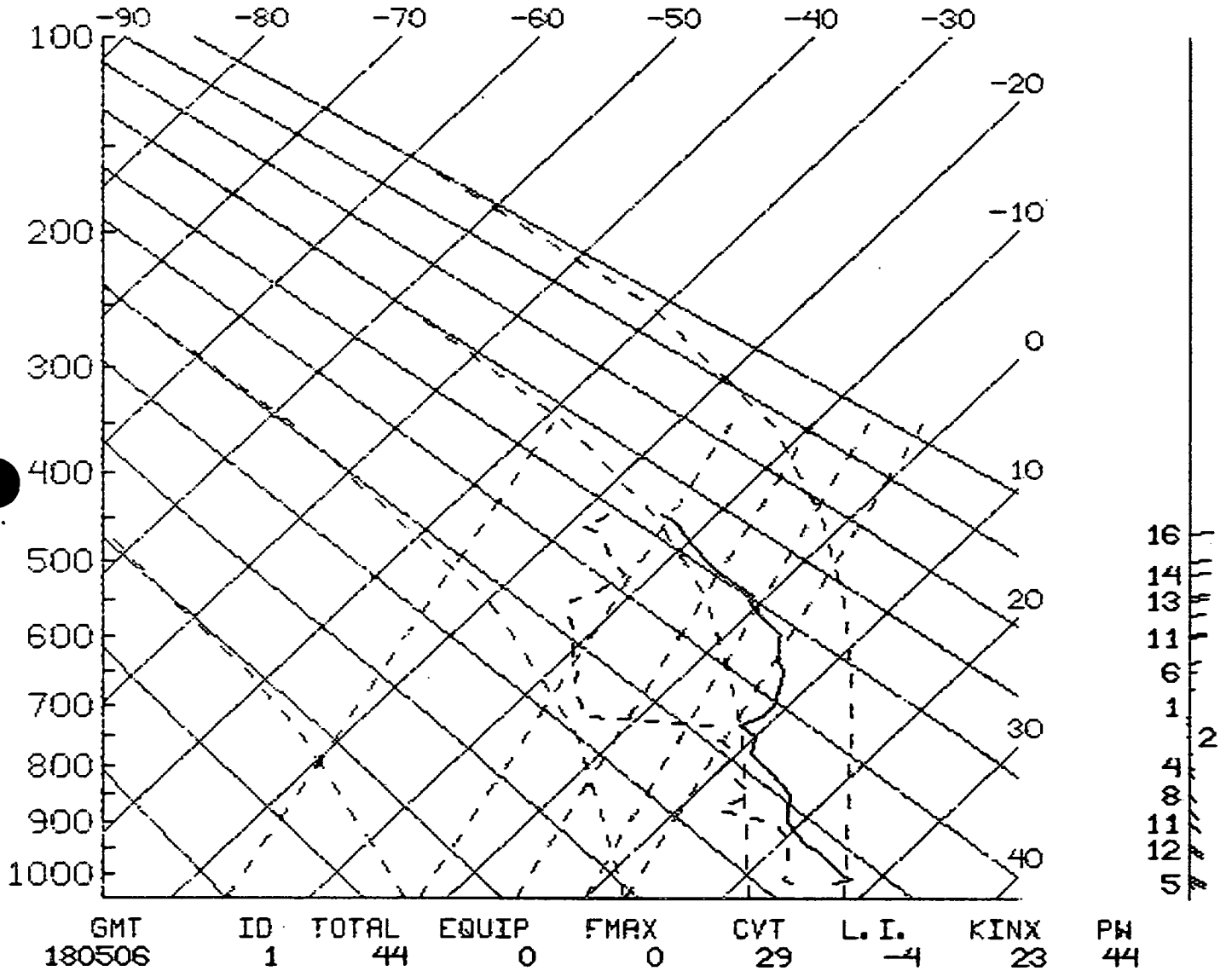

Figure 15 CCAFS Rawinsonde at 0506 UTC on 18 September 1991

ORIGINAL PAGE
COLOR PHOTOGRAPH

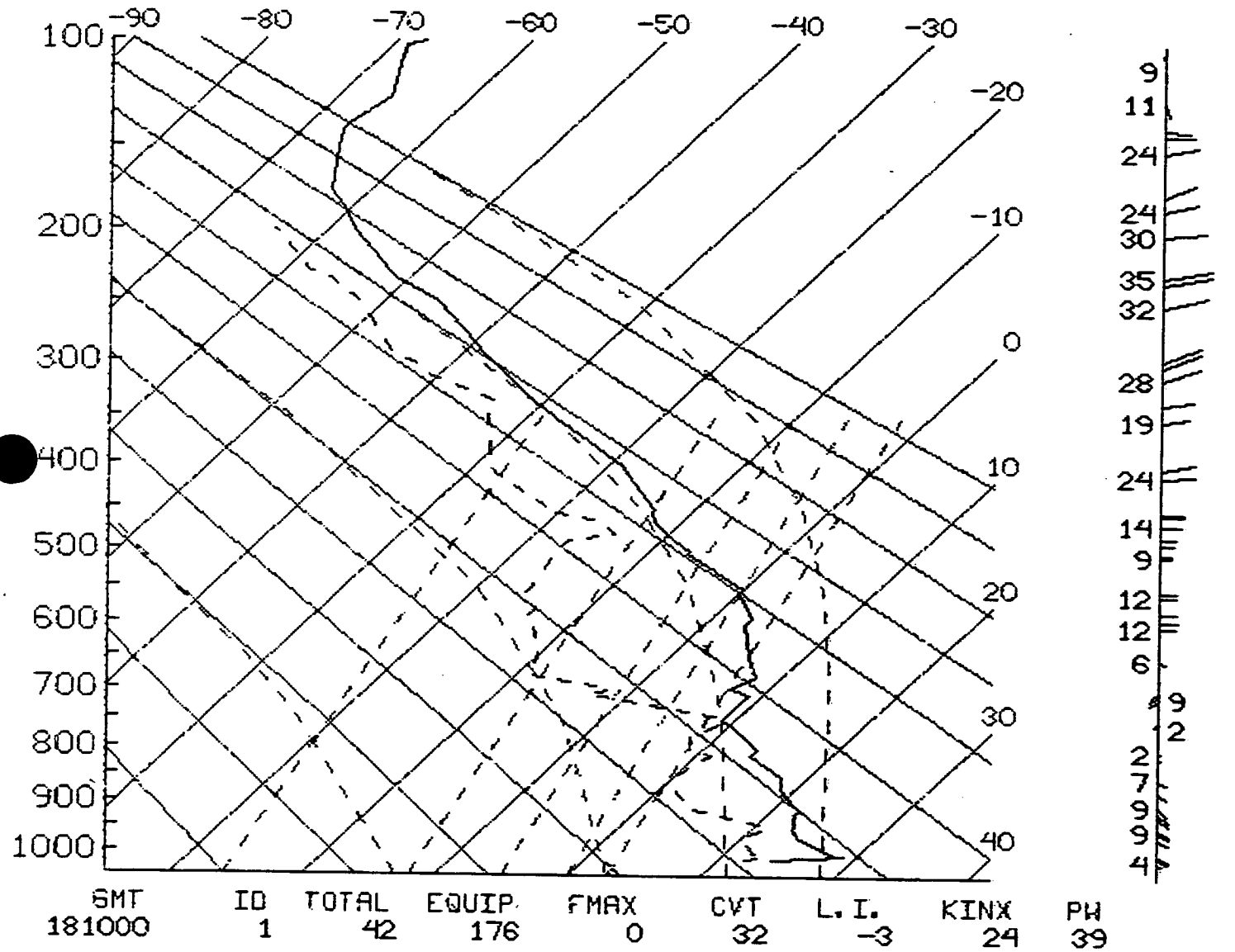

Figure 16 CCAFS Rawinsonde at 1000 UTC on 18 September 1991.

ORIGINAL PAGE
COLOR PHOTOGRAPH

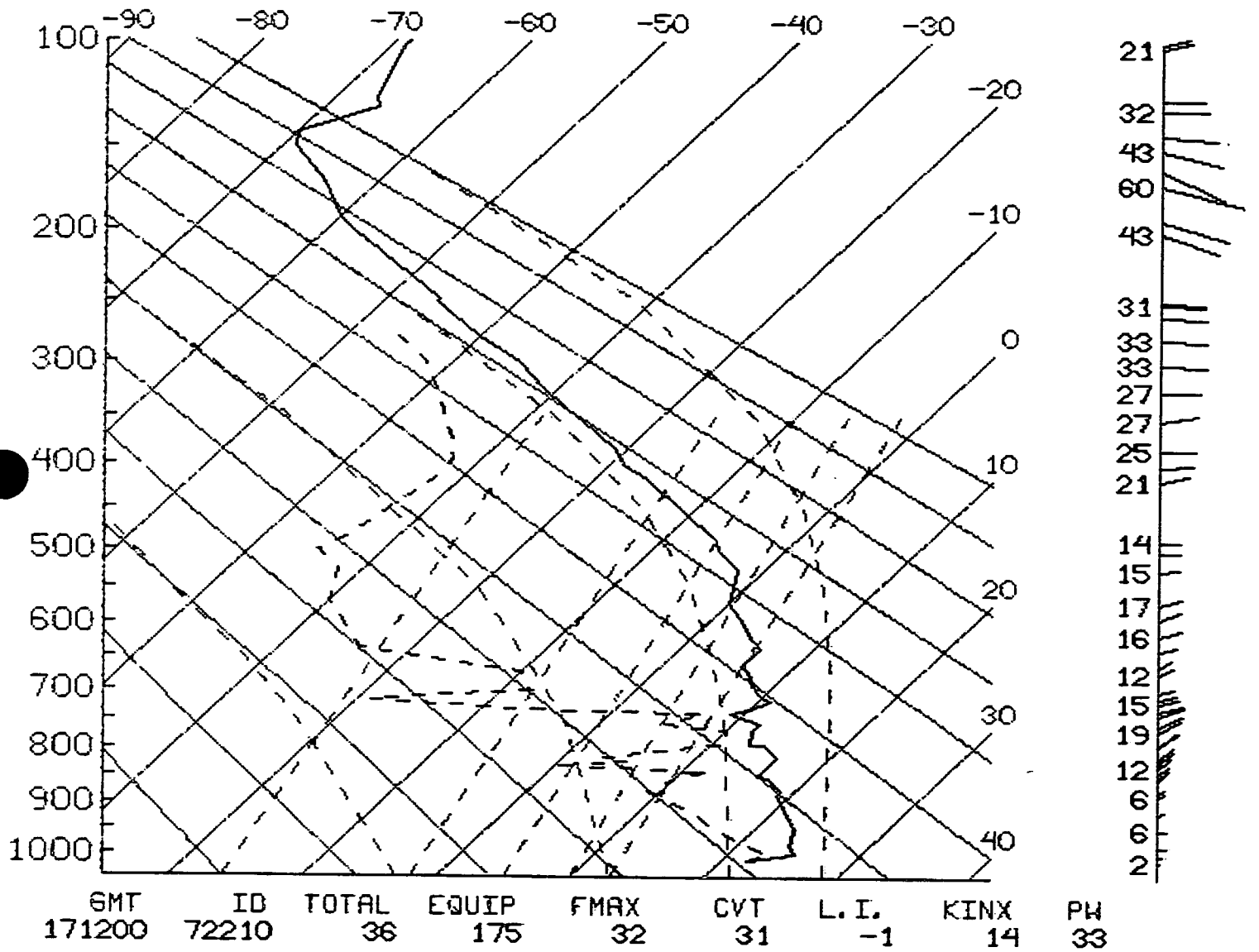

Figure 17 Tampa Rawinsonde at 1200 UTC on 17 September 1991

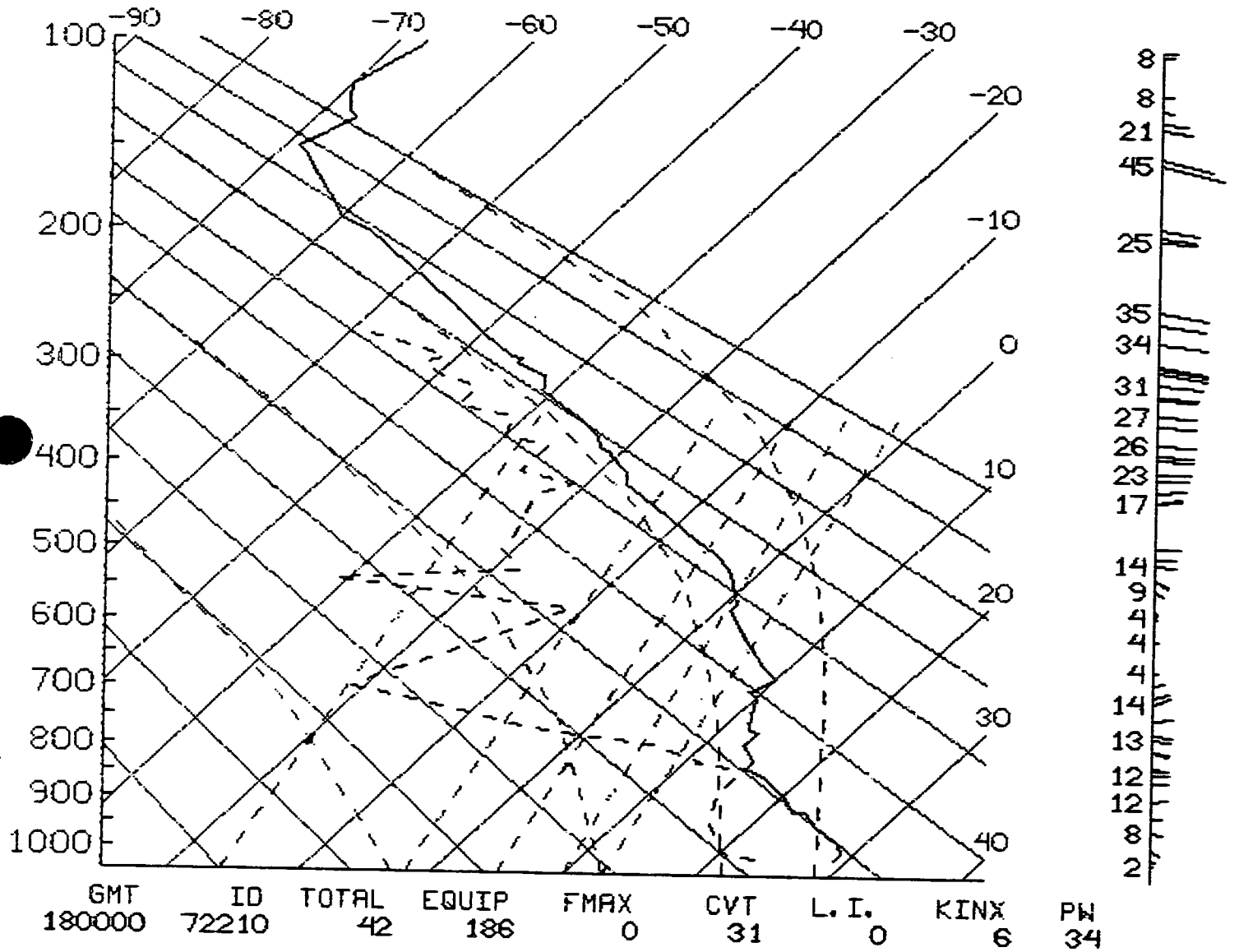

Figure 18 Tampa Rawinsonde at 0000 UTC on 18 September 1991.

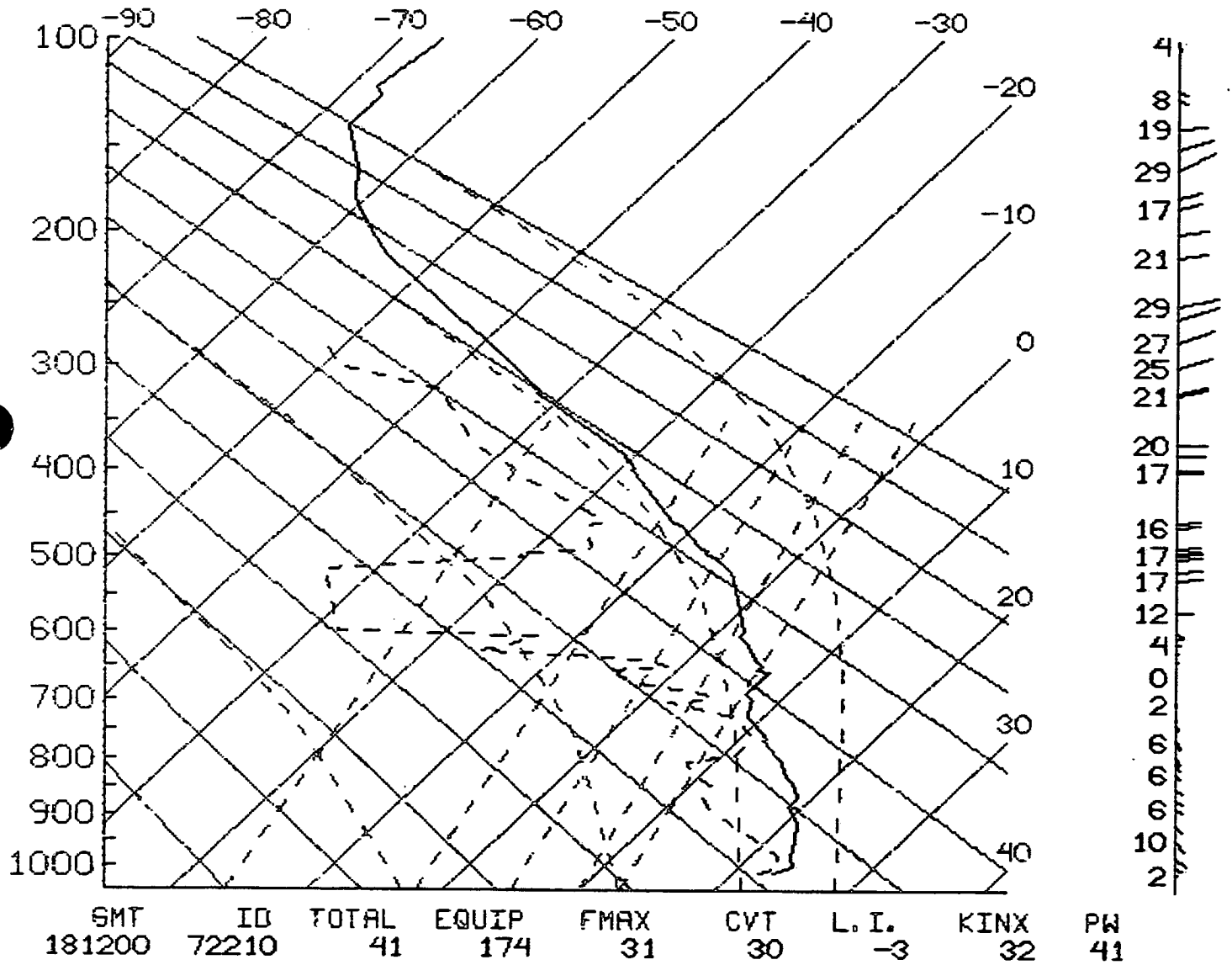

Figure 19 Tampa Rawinsonde at 1200 UTC on 18 September 1991.

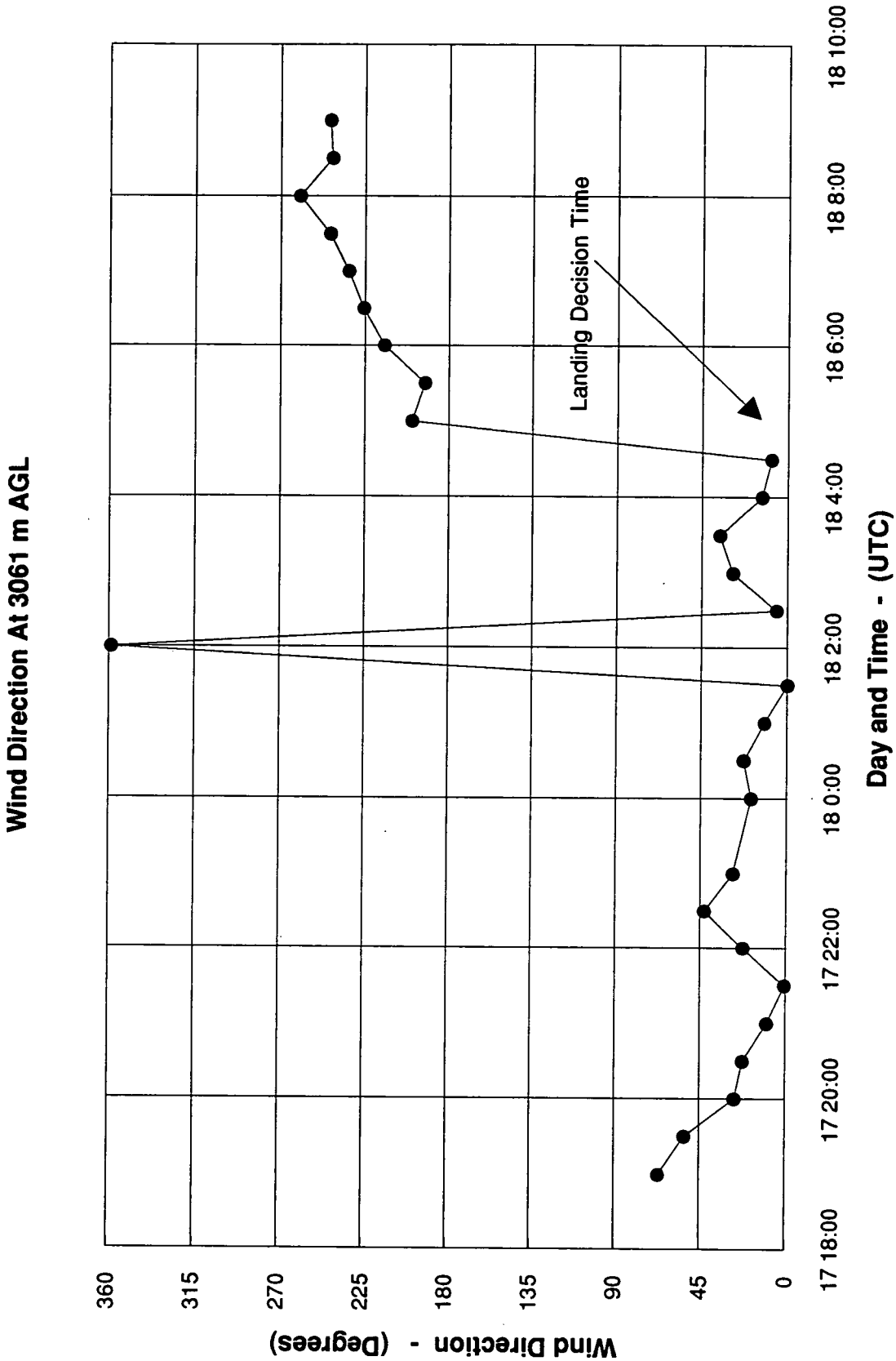

Figure 20 Time series of wind direction from the SLF Wind Profiler 1800 UTC 17 September to 1000 UTC 18 September 1991 at the 3061m (10040 ft.) level.

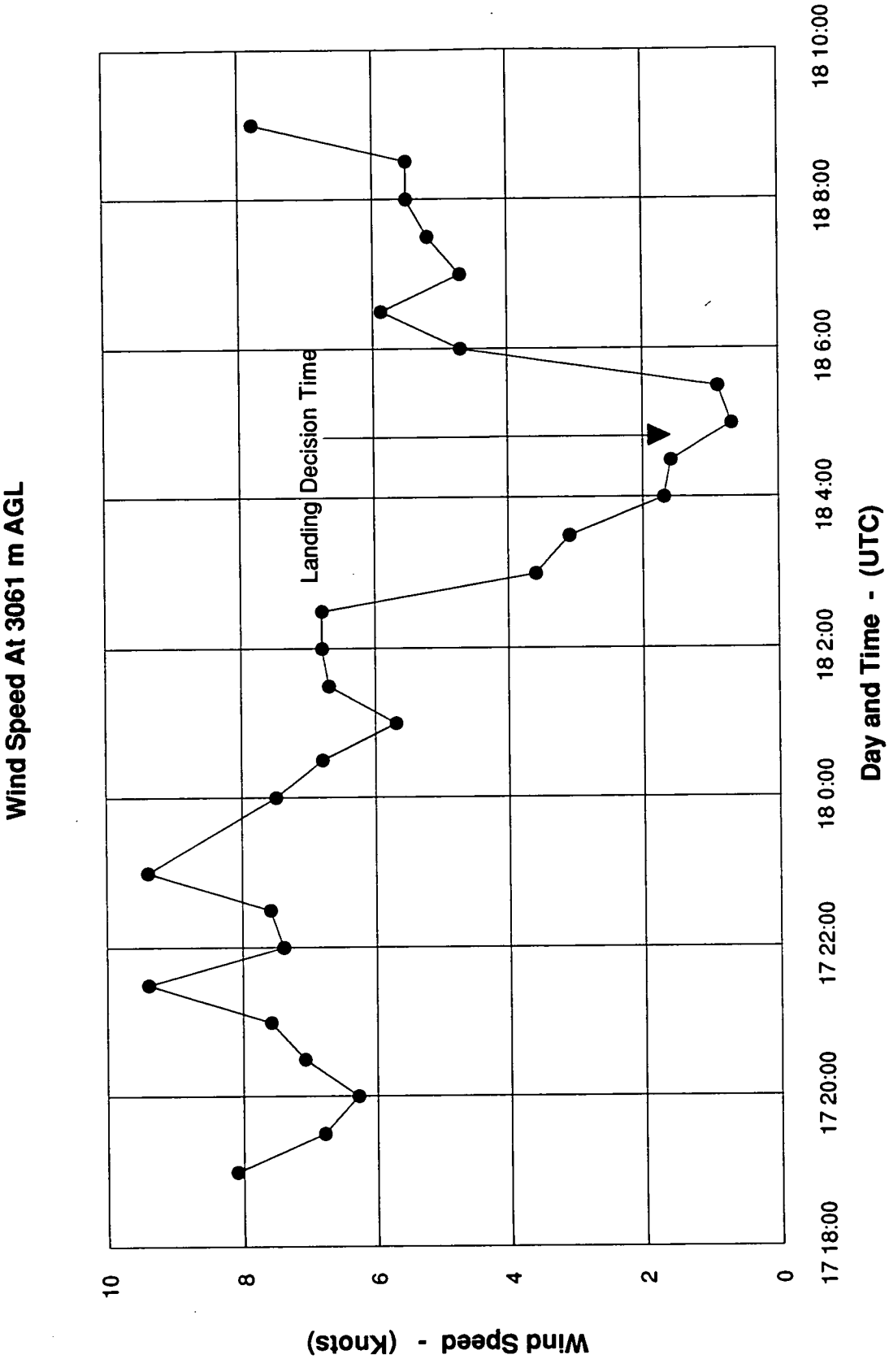

Figure 21 Time series of wind speed from the SLF Wind Profiler 1800 UTC 17 September to 1000 UTC 18 September 1991 at the 3061m (10040 ft.) level.

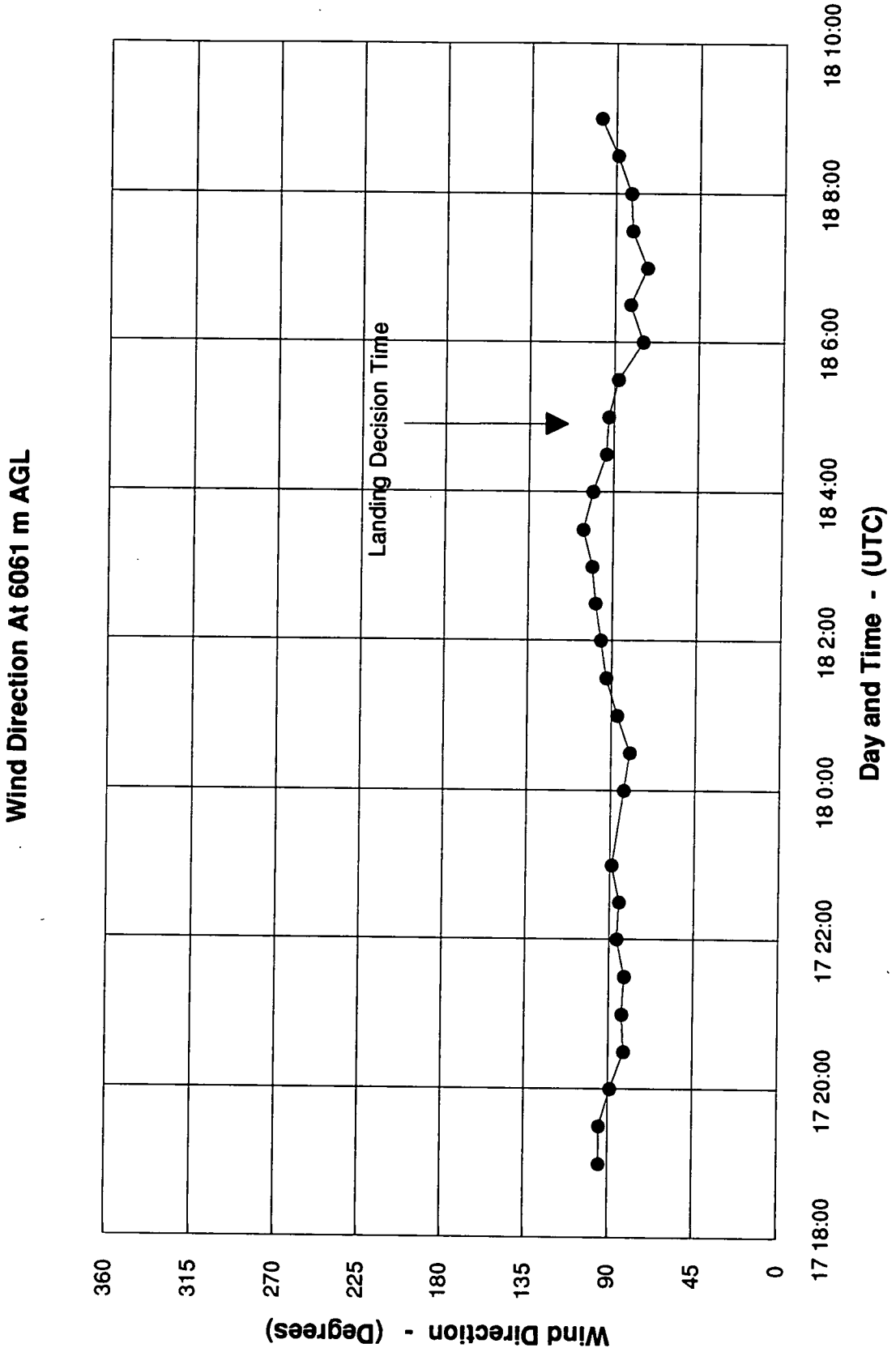

Figure 22 Time series of wind direction from the SLF Wind Profiler 1800 UTC 17 September to 1000 UTC 18 September 1991 at the 6061m (19880 ft.) level.

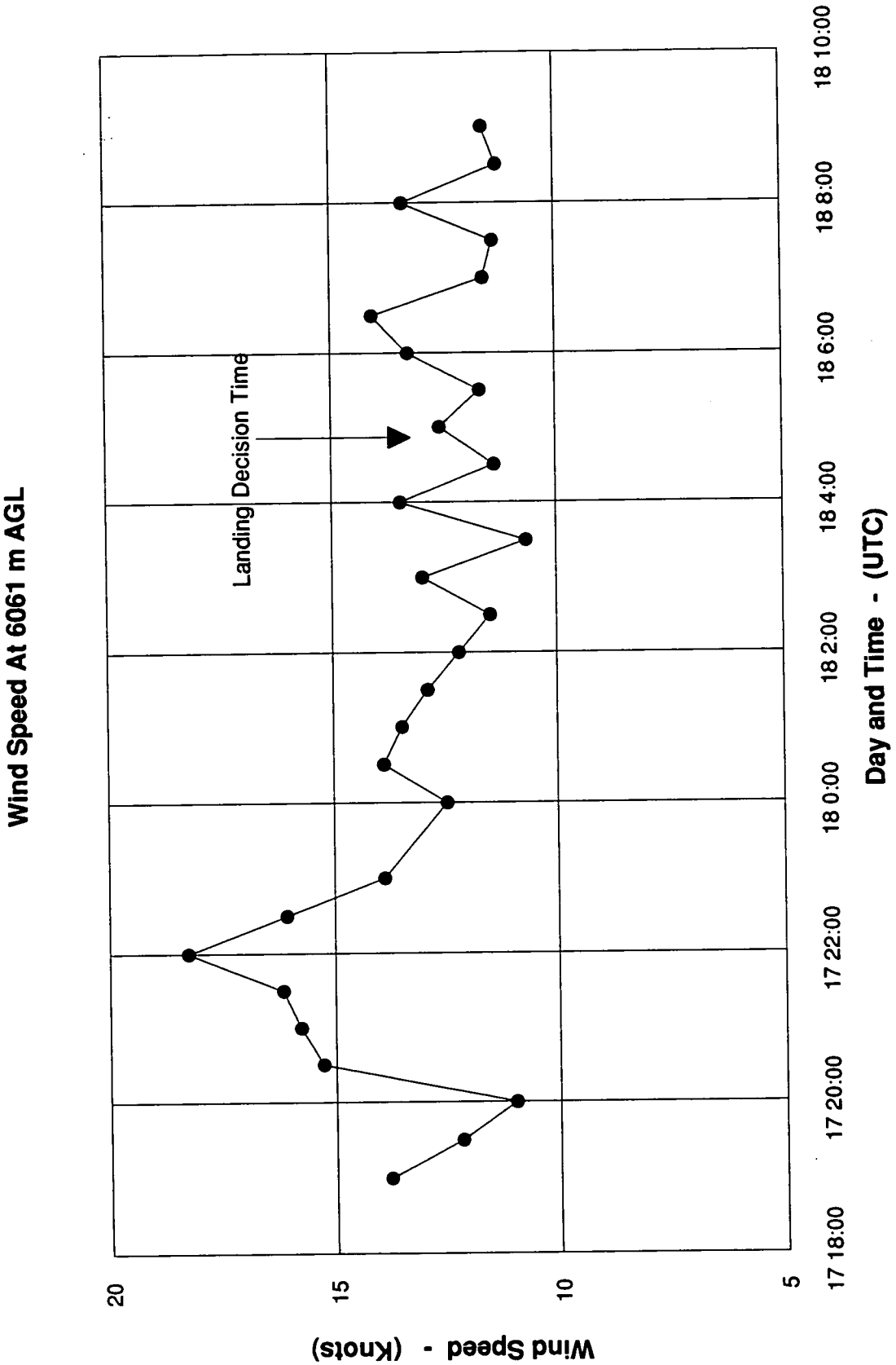

Figure 23 Time series of wind speed from the SLF Wind Profiler 1800 UTC 17 September to 1000 UTC 18 September 1991 at the 6061m (19880 ft.) level.

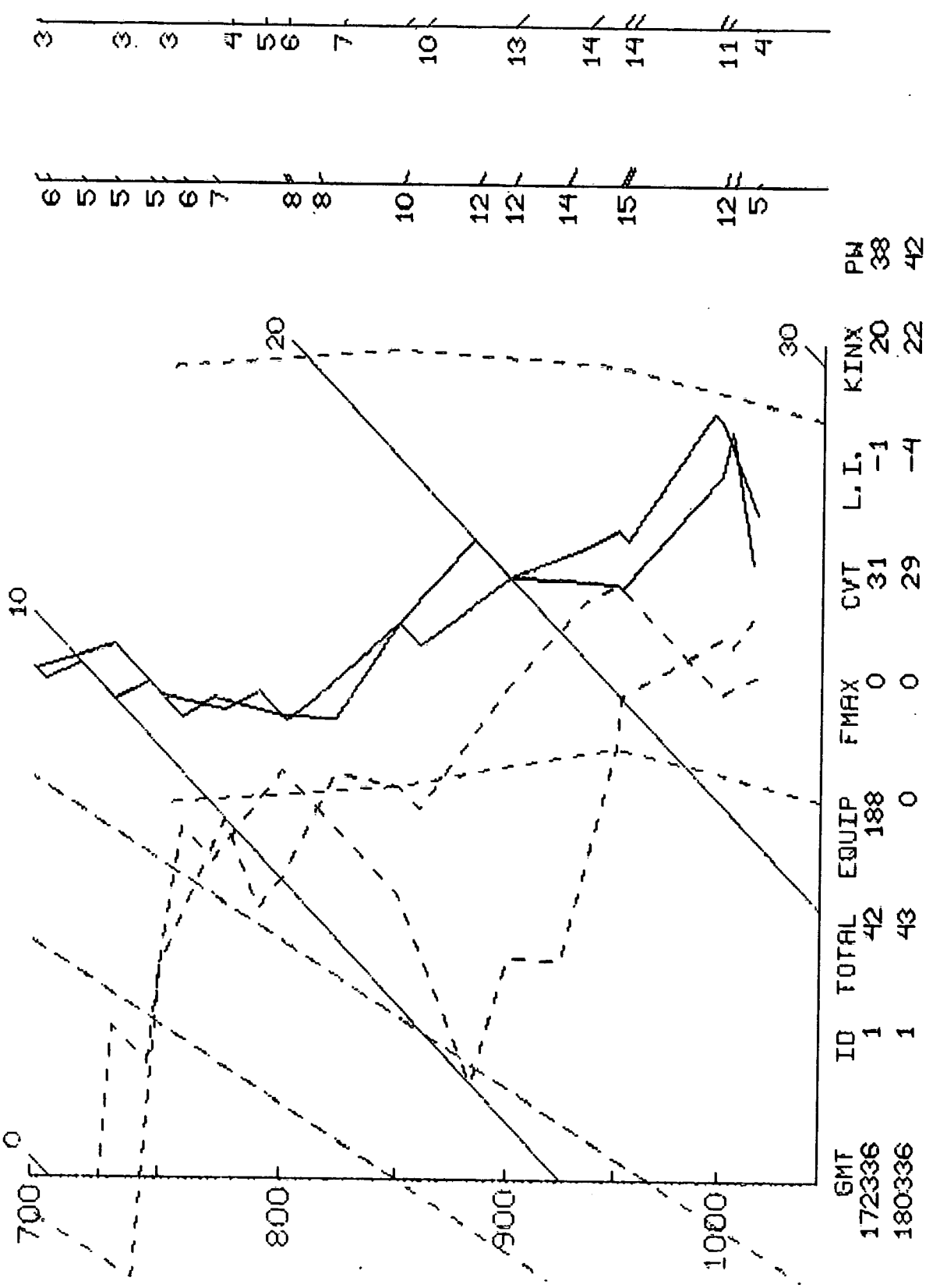

Figure 24 Comparison of low-level CCAFS soundings at 2336 UTC on 17 September and 0336 UTC on 18 September.

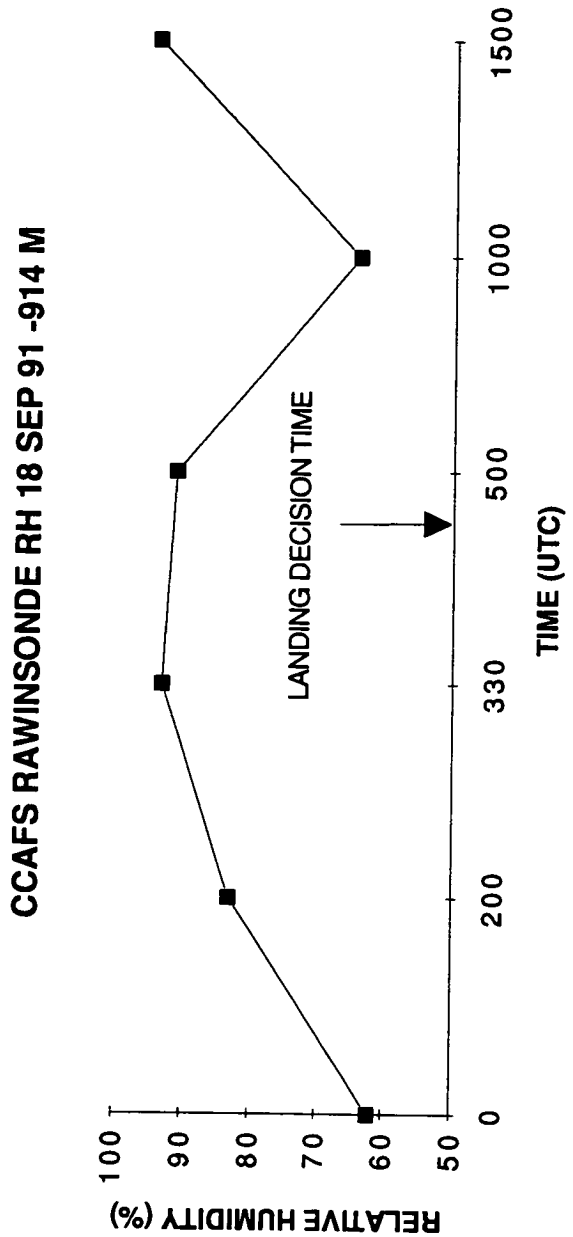

Figure 25 Time series of relative humidity from CCAFS rawinsondes , 2336 UTC 17 September to 1000 UTC 18 September 1991.

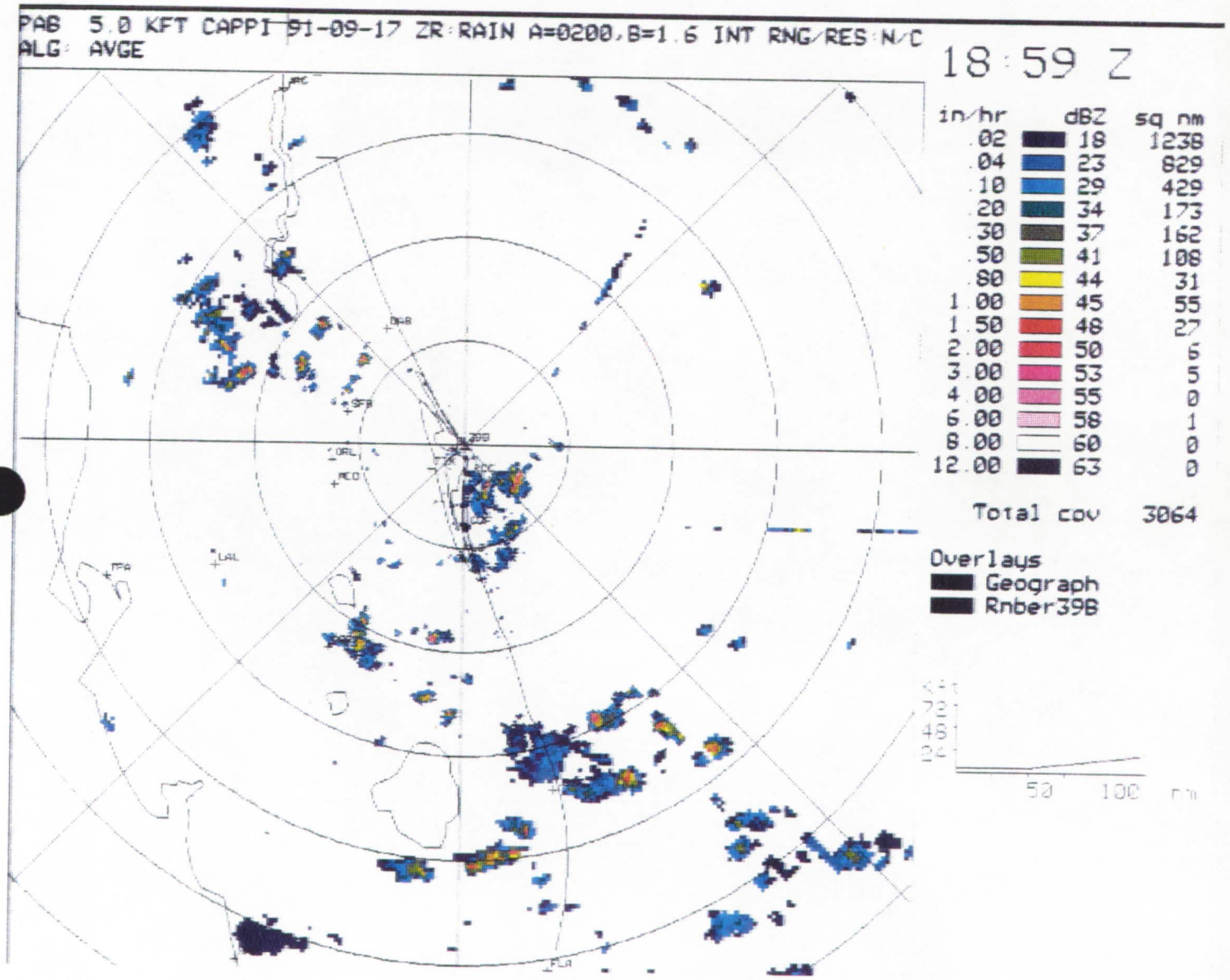

Figure 26 McGill Radar image at 1859 UTC on 17 September 1991.

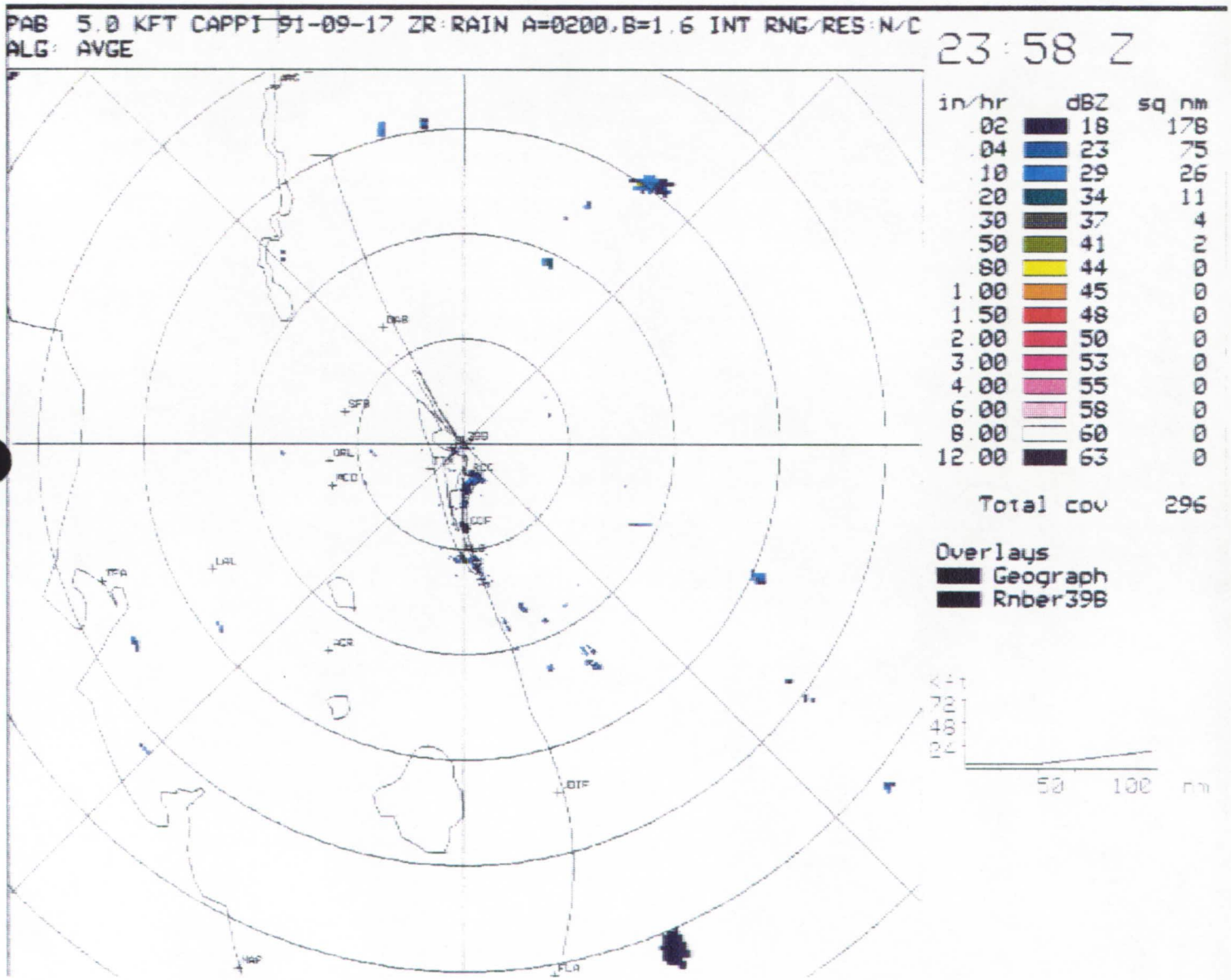

Figure 27 McGill Radar image at 2358 UTC on 17 September 1991.

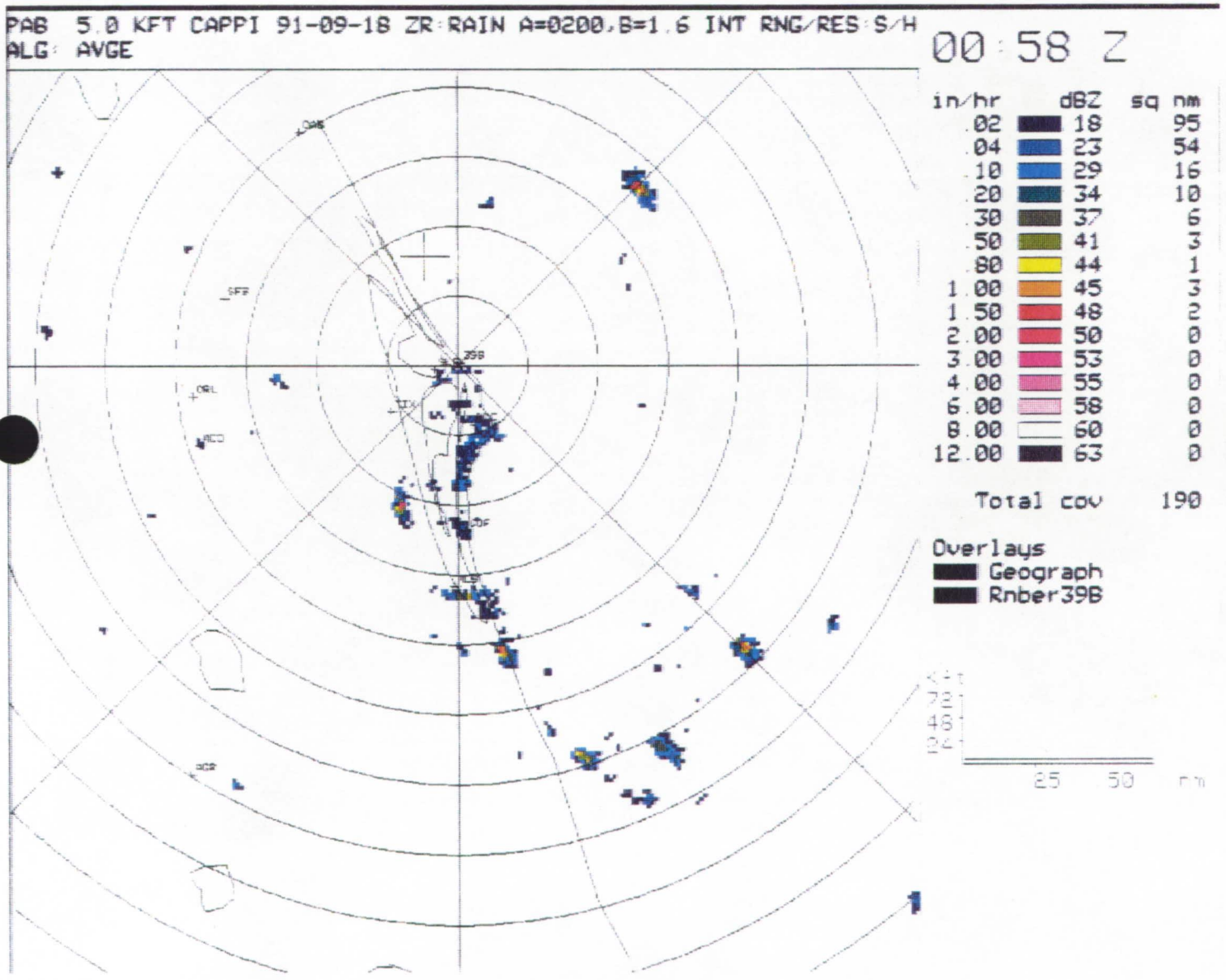

Figure 28 McGill Radar image at 0058 UTC on 18 September 1991.

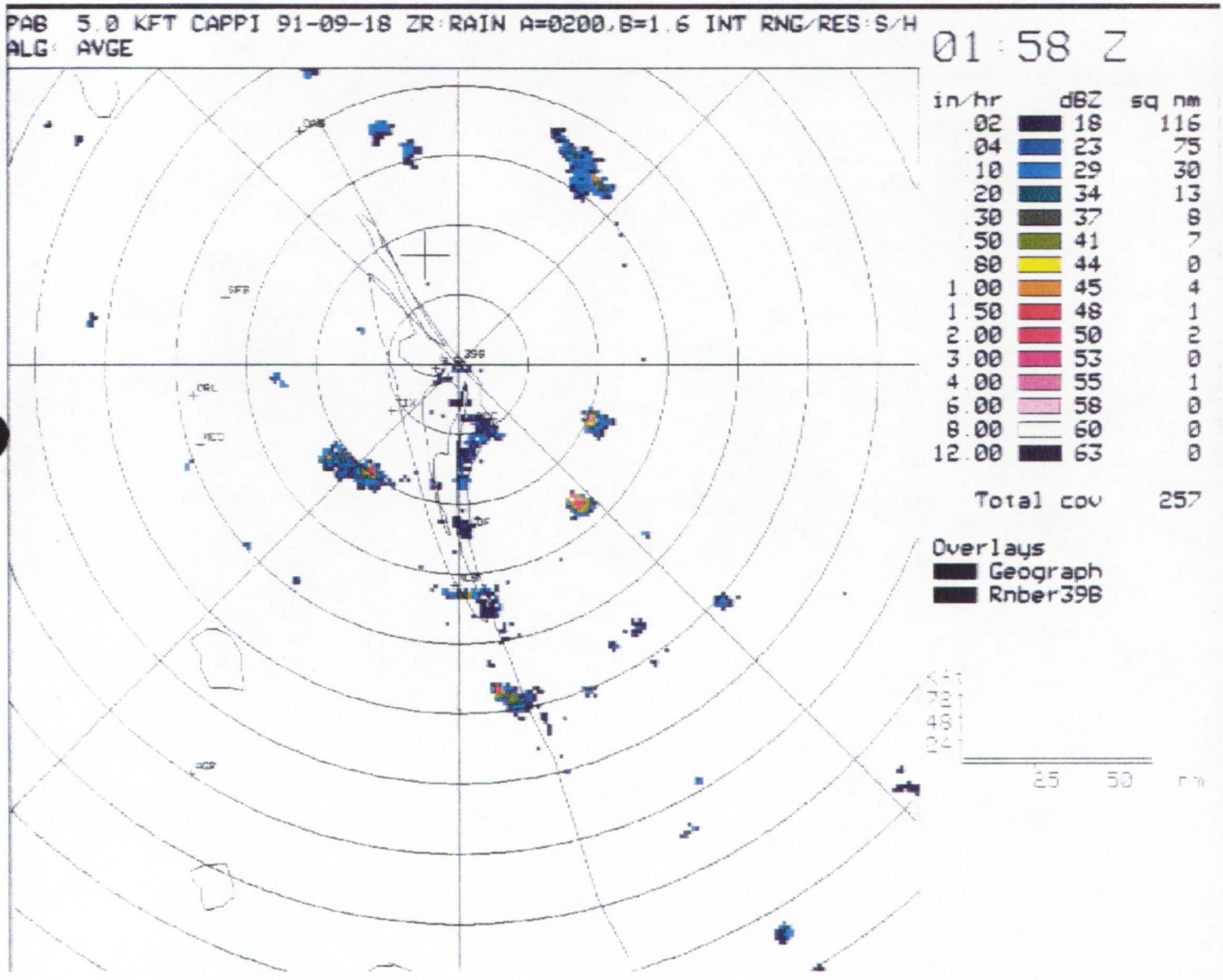

Figure 29 McGill Radar image at 0158 UTC on 18 September 1991.

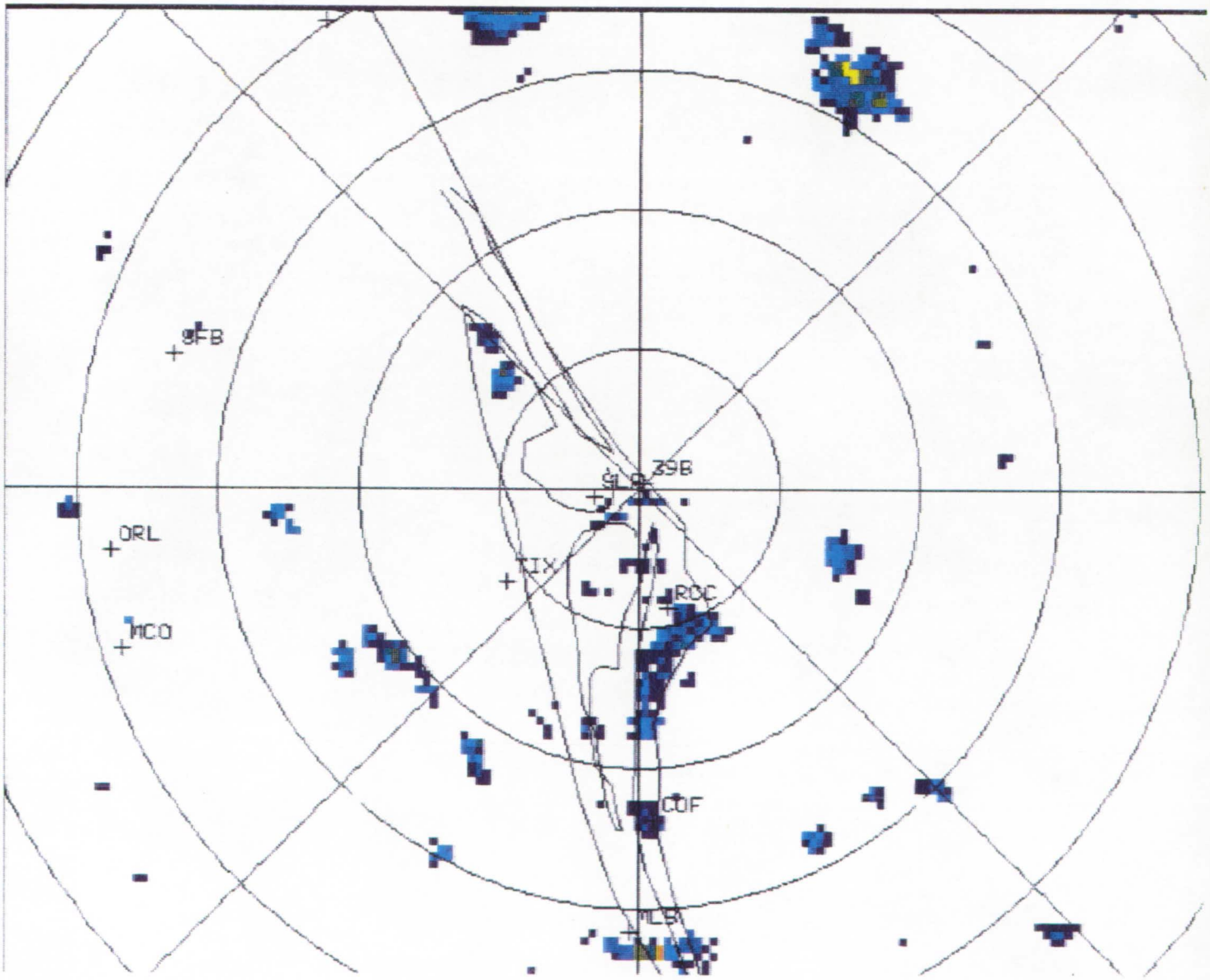

Figure 30 McGill Radar image at 0228 UTC on 18 September 1991.

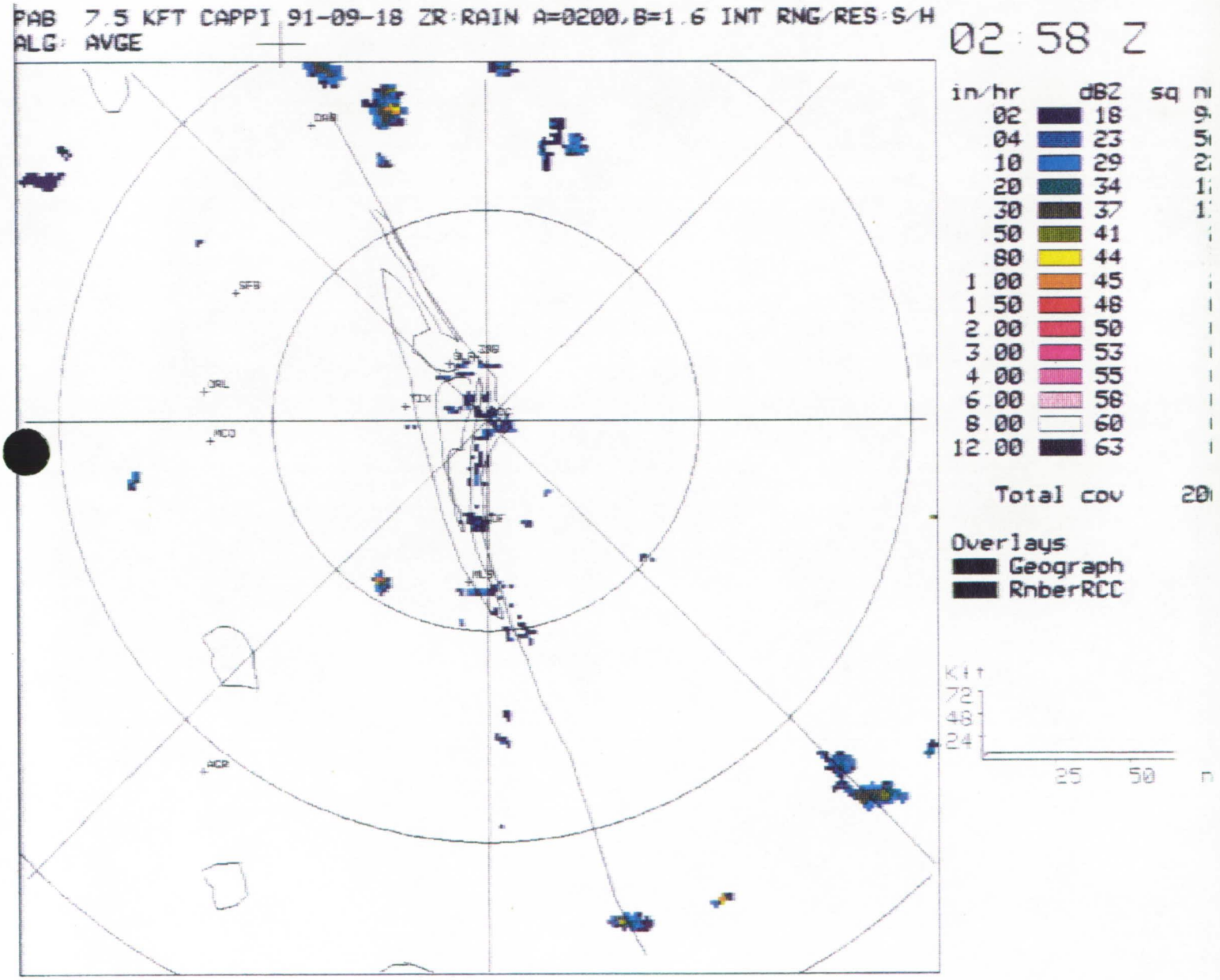

Figure 31 McGill Radar image at 0258 UTC on 18 September 1991.

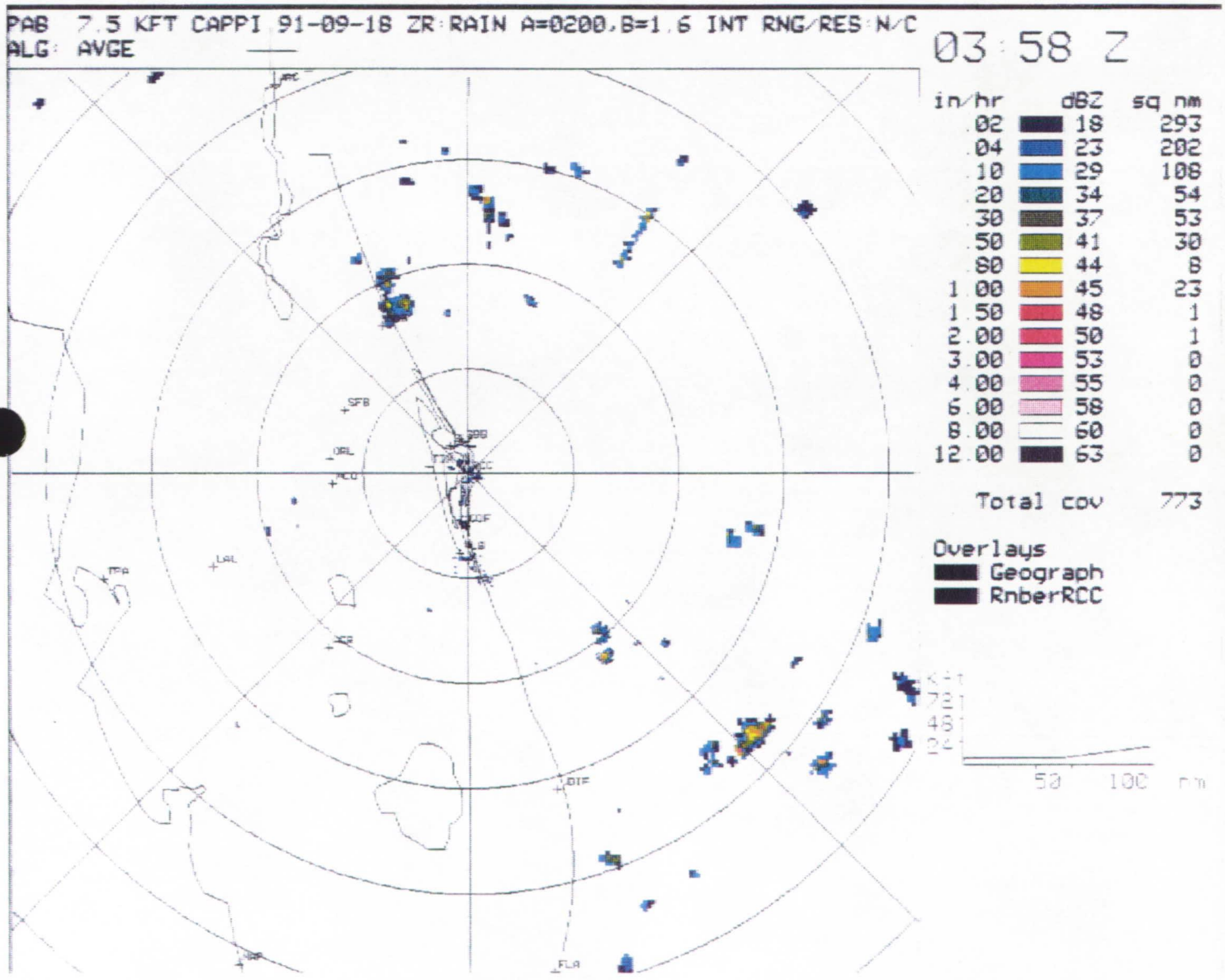

Figure 32 McGill Radar image at 0358 UTC on 18 September 1991.

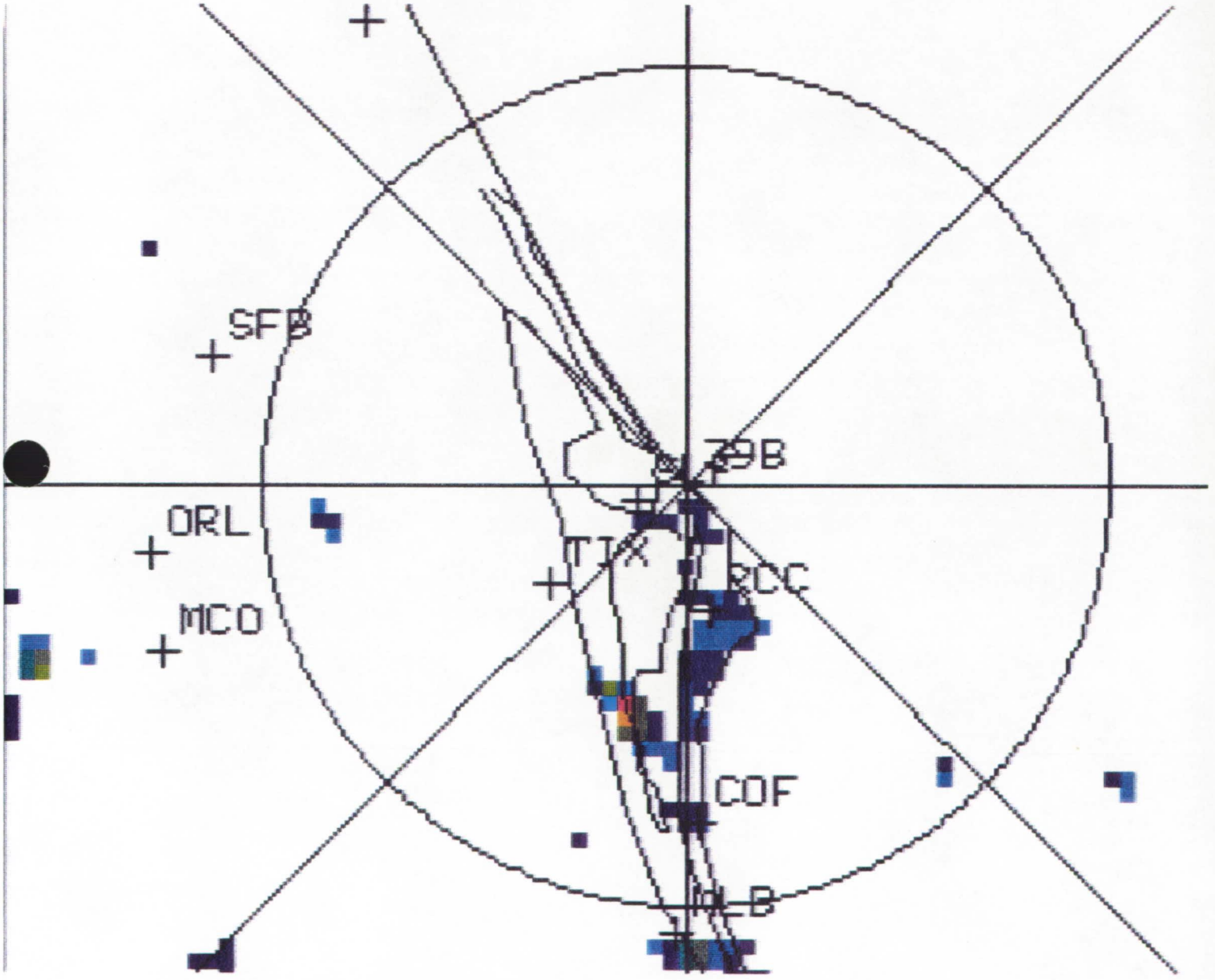

Figure 33 McGill Radar image at 0458 UTC on 18 September 1991.

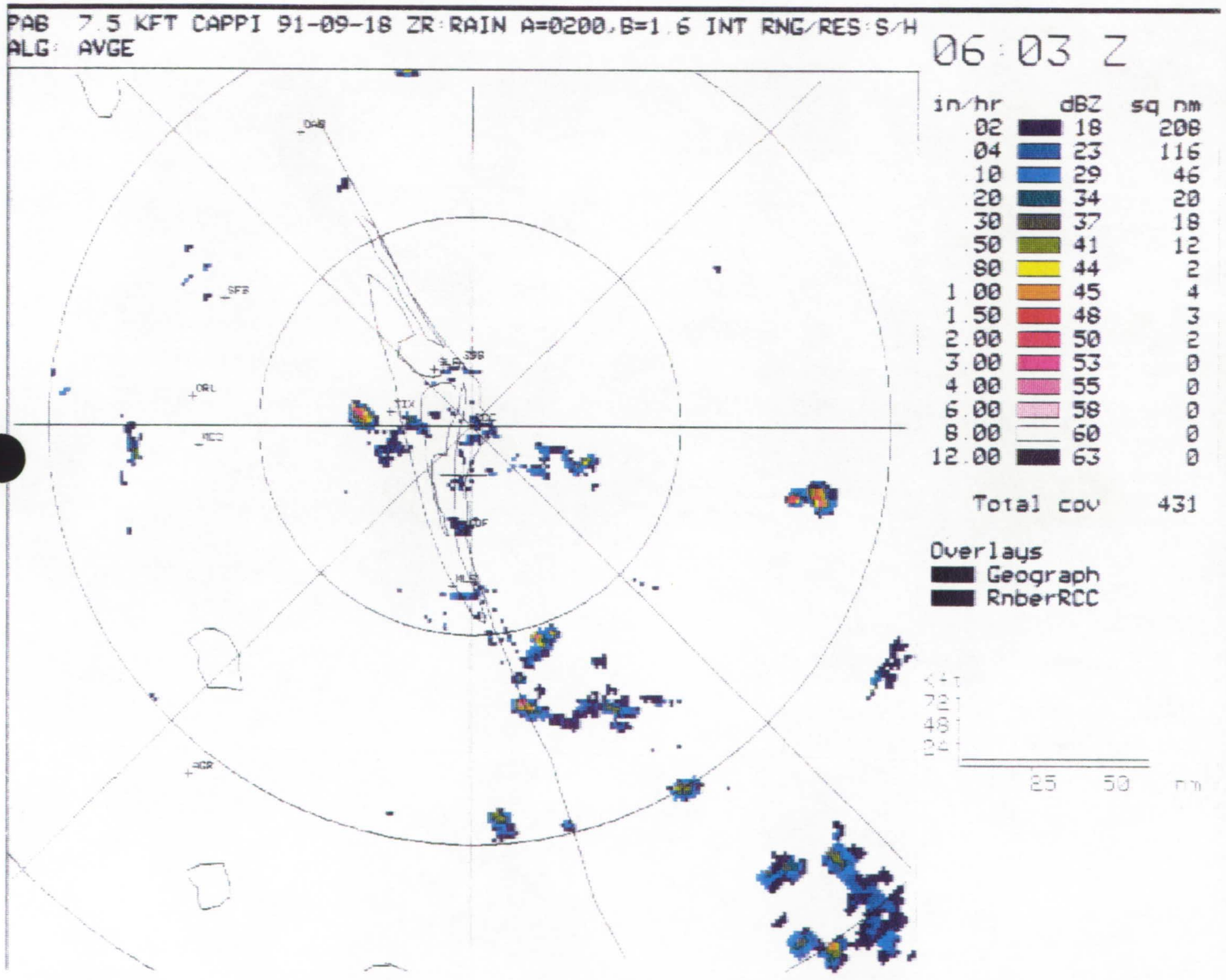

Figure 34 McGill Radar image at 0603 UTC on 18 September 1991.

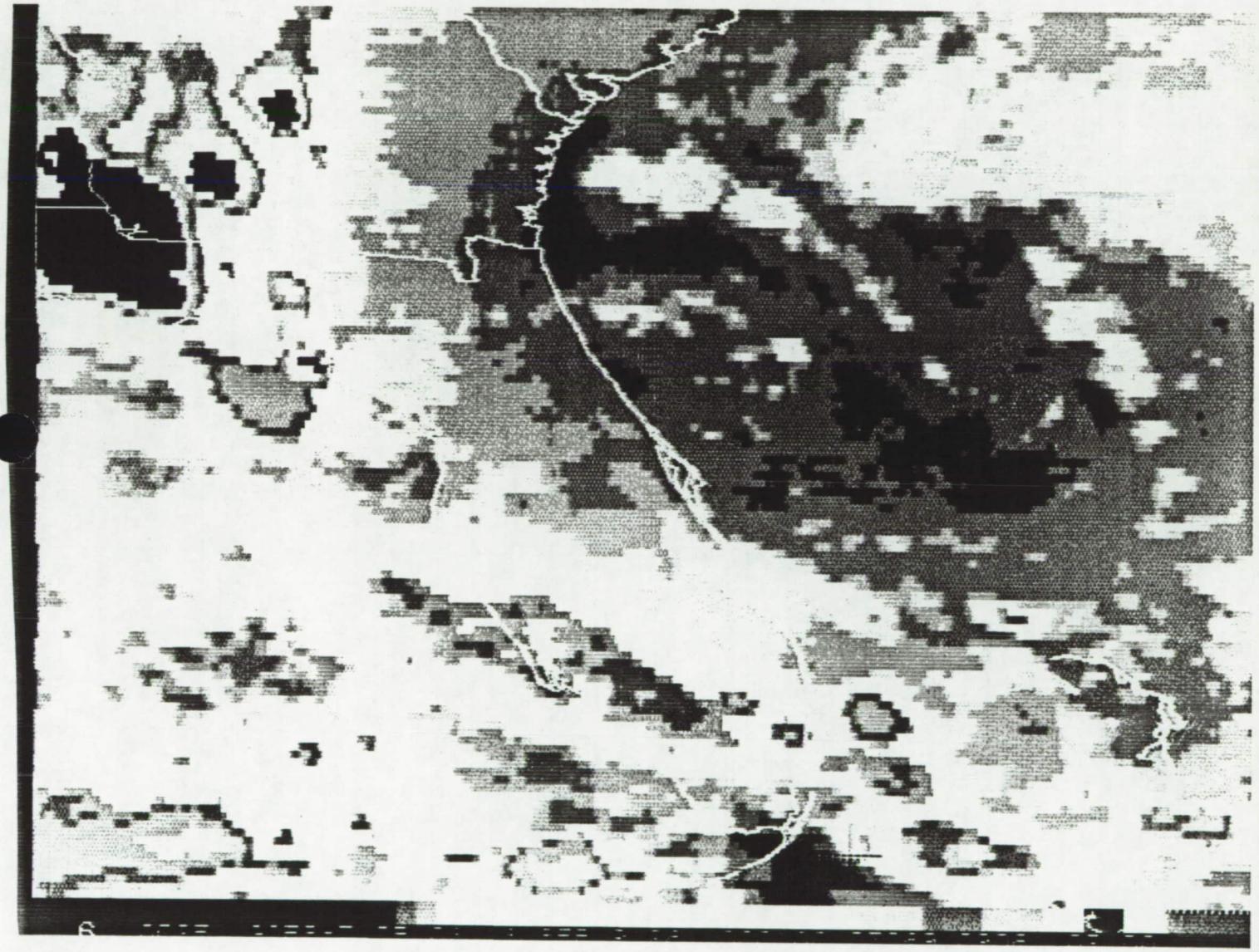

Figure 35a GOES Enhanced IR image at 0001 UTC on 18 September 1991.

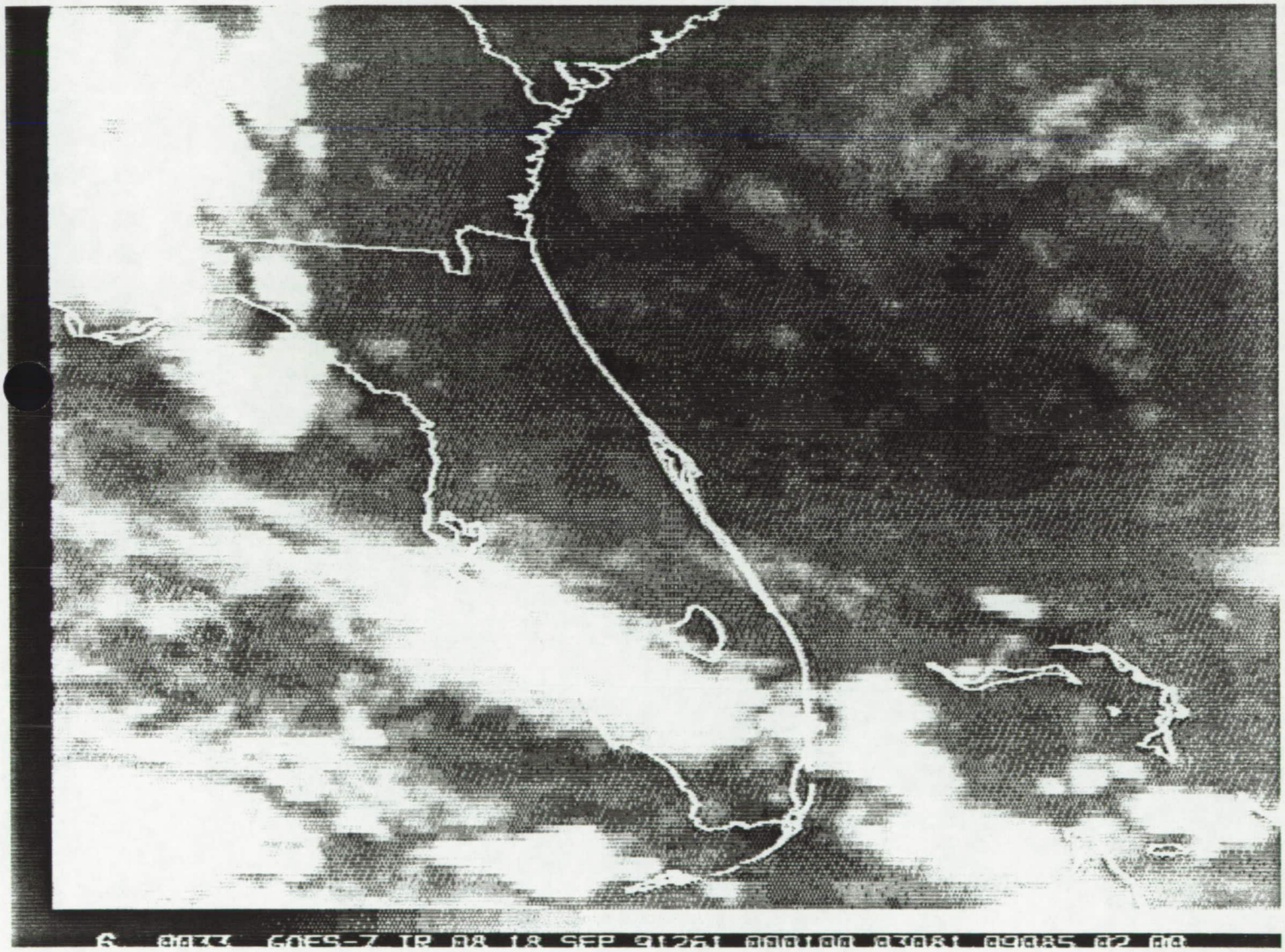

Figure 35b GOES IR image at 0001 UTC on 18 September 1991.

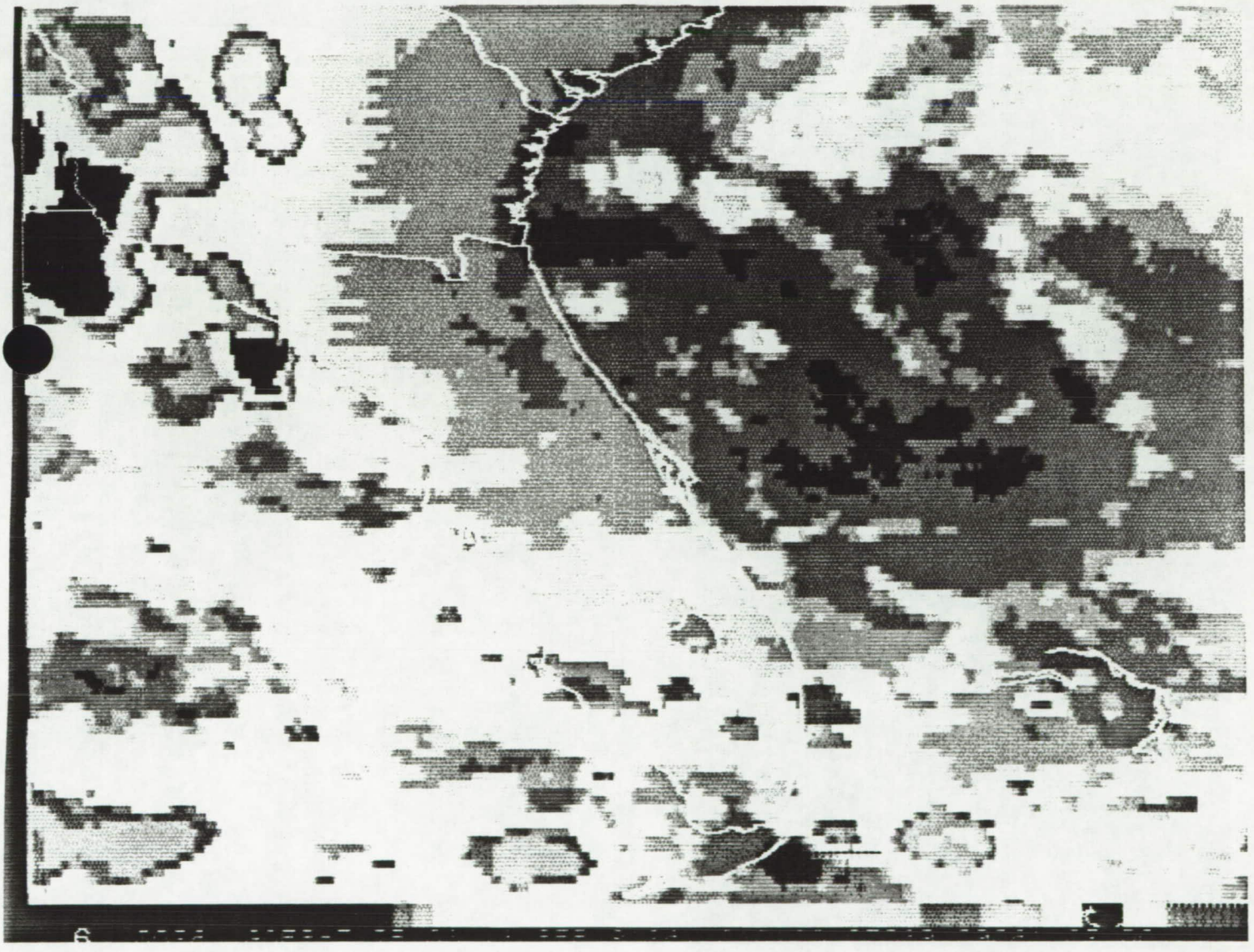

Figure 36a GOES Enhanced IR image at 0101 UTC on 18 September 1991.

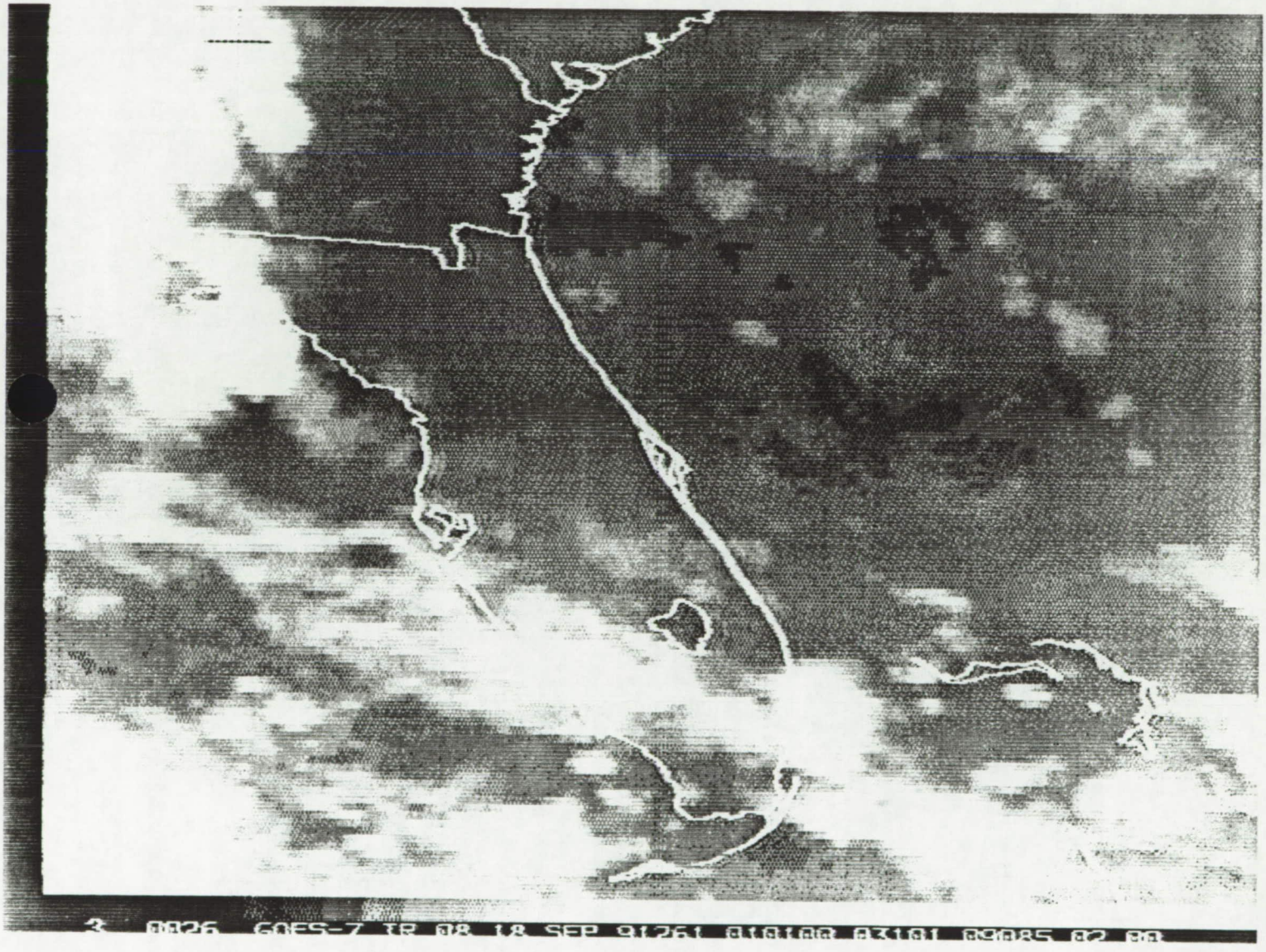

Figure 36b GOES IR image at 0101 UTC on 18 September 1991.

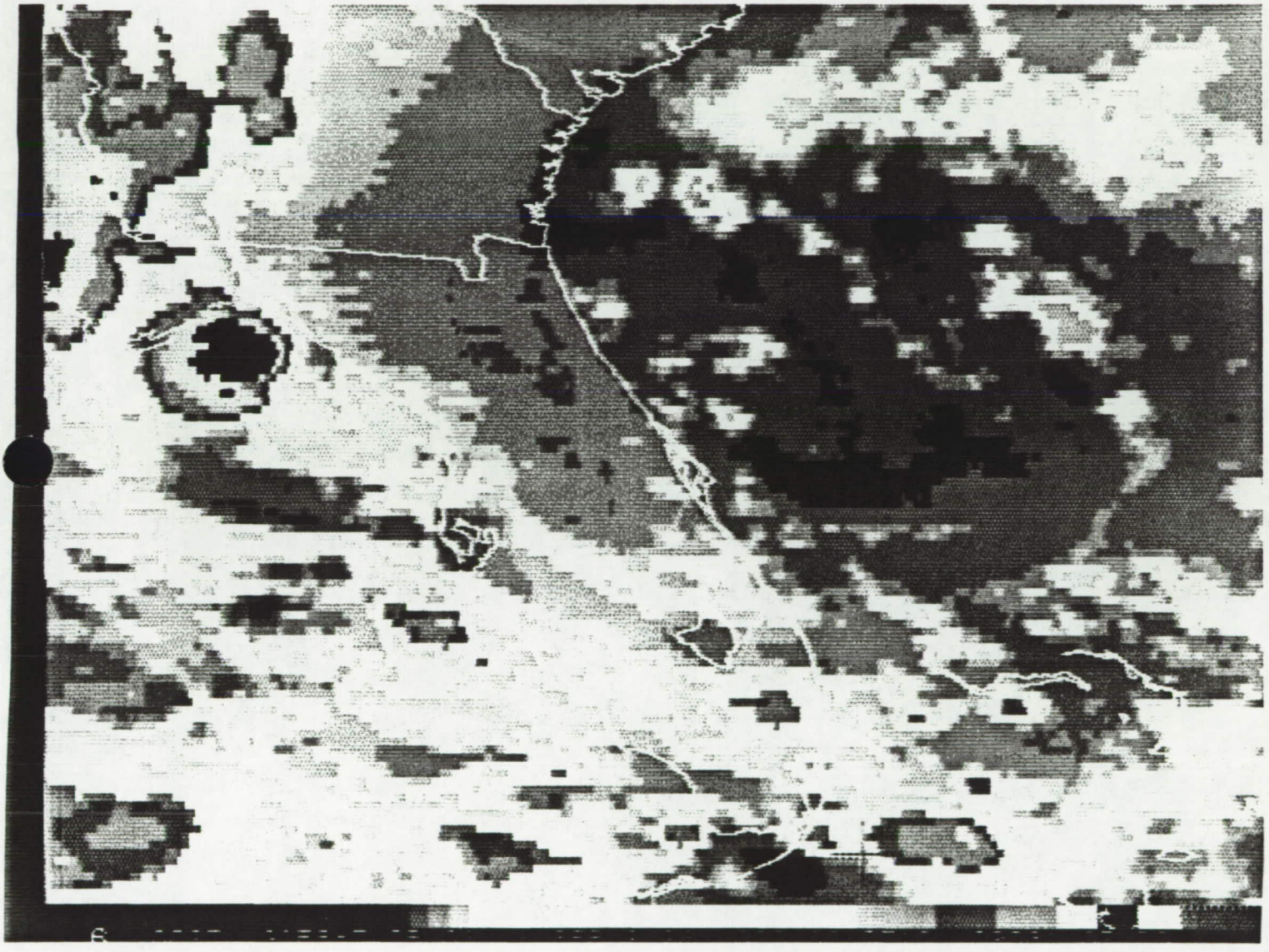

Figure 37a GOES Enhanced IR image at 0201 UTC on 18 September 1991.

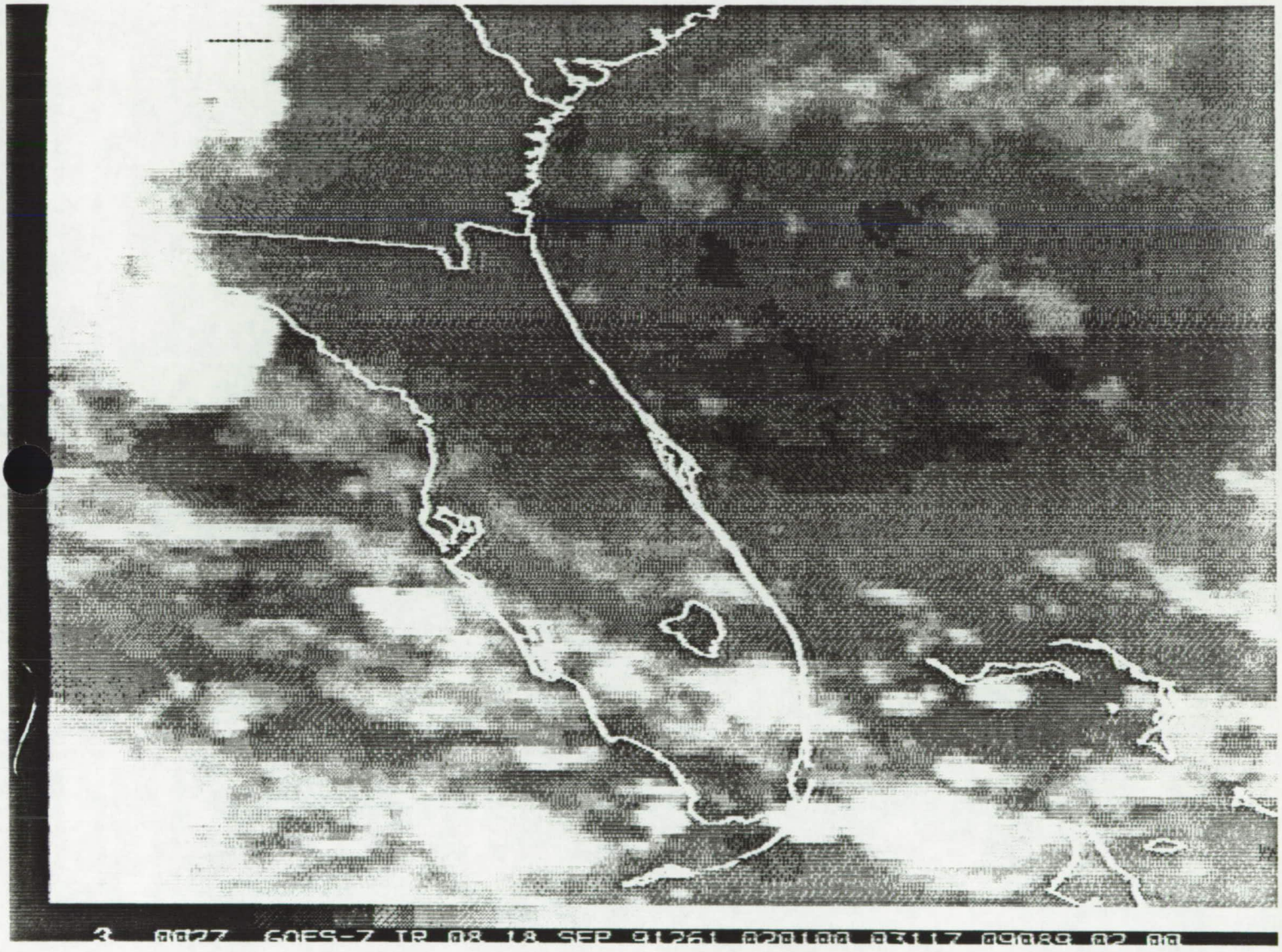

Figure 37b GOES IR image at 0201 UTC on 18 September 1991.

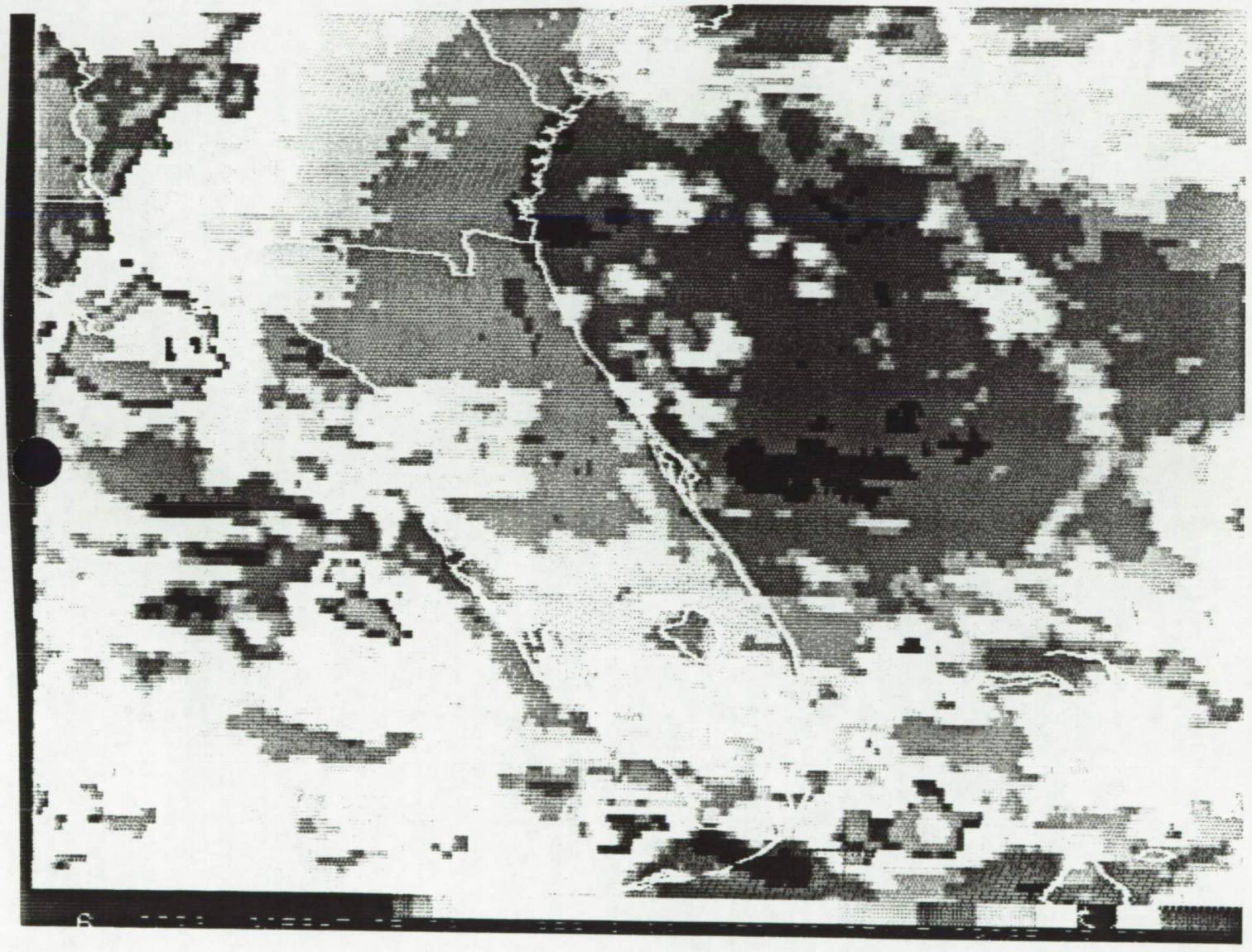

Figure 38a GOES Enhanced IR image at 0301 UTC on 18 September 1991.

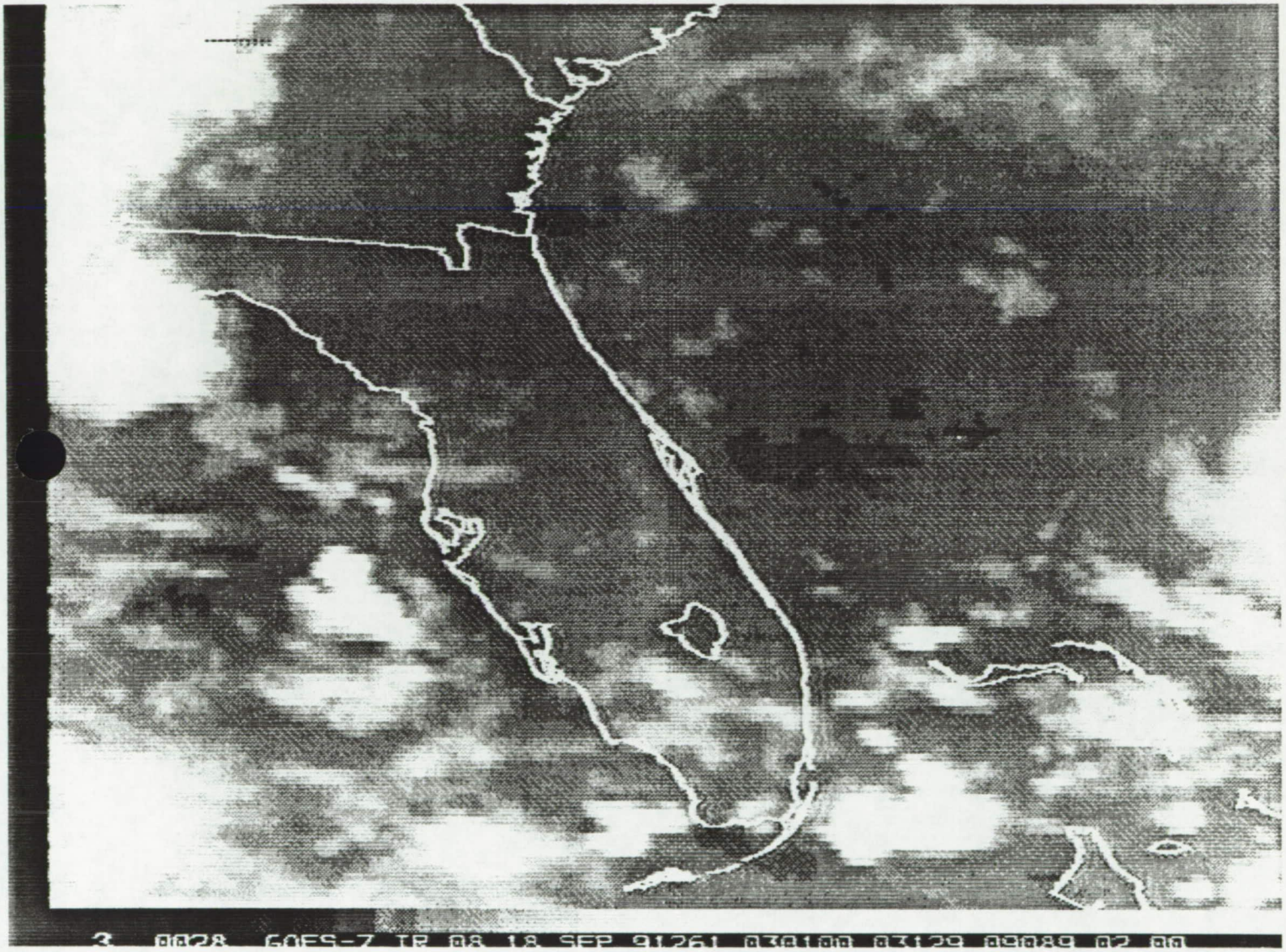

Figure 38b GOES IR image at 0301 UTC on 18 September 1991.

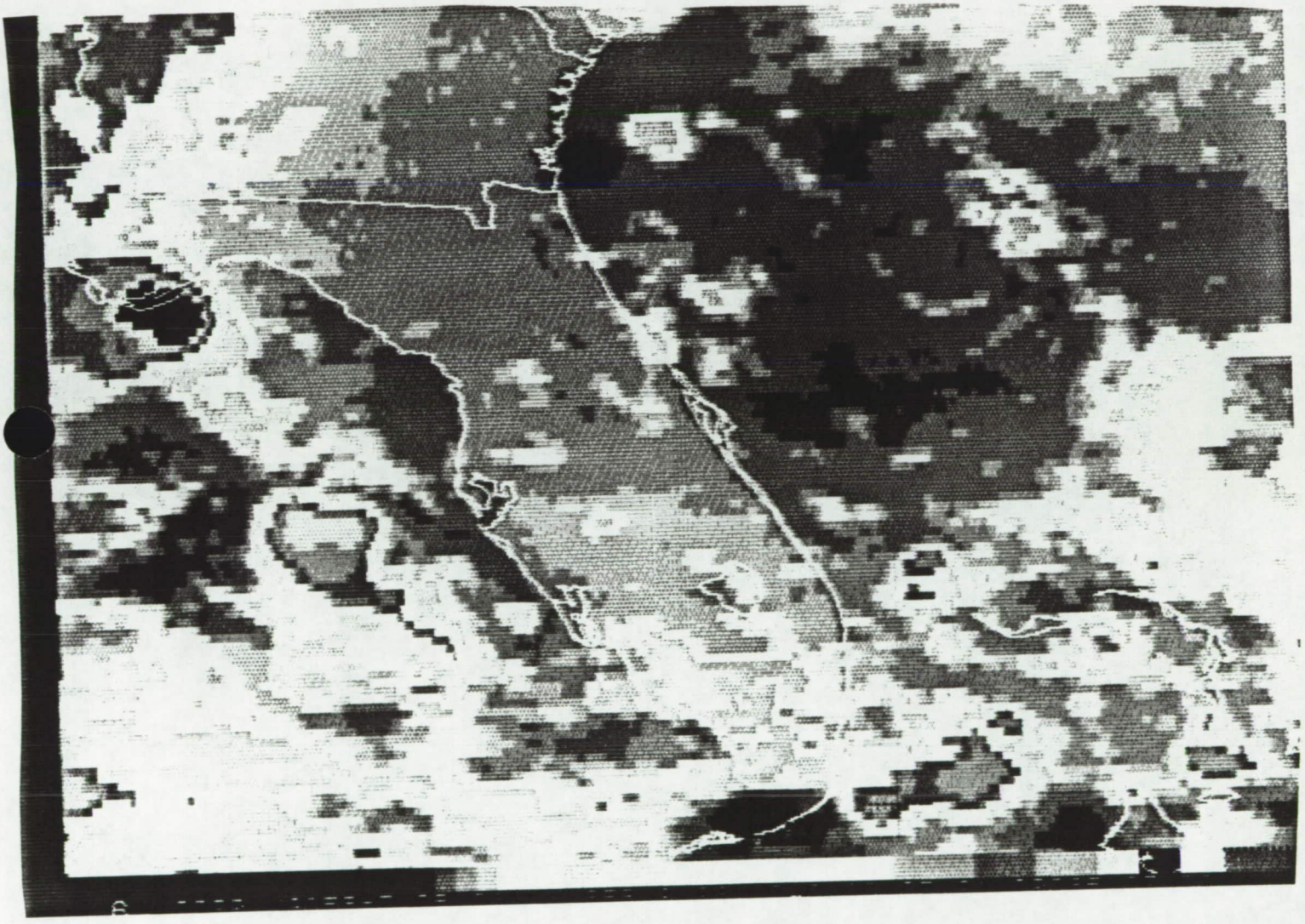

Figure 39a GOES Enhanced IR image at 0401 UTC on 18 September 1991.

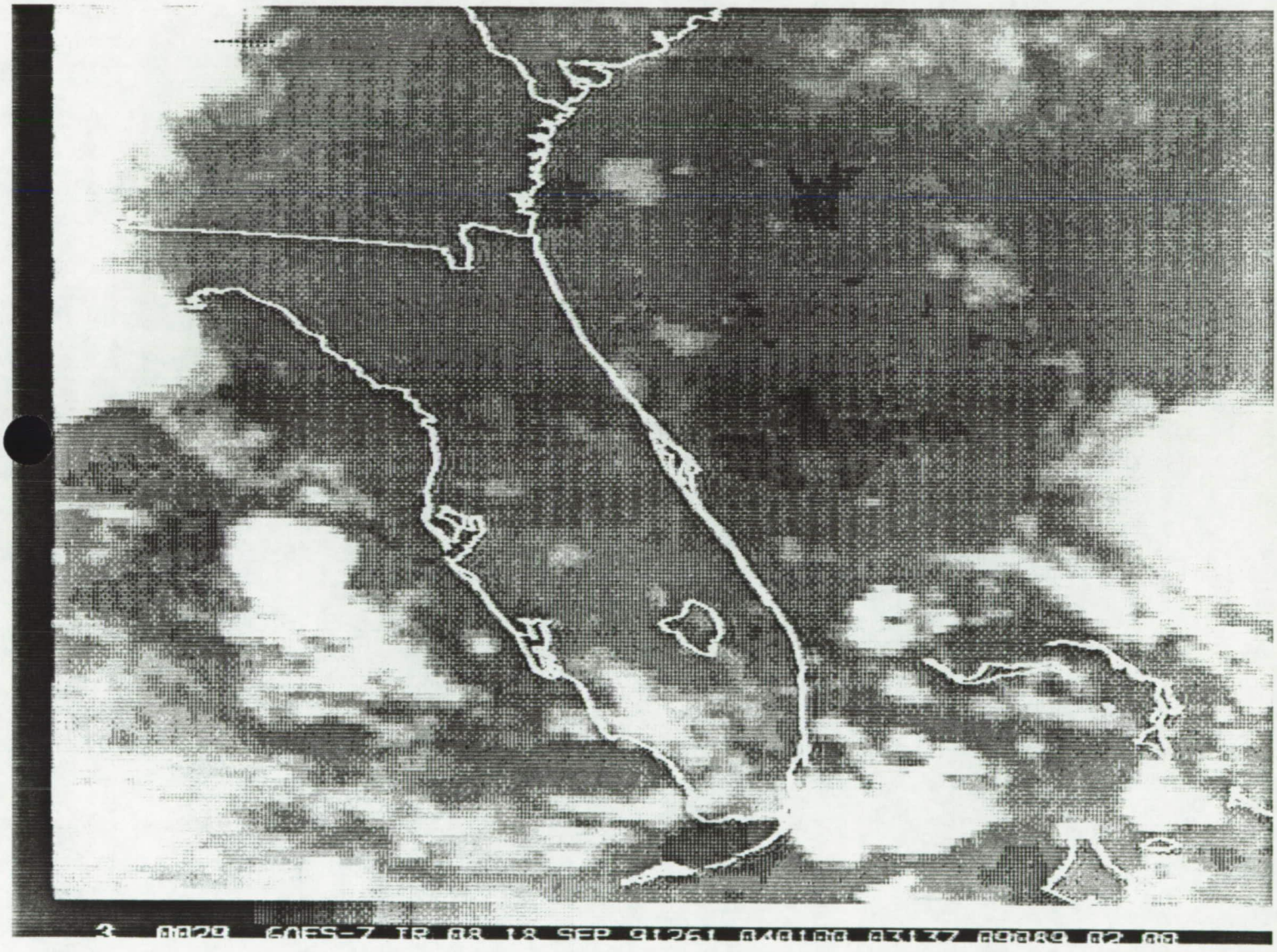

Figure 39b GOES IR image at 0401 UTC on 18 September 1991.

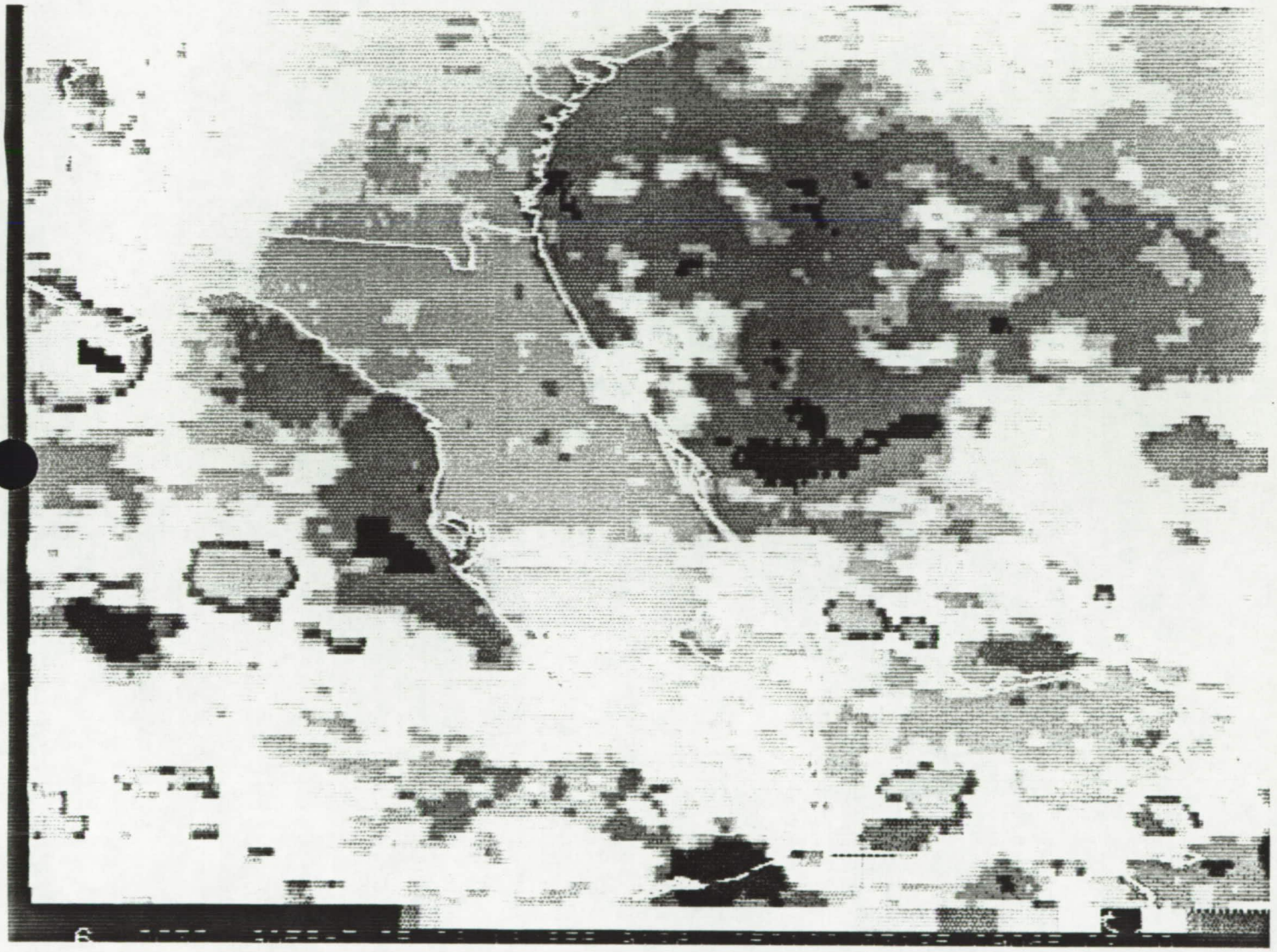

Figure 40a GOES Enhanced IR image at 0501 UTC on 18 September 1991.

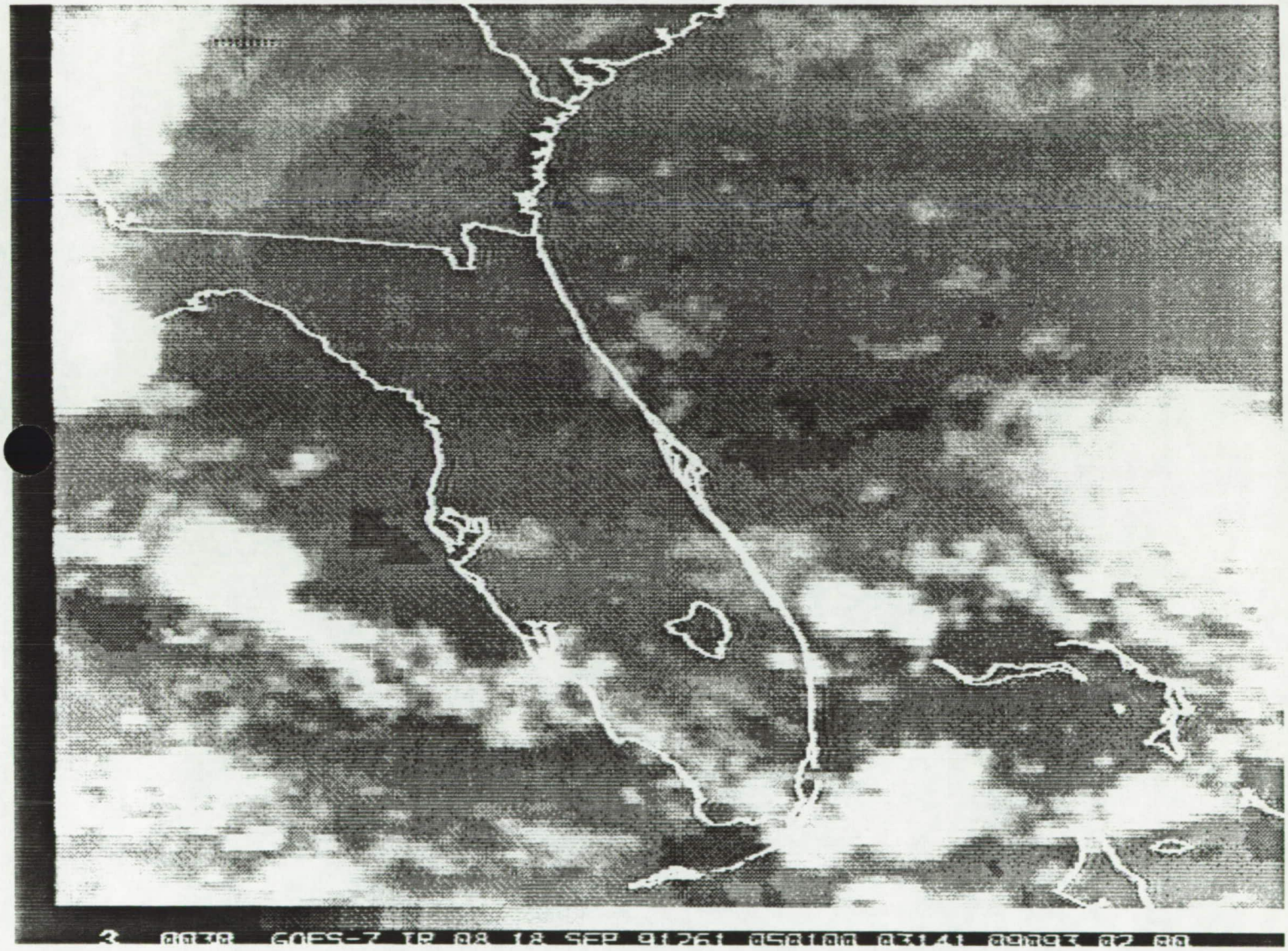

Figure 40b GOES IR image at 0501 UTC on 18 September 1991.

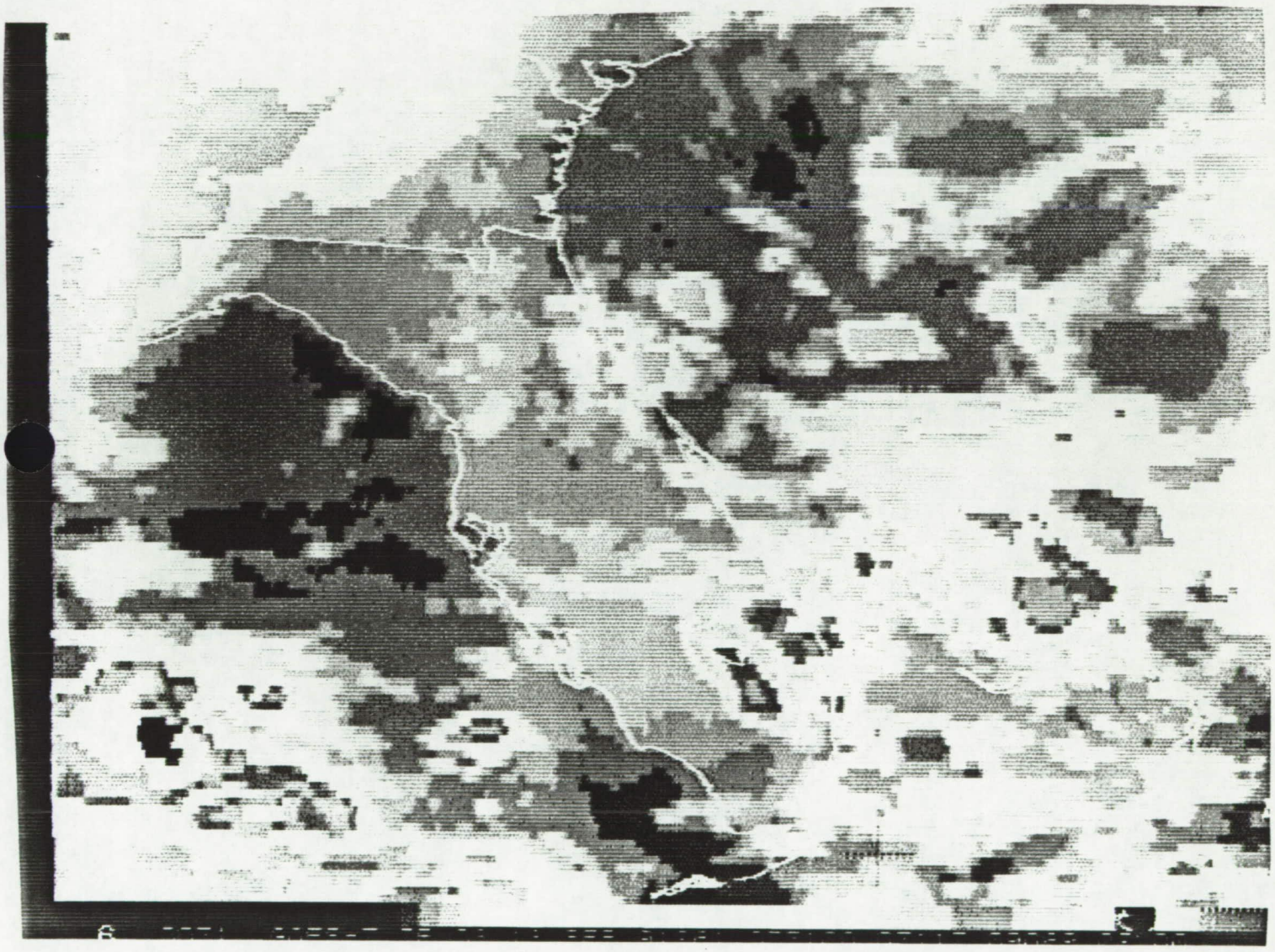

Figure 41a GOES Enhanced IR image at 0731 UTC on 18 September 1991.

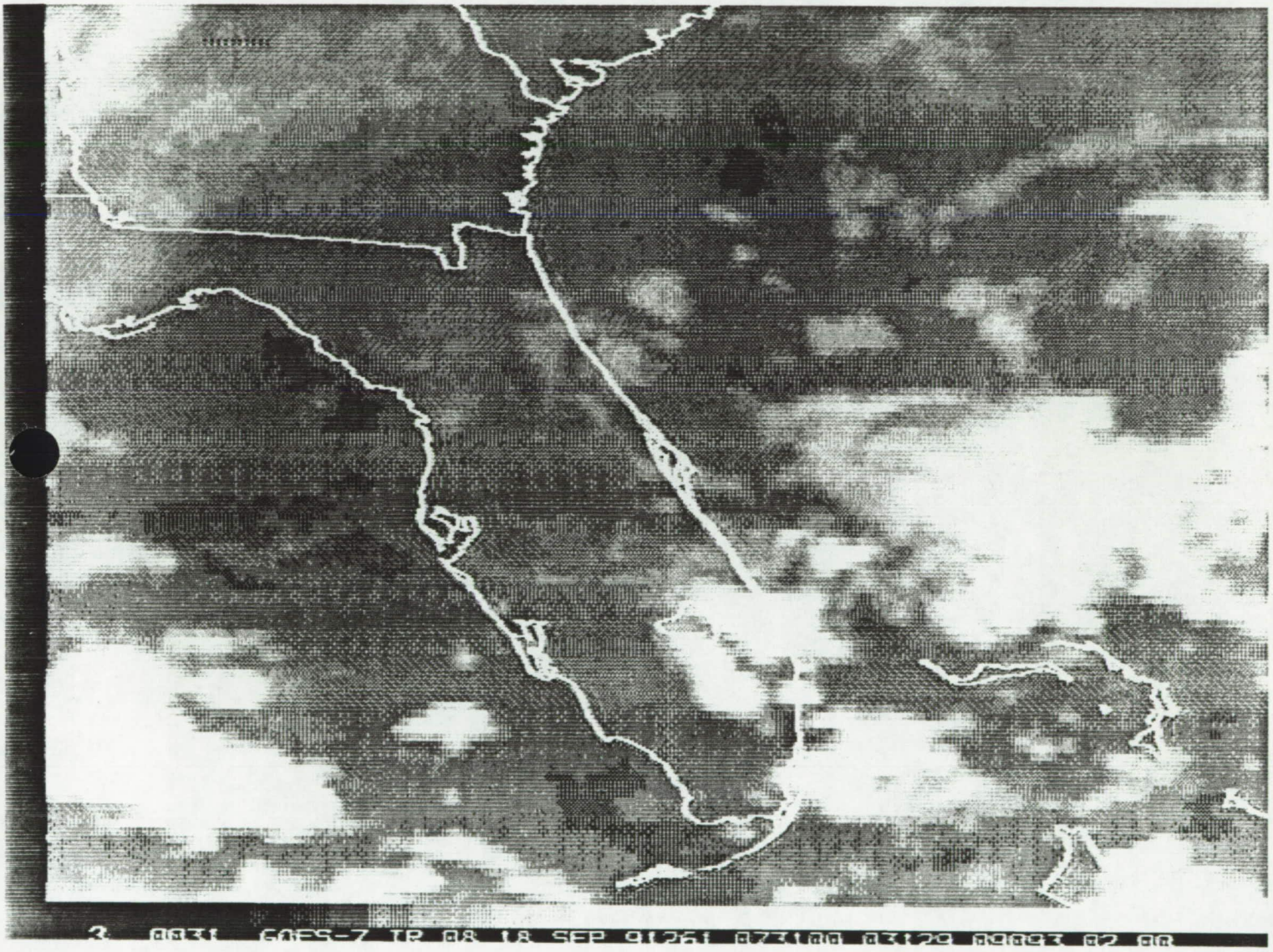

Figure 41b GOES IR image at 0731 UTC on 18 September 1991.

REPORT DOCUMENTATION PAGE

Form Approved
OMB No. 0704-0188

1. AGENCY USE ONLY (Leave blank)	2. REPORT DATE	3. REPORT TYPE AND DATES COVERED
	March 1992	Contractor Report

4. TITLE AND SUBTITLE	5. FUNDING NUMBERS
STS-48 Case Study 17-18 September 1991	C-NAS10-11844
6. AUTHOR(S) Michael K. Atchison, Mark M. Wheeler, Gregory E. Taylor, and John D. Warburton	
7. PERFORMING ORGANIZATION NAME(S) AND ADDRESS(ES) ENSCO, Inc., 445 Pineda Court, Melbourne, FL 32940	8. PERFORMING ORGANIZATION REPORT NUMBER 92-001
9. SPONSORING/MONITORING AGENCY NAME(S) AND ADDRESS(ES) NASA, John F. Kennedy Space Center, Code TM-LLP-2, Kennedy Space Center, FL 32899	10. SPONSORING/MONITORING AGENCY REPORT NUMBER NASA CR-190147
11. SUPPLEMENTARY NOTES	
12A. DISTRIBUTION/AVAILABILITY STATEMENT Unclassified--Unlimited	12B. DISTRIBUTION CODE

13. ABSTRACT (Maximum 200 Words)

This report documents weather conditions prior to and during the STS-48 attempted landing at the Shuttle Landing Facility at KSC on 18 September 1991. Major emphasis of this report focused on trends in meteorological data during 17 and 18 September and their relationship to the overall weather pattern observed over the KSC region. The primary weather problems during the landing of STS-48 were the formation of showers within 10 nautical miles of the SLF and any ceilings less than 10,000 feet. The controlling factor of the weather on 17-18 September was a high pressure ridge that was gradually weakening and moving off the northeast. As this occurred the low-level flow was switching from a easterly to a southeasterly direction. This change in wind direction was reflected by shower movement on the McGill radar and by trends in rawinsondes launched from the Cape. These rawinsondes also indicated that the boundary layer was becoming slightly more unstable several hours prior to the attempted landing which may have aided in the development of clouds and small isolated showers. In addition, analyses of KSC Doppler wind profiler and Cape rawinsondes indicated a possible mid-level disturbance in the easterly flow pattern near 700 mb (10000 ft.). This weak disturbance may have made the atmosphere a little more unstable early on 18 September. Finally, embedded within the southeasterly flow were several bands of low clouds. These clouds were rather difficult to see in unenhanced IR satellite imagery available to forecasters in real time. However, post analyses using several different enhancement curves, adapted from NESDIS, clearly reveals the presence of these clouds.

Analysis of the meteorological data surrounding the STS-48 attempted landing had led the AMU to identify two aspects that need further attention. First, forecasters need to be more aware of selecting optimum IR satellite enhancement curves to visualize low clouds during nighttime hours. Second, since the development of low-level clouds and showers are of prime concern for Shuttle landings, a low-level stability index should be developed and evaluated for use in easterly flow situations. Currently, MIDDS only provides the forecaster with information for the potential for thunderstorm and severe thunderstorm development.

14. SUBJECT TERMS	15. NUMBER OF PAGES 69
Space Shuttle, STS-48, Weather Analysis	16. PRICE CODE

17. SECURITY CLASSIFICATION OF REPORT	18. SECURITY CLASSIFICATION OF THIS PAGE	19. SECURITY CLASSIFICATION OF ABSTRACT	20. LIMITATION OF ABSTRACT
UNCLASSIFIED	UNCLASSIFIED	UNCLASSIFIED	NONE